Reprogramming Hepatocytes into Duct-like Cells

O'Neill, Kathy

Award date:
2010

Awarding institution:
University of Bath

Reprogramming Hepatocytes into Duct-like Cells

Kathy E. O'Neill

A thesis submitted for the degree of Doctor of Philosophy

University of Bath
Department of Biology and Biochemistry

July 2010

CONTENTS

TABLE OF FIGURES

Chapter 5

ACKNOWLEDGEMENTS

I am very grateful to my supervisors Professor Jonathan Slack and Dr. David Tosh.

I would also like to thank the past and present members of the Slack and Tosh labs, particularly Emily-jane Myatt, Shifaan Thowfeequ and Daniel Eberhard.

This work was funded by the Biotechnology and Biological Sciences Research Council (BBSRC).

ABSTRACT

Primary hepatocytes maintained in culture progressively downregulate liver-specific genes and lose their characteristic function and morphology. This process, termed dedifferentiation, is a hindrance to *in vitro* modelling of systems such as xenobiotic metabolism, liver disease and regeneration. However the results presented here demonstrate that dedifferentiated hepatocytes spontaneously induce expression of ductal genes, and therefore represent a useful model of cell reprogramming.

Rat hepatocytes were maintained in either a differentiated or a dedifferentiated state, and cells cultured under each condition were analysed by RT-PCR, western blotting and immunostaining. To determine the molecular basis of dedifferentiation and ductal gene activation, C/EBPα and Sox9 were selected as candidate transcriptional regulators and overexpressed in dedifferentiated and differentiated hepatocytes respectively. The contribution of chromatin-level systems and extracellular signalling cascades was also assessed.

This work shows that dedifferentiated hepatocytes downregulate *cebpα, cps1* and *gck*, and induce the ductal genes *sox9*, *ck19*, *osteopontin* and *cx43*. Overexpression of C/EBPα and Sox9 reveals that the repression of hepatocyte genes may be primarily due to downregulation of C/EBPα, while Sox9 may induce expression of ductal genes. It is also shown that C/EBPα and Sox9 are related by reciprocal transcriptional inhibition. At the chromatin level, dedifferentiation correlates with an increase in nuclear area, and with downregulation of the chromatin remodeller Brm. *Sox9* induction does not, however, require promoter-localised histone modification.

These results demonstrate that C/EBPα and Sox9, which activate hepatocyte and duct-specific gene expression respectively, are mutually antagonistic. The C/EBPα-mediated repression of *sox9* maintains lineage commitment in adult hepatocytes by blocking activation of the ductal program. This may explain why dedifferentiation, which involves downregulation of C/EBPα, facilitates reprogramming of hepatocytes into duct-like cells. Mutual antagonism of lineage-activating transcription factors is found in a range of tissue contexts, suggesting that dedifferentiation may also facilitate interconversion of non-hepatic cell types.

ABBREVIATIONS

ac	acetylated
Ad	adenovirus
AFP	alpha-fetoprotein
AID	activation induced deaminase
BAF	brahma-associated factor
BCECF	2',7'-bis-(2-carboxyethyl)-5-(and-6)-carboxyfluorescein
BECs	biliary epithelial cells
BMEL cells	bipotential mouse embryonic liver cells
BMP	bone morphogenetic protein
BrdU	5′-Bromo-2-deoxyuridine
Brg1	brahma-related gene 1
Brm	brahma
C/EBP	CCAAT/enhancer binding protein
CHD	chromodomain helicase DNA binding protein
ChIP	chromatin immunoprecipitation
CK	cytokeratin
CMV	cytomegalovirus
c-Myc	myelocytomatosis oncogene
Cps1	carbamoyl phosphate synthetase 1
C_t	threshold cycle
Cx	connexin
DAB	3,3'-diaminobenzidine
DAPI	4,6-diamidino-2-phenylindole dihydrochloride
DAPM	methylene dianiline
DAPT	N-[N-(3,5-difluorophenacetyl)-l-alanyl]-S-phenylglycine t-butyl ester
DEPC	diethylpyrocarbonate
DMEM	Dulbecco's modified Eagle's medium
DMSO	dimethylsulfoxide
DNA	deoxyribonucleic acid
Dnmt	*de novo* methyltransferase
Dox	doxycycline
DPPIV	dipeptidyl peptidase IV
DTT	dithiothreitol
EBF	early B-cell factor
EDTA	ethylenediaminetetraacetic acid
EGF	epidermal growth factor
eGFP	enhanced green fluorescent protein
EMT	epithelial-mesenchyme transition
ESCs	embryonic stem cells
FBS	foetal bovine serum
Fbx15	F-box protein 15
FGF	fibroblast growth factor
Fox	forkhead box
GATA	GATA-binding protein
Gck	glucokinase
GFP	green fluorescent protein

Glut2	facilitated glucose transporter 2
H3K4me3	histone 3 trimethylated on lysine 4
HEPES	4-(2-Hydroxyethyl)piperazine-1-ethanesulfonic acid
Hes1	hairy and enhancer of split 1
HMG	high mobility group
HNF	hepatic nuclear factor
HP1	heterochromatin protein 1
HRP	horse radish peroxidase
IHBD	intrahepatic bile duct
iPS cells	induced pluripotent stem cells
IRES	internal ribosome entry site
ISWI	imitation switch
Jag1	jagged1
Klf4	kruppel-like factor 4
KSFM	keratinocyte serum-free medium
LAP	liver activating protein
LIP	liver inhibitory protein
LRH1	liver receptor homolog 1
Mac1	macrophage 1
MafA	v-maf musculoaponeurotic fibrosarcoma oncogene family protein A
MBD4	methyl-CpG binding domain protein 4
MCSF	macrophage colony stimulating factor
MMP	matrix metallopeptidase
MOI	multiplicity of infection
mRNA	messenger ribonucleic acid
Myf5	myogenic factor 5
Myod1	myogenic differentiation 1
NeuroD1	neurogenic differentiation 1
Ngn3	neurogenin 3
NICD	notch intracellular domain
Nkx2.2	NK2 transcription factor related locus 2.2
OC-2	onecut 2
Pax	paired box gene
PBS	phosphate-buffered saline
PBS-T	phosphate-buffered saline-Tween 20
PC1/3	prohormone convertase 1/3
PCNA	proliferating cell nuclear antigen
PCR	polymerase chain reaction
Pdx1	pancreatic and duodenal homeobox 1
PET	positron emission tomography
PFA	paraformaldehyde
PH3	phospho-histone H3
POU5F1	POU domain class 5 transcription factor 1
PRDM16	PR domain containing 16
Ptf1a	pancreas specific transcription factor 1a
PVDF	polyvinylidene fluoride
Rbpj	recombination signal binding protein for immunoglobulin κJ region
RNA	ribonucleic acid
RSF	rat skin fibroblasts

RSV	Rous sarcoma virus
RT-PCR	reverse transcription-polymerase chain reaction
SAHA	suberoylanilide hydroxamic acid
Sall4	sal-like 4
SCNT	somatic cell nuclear transfer
SDS	sodium dodecyl sulphate
siRNA	short interfering ribonucleic acid
Sox	SRY-box containing gene
Suv39h	suppressor of variegation 3-9 homolog
SWI/SNF	switch/sucrose non-fermenting
Tbx	T-box
TGFβ	transforming growth factor β
TGFβR	transforming growth factor β receptor
TSA	trichostatin A
Ucp1	uncoupling protein 1
UGT	UDP-galactose transporter
Uhrf1	ubiquitin-like containing PHD and RING finger domains 1
VPA	valproic acid
Wnt	wingless-related
YFP	yellow fluorescent protein
Zeb2	zinc finger E-box binding homeobox 2

Chapter 1
Introduction

1.1 Specialised cell types arise by differential gene expression

The mammalian body is composed of hundreds of different cell types specialised for functions as varied as light perception and contraction (Arendt 2008). Despite this diversity, however, almost all cells in any given organism contain exactly the same genome. The distinctive character combinations that define individual cell types are created by differential expression of particular sets of genes (Orphanides and Reinberg 2002). In a hepatocyte (liver) cell, for example, genes encoding alcohol dehydrogenases are switched on, while those required for insulin synthesis, a function of pancreatic beta-cells, are repressed. Differential gene expression can reflect regulation at numerous different levels including transcription, ribonucleic acid (RNA) processing and export, translation and protein modification (Orphanides and Reinberg 2002) (*Figure 1.1*). The most important of these mechanisms is the regulation of transcription, which depends on the activity of promoter and enhancer sequences. Enhancers restrict gene expression in both time and space by binding transcription factors, which in turn influence chromatin structure and RNA polymerase II stabilisation at the promoter through deoxyribonucleic acid (DNA) looping (Tolhuis *et al.* 2002). Transcription factor binding to enhancers is combinatorial such that a single transcription factor expressed in more than one cell type can activate alternative sets of cell-type specific targets by synergising with other factors. The upstream region of many genes contains multiple enhancers that act in a modular fashion to control gene expression in different cell types. *Paired box gene 6* (*pax6*) expression, for example, is controlled by at least 6 different enhancers that regulate transcription in the eye, central nervous system and pancreas (Morgan 2004) (*Figure 1.2*). This differential deployment of genes in defined temporal and spatial contexts explains the existence of diverse specialised cell types that share the same genetic material.

1.2 Differentiation is stable under physiological conditions

During development, differentiated cell types are derived from a single celled zygote in a unidirectional process characterised by increasing and usually irreversible commitment to a single fate (Gurdon and Melton 2008).This idea can be illustrated

as a ball rolling downhill through a series of valleys. Where the valleys bifurcate, the ball travels in one of two possible directions, and the number of potential destinations becomes progressively restricted. Once it reaches the bottom of the hill, the ball is limited to a single destination (Hochedlinger and Plath 2009) (*Figure 1.3*). Similarly, a differentiated cell, although it retains genes encoding specialised characters of all other lineages, cannot switch to a different cell type.

The stability of differentiated cell types can be explained by mathematical modelling of gene regulatory networks. The architecture of a gene regulatory network describes all the genes in a system and the regulatory interactions between them (Huang 2009). As both protein-protein and protein-DNA interactions depend ultimately on the sequence of the genome, each cell in an organism possesses the same gene regulatory network. The distinct gene expression patterns of individual cell types reflect stable states of the network, known as attractors. Most network states are unstable due to constraints imposed by regulatory interactions. For example, if gene 1 inhibits gene 2, all network states in which both genes are highly expressed are forbidden (Huang 2009).

The state space is composed of all possible network states and has N dimensions. However it is often represented as a three-dimensional quasi potential energy landscape in which elevation and stability are inversely correlated (*Figure 1.4*). Gene regulatory networks are dynamic, and over time a system point, representing the current state of one cell, will "flow" downhill from unstable to stable states. Attractors, which occur at the bottom of valleys, are stable points in the multidimensional state space towards which trajectories converge from all directions. Hills correspond to unstable states and constitute the barriers that prevent a cell from spontaneously switching between stable gene expression patterns (Huang 2009). Each attractor is surrounded by a basin of attraction that is represented by a valley and defined as the set of initial states that will flow to the same attractor. If a network occupying an attractor is perturbed to a state within the basin of attraction, it will return over time to the same attractor. This self-stabilising behaviour underlies the robustness of differentiated cell types to small external perturbations (Huang 2009).

1.3 Reprogramming by somatic cell nuclear transfer

Although differentiation is largely stable under physiological conditions, it is not irreversible. In 1962, John Gurdon successfully generated cloned *Xenopus* tadpoles by somatic cell nuclear transfer (SCNT) of nuclei from differentiated cells. In 1.5% of transfers, nuclei from tadpole intestinal epithelial cells injected into enucleated recipient eggs could support development of normal feeding tadpoles, though not of adult frogs (Gurdon 1962). The first cloned mammal was created in 1997 by transfer of nuclei from adult sheep mammary gland (Wilmut *et al.* 1997). However the low efficiency of SCNT left open the possibility that surviving clones were selectively derived from rare somatic stem cells in the donor population rather than from terminally differentiated cells. During development, the DNA of B-cells and T-cells is rearranged at the immunoglobulin and T-cell receptor loci respectively, allowing clones established from differentiated cells to be retrospectively identified. Hochedlinger and Jaenisch (2002) generated viable B-cell and T-cell derived monoclonal mice that carried complete genomic rearrangements in all tissues, confirming the differentiated state of the donor nuclei. However successful cloning required a two-step procedure in which embryonic stem cell lines were established from cloned blastocysts and then employed as donors in tetraploid embryo complementation. The stem cell intermediate may have allowed reactivation of embryonic genes with fewer time constraints than direct blastocyst transfer and/or selected for cells that were successfully reprogrammed (Hochedlinger and Jaenisch 2002). Nevertheless, two-step cloning is not an absolute requirement for all differentiated cells, as blastocysts derived by SCNT of natural killer T-cell nuclei can develop into viable adults, albeit with low efficiency (Inoue *et al.* 2005). Mice have also been cloned from the nuclei of post-mitotic olfactory sensory neurons using both one and two-step procedures. In this case, lineage tracing was achieved by crossing mice that expressed Cre recombinase under control of the olfactory marker protein promoter with reporter animals, and selecting reporter-expressing cells as SCNT donors. Cloned blastocysts, embryonic stem cells or embryos were subsequently analysed for reporter expression or genetic recombination of the reporter locus (Eggan *et al.* 2004). Together, these experiments demonstrate that

even terminally differentiated nuclei can be reprogrammed to a pluripotent state that supports development of all differentiated cell types.

1.4 Induction of pluripotency in differentiated cells

In 2006, a significant breakthrough in reprogramming pluripotency was made by Takahashi and Yamanaka, who showed that ectopic expression of only four transcription factors is sufficient to establish a pluripotent-like state in differentiated cells. Mouse embryonic fibroblasts were transduced with retroviral vectors encoding POU domain class 5 transcription factor 1 (POU5F1), SRY-box containing gene 2 (Sox2), Kruppel-like factor 4 (Klf4) and myelocytomatosis oncogene (c-Myc), and selected on the basis of expression of *F-box protein 15* (*fbx15*), which is normally expressed specifically in embryonic stem cells (ESCs). The selected cells, which were named induced pluripotent stem (iPS) cells, activated embryonic stem cell markers and formed teratomas containing cells representing all three germ layers. However, endogenous *pou5f1*, *sox2* and *nanog* were expressed only at low levels, and the *pou5f1* and *nanog* promoters remained largely methylated, making maintenance of the pluripotent state dependent on continuous transgene expression. Furthermore, injection of these iPS cells into blastocysts did not result in live chimeras (Takahashi and Yamanaka 2006). The extent of iPS cell reprogramming was improved by adopting activation of endogenous *pou5f1* or *nanog* as a more stringent selection criterion for pluripotency than *fbx15* expression. Global gene expression in second generation iPS cells closely resembles that in embryonic stem cells, endogenous pluripotency genes are reactivated and viral vectors are silenced. In addition, endogenous *pou5f1* and *nanog* are demethylated and enriched for trimethylated lysine 4 on histone 3 (H3K4me3), and bivalent chromatin domains are established at genes encoding developmental regulators. Finally, *pou5f1* and *nanog*-selected iPS cells can contribute to development of viable postnatal chimeras, including germ line cells, and generate late gestation embryos by tetraploid complementation (Okita *et al.* 2007) (Wernig *et al.* 2007) (Mikkelsen *et al.* 2008). iPS cell generation and cloning therefore provide independent evidence that

differentiation depends on reversible processes, and cannot be considered as permanent or immutable, at least under experimental conditions.

1.5 The mechanism of reprogramming

Conversion of fibroblasts to iPS cells occurs with only 0.01 to 0.1% efficiency (Hochedlinger and Plath 2009), suggesting the existence of several barriers to reprogramming. POU5F1, Sox2, Klf4 and c-Myc can reprogram liver cells that have activated the albumin promoter (hepatoblasts or hepatocytes) (Aoi *et al.* 2008) and pancreatic beta-cells expressing the terminal differentiation marker insulin (Stadtfeld *et al.* 2008), demonstrating that iPS cells are not derived only from rare stem cells in the starting population. The low efficiency of iPS generation is also unlikely to reflect a requirement for gene expression changes induced by insertional mutagenesis at certain genomic loci, as mapping of vector insertions in different iPS lines has not identified any common sites (Aoi *et al.* 2008). In addition, iPS cells can be created from fibroblasts and liver by transient expression of POU5F1, Sox2, Klf4 and c-Myc from nonintegrating adenoviral vectors, albeit with only 0.0001% to 0.001% efficiency (Stadtfeld *et al.* 2008). An important limiting factor in iPS generation may therefore be that transgene expression is required at the correct stoichiometry, consistent with the sensitivity of embryonic stem cells to the dosage of POU5F1 (Niwa *et al.* 2000). Stochastic epigenetic events are also expected to be critically important, and may accumulate slowly, thus accounting for the observation that reprogramming takes 1-2 weeks (Jaenisch and Young 2008).

Further insight into the mechanism of reprogramming can be gained by analysing stable, partially reprogrammed cell lines. Partially reprogrammed cells downregulate fibroblast genes and highly express proliferation-associated factors, but pluripotency genes are expressed at low or undetectable levels and are associated with DNA hypermethylation (Mikkelsen *et al.* 2008). Inactivity of endogenous pluripotency genes correlates with inappropriate activation or incomplete repression of lineage-specific transcription factors such GATA-binding protein 6 (Gata6), Pax7, Pax3 and SRY-box containing gene 9 (Sox9). siRNA-mediated knockdown of these factors, in combination with inhibition of DNA methylation, promotes complete

reprogramming to a fully pluripotent state (Mikkelsen *et al.* 2008). DNA hypermethylation and expression of lineage specifying transcription factors are therefore incompatible with activation of endogenous pluripotency regulators.

1.6 Direct interconversion of differentiated cells

iPS cell technology can be used to interconvert differentiated cells by reprogramming a starting population to pluripotency and then inducing differentiation into an alternative cell type. For example, human fibroblast-derived iPS cells can be converted into insulin-producing cell clusters via definitive endoderm and pancreatic endoderm intermediates (Tateishi *et al.* 2008). However Zhou *et al*. (2008) showed that insulin-secreting pancreatic beta-cells can also be generated directly from differentiated exocrine cells. Adenovirus-mediated expression of pancreatic and duodenal homeobox 1 (Pdx1), neurogenin 3 (Ngn3) and v-maf musculoaponeurotic fibrosarcoma oncogene family protein A (MafA) in the pancreas of adult mice induced ectopic insulin positive cells within 3 days that contained a comparable amount of insulin protein to endogenous beta cells by day 10. The exocrine origin of induced beta-cells was confirmed in Cpa1-CreER^{T2}; R26R mice, in which an inducible form of Cre recombinase is expressed specifically in mature exocrine cells, resulting in permanent β-galactosidase labelling. Reprogrammed cells were negative for the exocrine markers amylase and pancreas specific transcription factor 1a (Ptf1a), but coexpressed insulin with gene products essential for beta-cell function including facilitated glucose transporter 2 (Glut2), glucokinase (Gck), prohormone convertase 1/3 (PC1/3), neurogenic differentiation 1 (NeuroD1), NK2 transcription factor related locus 2.2 (Nkx2.2) and Nkx6.1. Furthermore, induced beta-cells synthesised C-peptide, a by-product of insulin processing, and stored insulin in small dense secretory granules. In mice rendered hyperglycaemic by streptozotocin, which specifically ablates beta-cells, injection of Ad-Pdx1, Ad-Ngn3 and Ad-MafA significantly improved fasting blood glucose, glucose tolerance and the level of serum insulin (Zhou *et al.* 2008). The combined activity of three transcription factors can therefore directly reprogram differentiated exocrine cells into functional beta-cells. This conversion could in principle have

occurred via dedifferentiation to the $Sox9^{+}$ hepatic nuclear factor 6 $(HNF6)^{+}$ endodermal progenitor shared by exocrine and beta-cells, but Sox9 and Hnf6 were not expressed during reprogramming, and few induced beta-cells divided in the first 10 days after adenovirus infection (Zhou *et al.* 2008). Notably, maintenance of the beta-cell phenotype did not require continued transgene expression, which was substantially diminished after one month and undetectable after two months. Pdx1 and MafA protein, in contrast, were consistently expressed after two months, indicating activation of the endogenous genes (Zhou *et al.* 2008). Transient transcription factor expression can thus give rise to stable changes in cell identity.

In addition to reprogramming exocrine cells to beta cells, ectopic transcription factor expression can convert B cells to macrophages. Xie *et al*. (2004) showed that retrovirus-mediated expression of CCAAT/enhancer binding protein α (C/EBPα) in primary B cell precursors induced the macrophage marker macrophage 1 (Mac1), and suppressed the B cell marker CD19 antigen 19 (CD19) in 60% of B cell precursors after 4 days. Gene expression profiling revealed repression of additional lymphoid genes (such as *E2A*, *early B-cell factor* (*EBF*) and *pax5*), and induction of monocytic markers (including *macrophage colony stimulating factor receptor* (*MCSFR*) and *PU.1*). Reprogrammed cells were also characterised by the large granular morphology of their *bone fide* counterparts and were capable of phagocytosis. The B cell origin of induced macrophages was confirmed by heavy and light chain immunoglobulin rearrangements, and by lineage tracing B cells derived from CD19-Cre; R26R EYFP mice, in which B cells are labelled by EYFP (Xie *et al.* 2004). Coexpression of C/EBPα and PU.1 in B cell precursors increased the percentage of Mac1-expressing cells compared to expression of C/EBPα alone, while in a PU.1 defective pre-B cell line, activation of Mac1 required exogenous expression of both C/EBPα and PU.1. C/EBPα-mediated induction of macrophage genes in B cell precursors therefore occurred by synergism with endogenous PU.1. However C/EBPα did not require PU.1 to repress CD19 (Xie *et al.* 2004). C/EBPα therefore has two separable activities: It cooperates with PU.1 to activate macrophage genes, and also represses the B cell gene expression program in a PU.1 independent manner.

The reciprocal control of alternative gene expression programs is also a feature of cell fate switching between the skeletal muscle and brown fat lineages. Seale *et al*. (2008) reported that shRNA-mediated knockdown of the zinc finger protein PR domain containing 16 (PRDM16) in primary brown fat preadipocytes ablated expression of selected brown fat genes such as *uncoupling protein 1* (*ucp1*), induced expression of myogenic genes including *myogenic differentiation 1* (*myod1*) and promoted long tube-like morphology. PRDM16 deficient brown adipose pads also expressed reduced levels of brown adipocyte genes and induced myogenic genes. Conversely, retroviral expression of PRDM16 in C2C12 myoblasts blocked induction of myotube-specific genes in response to pro-myogenic culture conditions (Seale *et al.* 2008). Under adipogenic conditions, PRDM16-expressing C2C12 cells and primary myoblasts differentiated into lipid-storing adipocytes, induced brown fat genes and downregulated myogenic genes, while control cells developed into multinucleated skeletal myotubes. PRDM16 therefore controls a bidirectional switch between brown fat and skeletal muscle (Seale *et al.* 2008). The ability of PRDM16 to induce reprogramming of myoblasts to brown adipocytes was dependent on formation of a complex with the activating isoform of C/EBPβ, liver activating protein (LAP). Accordingly, if PRDM16 was expressed in C2C12 myoblasts in the presence either of shRNA targeted against C/EBPβ or a dominant negative form of C/EBPβ, liver inhibitory protein (LIP), induction of adipogenesis and brown fat gene expression was blunted. In C/EBPβ-deficient embryos, a broad reduction of brown fat-selective gene expression and induction of skeletal muscle gene expression was observed (Seale *et al.* 2008). PRDM16 and C/EBPβ therefore function synergistically to induce expression of brown fat genes in both brown adipocytes and myoblasts, and repress skeletal muscle genes in brown fat.

PRDM16 and C/EBPβ not only activated the brown fat program in myoblasts, but also reprogrammed fibroblasts to brown adipocyte-like cells (Kajimura *et al.* 2009). Fibroblasts ectopically expressing PRDM16 and C/EBPβ induced brown fat genes, and further enhanced expression of thermogenic genes in response to cAMP, a characteristic of *bone fide* brown adipocytes. However engineered brown fat cells had significantly higher basal levels of total and uncoupled respiration than normal brown adipocytes, and did not display cAMP-mediated increases in either activity.

Nevertheless, when transplanted *in vivo* these cells formed distinct brown fat pads that expressed brown adipocyte genes including *ucp1*. Moreover, positron emission tomography (PET) with fluorodeoxyglucose showed that the engineered adipose, like its *bone fide* counterpart, is a sink for active glucose disposal. Ectopic expression of just two factors can therefore reprogram fibroblasts to functional brown adipocytes (Kajimura *et al.* 2009).

The induction of skeletal muscle in brown fat preadipocytes treated with PRDM16-targetted shRNA suggested that the two cell types may be developmentally related. Seale *et al*. (2008) investigated this hypothesis using Myf5-Cre; R26R3-YFP mice, which express Cre under the control of the myogenic factor 5 (Myf5) promoter, previously thought to be activated only in committed skeletal myogenic precursors. Yellow fluorescent protein (YFP) expression was detected in skeletal muscle and brown fat, but not white fat, demonstrating that skeletal muscle and brown fat are derived from a shared Myf5-expressing progenitor (Seale *et al.* 2008). This data emphasises the importance of developmental relatedness in facilitating reprogramming of differentiated cells, and is consistent with the successful conversion of additional cell types that are derived from a common precursor, including exocrine and endocrine pancreas, and B cells and macrophages.

1.7 Chromatin-mediated control of reprogramming

Reprogramming of differentiated cell types by transcription factors highlights the importance of these proteins in establishing cell identity. However lineage-specific gene expression patterns are additionally regulated at the level of chromatin. Mammalian cells contain 1.7m of DNA that must be packaged into a 5μm nucleus but still remain available for transcription, replication and repair. A 7-fold compaction is achieved by assembling DNA into nucleosomes, the fundamental structural units of chromatin (Ho and Crabtree 2010), each of which consists of an octamer of core histone proteins (two copies of histone H2A (H2A), H2B, H3 and H4) encircled by 146bp of DNA (*Figure 1.6*). An iterated series of nucleosomes forms a lower order structure that resembles “beads on a string”, which is in turn

compacted several thousand fold into undefined higher order structures (Ruthenburg *et al.* 2007).

Chromatin not only packages DNA, but also provides an opportunity to regulate gene expression. Histone proteins are subject to posttranslational modifications including acetylation, methylation and phosphorylation. These localise predominantly to the N-terminal tails of histones that project from the alpha-helical core of the nucleosome. Histone modifications can directly affect histone-DNA contacts by neutralisation or addition of charge, or alternatively they can toggle the ability of nucleosomes to form higher order structures by modulating internucleosomal interactions (Ruthenburg *et al.* 2007). Aceylation of lysine 16 on histone 4 (H4K16ac), for example, inhibits formation of compact 30nm-like fibres and impedes the ability of chromatin to form cross-fibre interactions (Shogren-Knaak *et al.* 2006). Histone modifications are also bound by effector proteins that cross-link nucleosomes, enhance occupancy of RNA-polymerase II, or recruit remodelling complexes. By modulating the packaging of chromatin, histone modifications alter the accessibility of gene regulatory regions to transcription factors and therefore contribute to differential gene expression (Cairns 2009).

As histone modification is an important component of cell-type specific transcription, it can be a rate limiting step in cell reprogramming. The efficiency of iPS cell derivation from neural progenitor cells, for example, can be improved by BIX01294-mediated inhibition of the histone methyltransferase G9a. Transduction of neural progenitor cells with POU5F1 and Klf4 in the presence of BIX01294 gives rise to approximately the same number of iPS colonies as transduction with POU5F1, Klf4, Sox2 and c-Myc, and to significantly more colonies than POU5F1 and Klf4 alone (Shi *et al.* 2008). Similarly, the histone deacetylase inhibitors suberoylanilide hydroxamic acid (SAHA), trichostatin A (TSA) and valproic acid (VPA) improve the efficiency of iPS cell generation from mouse embryonic fibroblasts expressing POU5F1, Sox2, Klf4 and c-Myc. VPA also allows efficient iPS induction without c-Myc (Huangfu *et al.* 2008). The changes in gene expression that underlie reprogramming therefore require chromatin-level control of transcription.

ATP-dependent chromatin remodelling complexes provide access to nucleosomal DNA by sliding nucleosomes along the DNA strand, and therefore represent a second chromatin-level mechanism of gene regulation. In vertebrates, there are four main families of remodellers based on the ATPase subunit: Switch/sucrose non-fermenting (SWI/SNF), imitation switch (ISWI), chromodomain helicase DNA binding protein (CHD) and INO80, the best studied of which is SWI/SNF. The ATPase subunit of mammalian SWI/SNF, either brahma (Brm) or brahma-related gene 1 (Brg1), is complexed with ten brahma-associated factors (BAFs), several of which are encoded by gene families. SWI/SNF complexes can therefore be combinatorially assembled to generate cell-type specific variants with distinct biological functions (Ho and Crabtree 2010). The ability of remodelling complexes to modulate availability of gene regulatory elements means that, like histone modifications, they can be essential mediators of reprogramming. For example, non-cardiogenic mouse mesoderm can be converted to contractile cardiac myocytes by ectopic expression of Gata4, T-box 5 (Tbx5) and the cardiac specific BAF complex subunit Baf60c. Baf60c is necessary for successful reprogramming as it allows Gata4 to bind to cardiac genes (Takeuchi and Bruneau 2009), suggesting that the reprogramming activity of ectopic transcription factors is dependent on chromatin remodelling.

In addition to histone modification and nucleosome remodelling, lineage-specific gene expression in mammals depends on DNA methylation. DNA methylation occurs almost exclusively on cytosine residues in a CG context and covers most of the genome. The 20-30% of CG dinucleotides that are unmethylated are mainly densely clustered in CpG islands near gene promoters (Law and Jacobsen 2010). DNA methylation is patterned during early embryogenesis by the *de novo* methyltransferases Dnmt3a and Dnmtb, but is erased and reestablished in primordial germ cells during postimplantation development (Kaneda *et al.* 2004). Maintenance of DNA methylation requires DNMT1, which is recruited to replication foci by ubiquitin-like containing PHD and RING finger domains 1 (UHRF1). The SRA domain of UHRF1 binds specifically to hemimethylated DNA, allowing DNMT1 to methylate newly replicated CpGs according to the methylation pattern on the mother strand (Bostick *et al.* 2007) (Sharif *et al.* 2007). The mechanism of DNA

demethylation in mammals has not been elucidated, but in zebrafish requires tight coupling of 5-methylcytosine deamination by activation induced deaminase (AID) with T/G mismatch repair mediated by the thymine glycosylase methyl-CpG binding domain protein 4 (MBD4) (Rai *et al.* 2008).

Mikkelsen *et al*. (2008) showed that relief of DNA methylation is required to produce second generation iPS cells from embryonic fibroblasts of iPS cell-derived chimeric mice (*Figure 1.5*). The first generation iPS line carried integrated doxycycline (Dox)-inducible lentiviral vectors encoding POU5F1, Sox2, Klf4 and c-Myc, which were activated in second generation embryonic fibroblasts to produce both iPS cells and partially reprogrammed cells. Stable lines derived from partially reprogrammed cells did not express pluripotency-related genes, and were characterised by DNA hypermethylation at these loci. However complete reprogramming could be induced by treatment with either the DNA methyltransferase inhibitor 5-azacytidine or siRNA against DNMT1 (Mikkelsen *et al.* 2008). Demethylation of DNA is also necessary for nuclear reprogramming in heterokaryons arising from cell fusion of mouse embryonic stem cells and human fibroblasts. Accordingly, si-RNA-mediated knockdown of AID blocks induction of POU5F1 and Nanog in the fibroblast nucleus by preventing promoter demethylation (Bhutani *et al.* 2010). Modulation of the chromatin environment by a combination of histone modification, chromatin remodelling and DNA methylation is therefore a central component of the mechanism that underlies reprogramming.

1.8 Dedifferentiation facilitates reprogramming

The term dedifferentiation describes loss of the cell-type specific characters that define a terminally differentiated cell. The most important aspect of this process is selective repression of gene expression, which in turn results in altered cell morphology and function. Dedifferentiated cells may be more amenable to reprogramming than their differentiated counterparts. Rooman *et al*. (2000) demonstrated that exocrine cells dedifferentiate in culture and spontaneously express proteins characteristic of the pancreatic duct. During five days of suspension culture, 90% pure preparations of amylase-positive rat exocrine acini formed spheroids that

contained 87% amylase negative, cytokeratin 20 (CK20) positive cells. Electron microscopy revealed loss of the zymogen granules and stacked endoplasmic reticulum characteristic of acinar cells and acquisition of several features of duct cells, including a relative abundance of mitochondria, microvilli and intercellular junctions. The cultures did not contain 5′-Bromo-2-deoxyuridine (BrdU)/CK20 double positive cells, implying that the duct-like population was derived from acini, rather than selective outgrowth of contaminating ductal cells (Rooman *et al.* 2000). The acinar-ductal switch could be blocked or reversed by adding nicotinamide, otherwise known as vitamin B3, to the culture medium. In each case, maintenance or reexpression of the acinar phenotype occurred in tight association with repression of the ductal phenotype (Rooman *et al.* 2000). This mutually exclusive behaviour of the acinar and ductal programs suggests that dedifferentiation may be required for the expression of duct genes in acinar cells.

Dedifferentiation also facilitates Pdx1-mediated conversion of hepatocytes to pancreatic beta-cell like cells. Meivar-Levy *et al*. (2007) report that when Pdx1, a master regulator of pancreatic development, was ectopically expressed in cultured human liver cells, it induced expression of pancreatic genes such as endogenous Pdx1 and insulin. Notably, however, Pdx1 also suppressed expression of a range of hepatic markers including albumin, glutamine synthetase, and the transcription factor C/EBPβ. If hepatocytes were co-infected with adenoviruses expressing full-length C/EBPβ (LAP) and Pdx1, the hepatic program was maintained, and Pdx1-mediated activation of pancreatic genes was inhibited. Therefore the dedifferentiation-inducing activity of Pdx1 was required for its ability to induce pancreatic genes (Meivar-Levy *et al.* 2007). *In vivo*, LAP function is opposed by a dominant negative form of C/EBPβ known as LIP. By overexpressing LIP in the absence of Pdx1, the dedifferentiation and transactivation activities of Pdx1 could therefore be uncoupled. LIP activated expression of insulin and Ngn3, and in addition synergised with Pdx1 in inducing endogenous Pdx1, Ngn3 and Islet1. However LIP alone could not induce the complete repertoire of pancreatic genes (Meivar-Levy *et al.* 2007). Dedifferentiation is therefore required for the induction of most pancreatic genes in hepatocytes, but is not sufficient for complete reprogramming.

The gene repression that characterises dedifferentiation is a necessary prerequisite for reprogramming terminally differentiated B cells to pluripotency. Hanna *et al*. (2008) were able to convert pro- and pre-B cells isolated from primary iPS cell-derived chimeras into secondary iPS cells by transgenic expression of POU5F1, Sox2, Klf4 and c-Myc (*Figure 1.5*). In contrast, reprogramming of mature B cells additionally required knockdown of the B cell transcription factor Pax5 (or overexpression of C/EBPα) (Hanna *et al.* 2008). Pax5 activates B-cell specific genes and is required to maintain both the B-lymphoid transcription program and lineage commitment (Mikkola *et al.* 2002). Therefore suppression of the B cell gene expression profile appears to promote acquisition of an alternative cell fate. The role of dedifferentiation in facilitating conversion of B cells to iPS cells is reminiscent of its ability to promote exocrine pancreas and hepatocyte reprogramming, suggesting that dedifferentiation could facilitate cell type interconversions in a range of developmental contexts, and may be adopted as a strategy to improve the efficiency of reprogramming.

1.9 Liver architecture and development

The epithelial component of the liver is composed of hepatocytes and biliary epithelial cells (BECs), which are derived from a common progenitor (Tanimizu and Miyajima 2004) (Suzuki *et al.* 2008) (Strick-Marchand and Weiss 2002). Given the importance of a close developmental relationship in facilitating the interconversion of differentiated cells, the liver epithelium may therefore be a useful model in which to study reprogramming. The architectural subunit of the liver is the liver lobule, which is roughly hexagonal in shape and is composed of cords of hepatocytes separated by sinusoidal capillaries that radiate towards the central vein. Each corner of the lobule is demarcated by a single branch of the portal vein, hepatic artery and bile duct network, known collectively as a portal triad (*Figure 1.7*). Hepatocytes constitute approximately 70% of the liver and are responsible for secretion of plasma proteins and bile, metabolism of glucose/glycogen, cholesterol and urea, and drug detoxification. BECs (cholangiocytes), which make up 3% of the hepatic volume, line the bile ducts that transport bile out of the liver and control bile pH (Si-Tayeb *et*

al. 2010). The non-epithelial compartment of the liver includes endothelial cells (arterial, venous and sinusoidal), Kupffer cells (resident liver macrophages), pit cells (natural killer cells), and stellate cells (Si-Tayeb *et al.* 2010).

Interconversion of differentiated cell types often involves recapitulation of the processes that govern tissue development (Zhou *et al.* 2008). In mouse, the liver is specified from the ventral foregut endoderm at E8.25, when albumin, transthyretin and alpha-fetoprotein (AFP) are first expressed by endodermal cells known as hepatoblasts (Zaret 2008) (*Figure 1.8*). Hepatic differentiation is induced by a combination of fibroblast growth factor (FGF) signalling from the cardiac mesoderm and bone morphogenetic protein (BMP) signalling from the septum transversum mesenchyme (Jung *et al.* 1999) (Rossi *et al.* 2001). Competence of the foregut endoderm to respond to these cues depends on the activity of forkhead box A (FoxA) and GATA4. *In vivo* footprinting of the albumin enhancer in undifferentiated mouse gut endoderm revealed that FoxA and GATA sites are bound prior to activation of gene transcription (Gualdi *et al.* 1996) (Bossard and Zaret 1998). Furthermore, both FoxA and GATA4 can bind the albumin enhancer when it is assembled *in vitro* into Histone 1 (H1)-compacted nucleosome arrays. Although this binding is insufficient to activate transcription, it results in opening of the local chromatin structure, even in the absence of ATP-dependent enzymes (Cirillo *et al.* 2002). FoxA and GATA4 may therefore act as pioneer factors that allow access of other transcription factors to the DNA. Consistent with this hypothesis, conditional deletion of *foxa1* and *foxa2* in the foregut endoderm (Foxa3-Cre; $Foxa1^{-/-}$, $Foxa2^{LoxP/LoxP}$) blocks both AFP induction and liver bud formation (Lee *et al.* 2005).

Following liver specification, a diverticulum lined by hepatoblasts forms from the foregut. The hepatoblasts proliferate to create a liver bud before migrating away from the endoderm epithelium and invading the adjacent septum transversum mesenchyme (Lemaigre 2009). Hepatoblasts are bipotential and differentiate either into hepatocytes or BECs (Tanimizu and Miyajima 2004) (Strick-Marchand and Weiss 2002) (Suzuki *et al.* 2008). Segregation of hepatobiliary lineages requires the activity of C/EBPα, a member of the bZIP family of transcription factors that is expressed in hepatoblasts and hepatocytes but not in biliary cells (Yamasaki *et al.* 2006). In $cebpa^{-/-}$ animals, pseudoglandular structures are formed throughout the

liver parenchyma that coexpress hepatocyte and biliary markers. However in wildtype livers, biliary genes are expressed only in periportal hepatoblasts (Yamasaki *et al.* 2006).

In addition to C/EBPα, lineage segregation requires the ONECUT transcription factors HNF6 and onecut-2 (OC-2), which are highly expressed in biliary cells, but also present in hepatoblasts and hepatocytes (Clotman *et al.* 2005). In *hnf6*/*oc-2*$^{-/-}$ livers, hepatoblasts differentiate into hybrid cells coexpressing hepatocyte and biliary markers, a phenotype similar to that of *cebpa*$^{-/-}$ mutants. Increased activin/transforming growth factor β (TGFβ) signalling is also observed, as indicated by repression of the TGFβ antagonist α2-macroglobulin and the activin antagonist follistatin, and upregulation of TGFβ receptor type II (Clotman *et al.* 2005). Analysis of CAGA12/GFP mice, which harbour an activin/TGFβ responsive green fluorescent protein (GFP) gene, reveals that at E12.5 a gradient of activin/TGFβ signalling exists in the liver, with high activity in the vicinity of the portal vein, where hepatoblasts differentiate into BECs, and lower activity in the parenchyma, where hepatoblasts give rise to hepatocytes. However when CAGA12/GFP animals are crossed with *hnf6/oc-2* double knockouts, high activin/TGFβ signalling extends further away from the portal vein and into the parenchyma. The spatial correlation between high activin/TGFβ signalling and abnormal hepatoblast differentiation suggests that HNF6 and OC-2 inhibit activin/TGFβ signalling in the parenchyma to allow hepatocyte differentiation at the expense of biliary differentiation (Clotman *et al.* 2005).

Gene knockout strategies have identified several transcription factors that are required for terminal hepatocyte differentiation. The nuclear hormone receptor HNF4α controls expression of apolipoproteins, serum proteins (e.g. albumin and transferrin), and enzymes involved in glucose metabolism (e.g. phosphoenolpyruvate carboxykinase, glucose-6-phosphatase and glycogen synthase) (Li *et al.* 2000) (Parviz *et al.* 2003). It also regulates the activity of genes encoding cell adhesion proteins (e.g. E-cadherin) and gap junction proteins (e.g. connexin 32), and is therefore necessary for generation of a hepatic epithelium (Parviz *et al.* 2003). HNF1α is a member of the POU-Homeodomain transcription factor family that activates serum protein genes and contributes to cholesterol, glucose, lipid, amino

acid and xenobiotic metabolism (Shih *et al.* 2001). Similarly, C/EBPα regulates transcription of genes involved in ammonia detoxification, and glucose and lipid homeostasis (Inoue *et al.* 2004).

Segregation of the biliary lineage occurs in association with bile duct tubulogenesis, which proceeds from the hilum towards the periphery of the liver lobes (Antoniou *et al.* 2009). Liver-specific deletion of HNF1β (Alfp-Cre; $hnf1\beta^{fl/fl}$), which is required for biliary morphogenesis, results in a paucity of small intrahepatic bile ducts and dysplasia of larger ducts (Coffinier *et al.* 2002). $Hnf6^{-/-}$ livers display a similar phenotype combined with transient repression of HNF1β, suggesting that HNF6 regulates morphogenesis by activating HNF1β (Clotman *et al.* 2002). However the morphogenetic defects in *hnf6* mutants may be a secondary consequence of disrupted lineage segregation.

1.10 The liver as a model for cell reprogramming

The potential of liver epithelium as a model for cell reprogramming is highlighted by the conversion of hepatocytes to biliary cells. Michalopoulos *et al.* (2005) investigated hepatocyte plasticity *in vivo* using rats with hybrid livers, which contained clones of hepatocytes expressing dipeptidyl peptidase IV (DPPIV). The chimeric animals were generated by injecting DPPIV-positive donor hepatocytes into DPPIV-negative recipients that were previously treated with retrorsine (to inhibit hepatocyte proliferation) and partially hepatectomised. This model relies on the ability of differentiated hepatocytes, which are normally quiescent, to divide rapidly in response to liver injury and thereby restore liver mass. Hepatocyte replication is responsible for liver regeneration after partial hepatectomy (without retrorsine treatment) or necrotic injury caused by carbon tetrachloride (Fausto and Campbell 2003). Where the ability of hepatocytes to undergo mitosis is impaired, for example following administration of D-galactosamine, facultative progenitors are activated that give rise to oval cells. Oval cells are thought to differentiate into both hepatocytes and biliary epithelium, but their apparent multipotentiality has not been demonstrated by lineage tracing (Zaret and Grompe 2008). A second progenitor population consisting of small hepatocyte-like cells is the primary source of new

hepatocytes after partial hepatectomy and retrorsine treatment in the absence of exogenous hepatocytes (Gordon *et al.* 2000). In the chimeric model, activation of both oval cells and small hepatocytes is observed, but exogenous hepatocytes repopulate 40-60% of the liver (Dabeva *et al.* 1998).

Michalopoulos *et al*. subjected rats with DPPIV chimeric livers to bile duct ligation and treatment with the biliary toxin methylene dianiline (DAPM). 30 days after bile duct ligation, periportal ductules bearing the donor hepatocyte marker DPPIV were observed, suggesting that following biliary injury, hepatocytes can differentiate into bile duct cells (Michalopoulos et al. 2005). Prior to bile duct ligation and DAPM treatment, DPPIV-positive duct cells were never observed in hybrid livers. However it remains possible that biliary cells expressing DPPIV were derived from contaminating duct or progenitor cells in the donor population.

Reprogramming has been described not only in rat liver, but also in primary cultures of murine hepatocytes. Weiss *et al*. (2006) isolated hepatocytes from adult mice and allowed them to dedifferentiate in culture, a process which was characterised by increased motility, a plastic morphology, enhanced mitotic activity, loss of polarity and downregulation of the liver marker tyrosine aminotransferase. By 3 days after plating, the dedifferentiated cells had also activated CK19, A6 antigen and α6 integrin, all of which are expressed in mouse bile duct cells. However as these markers are shared by adult liver progenitors, or oval cells, they do not definitively demonstrate biliary differentiation. The origin of the biliary/oval-like cells is likely to be hepatocytic, as CK19 was frequently coexpressed with albumin in binucleate cells (Fougere-Deschatrette *et al.* 2006). Albumin expression is characteristic of both hepatoblasts and hepatocytes, but only the latter are binucleate. Primary hepatocytes may therefore provide an easily accessible and well-characterised model in which to study the molecular mechanisms of cell reprogramming and establish the relative importance of dedifferentiation in this process.

1.11 Aims and objectives

There is some evidence for the conversion of hepatocytes to BECs in both rat liver (Michalopoulos *et al.* 2005) and primary mouse hepatocytes (Fougere-Deschatrette *et al.* 2006). However these studies were limited by a lack of duct-specific markers and the absence of reliable lineage tracing. Furthermore, the molecular regulation of hepatic lineage-switching was not investigated. The aim of the work presented here was therefore to address the technical limitations of previous studies, and dissect the molecular mechanism of hepatocyte to BEC reprogramming. Objectives included the following:

1. Develop an *in vitro* model of hepatocyte to BEC reprogramming.

   In vivo analysis of the mechanism of hepatocyte to BEC reprogramming is hindered by the heterogeneity of liver tissue and the difficulty of manipulating the external signalling environment. Rat hepatocytes were therefore cultured *in vitro*, either under conditions that maintained differentiation (Li *et al.* 2007), or under conditions that promoted dedifferentiation. Evaluation of hepatocyte to BEC reprogramming required analysis of specific hepatocyte and biliary markers. Widely used markers of biliary differentiation, including Ck7, Ck19 and connexin 43 (Cx43) are also expressed in oval cells (Yovchev *et al.* 2007). However it was possible to distinguish biliary and oval cell fate by expression of Sox9 and osteopontin, recently described as novel biliary markers by Antoniou *et al*. (2009).

2. Determine whether dedifferentiation facilitates hepatocyte-BEC reprogramming.

   Dedifferentiation facilitates reprogramming of exocrine pancreas to pancreatic duct (Rooman *et al.* 2000), hepatocytes to β-cells (Meivar-Levy *et al.* 2007) and B-cells to iPS cells (Hanna *et al.* 2008) (see *section 1*.8). The extent to which dedifferentiation is necessary and sufficient for conversion of hepatocytes to BECs was therefore investigated using the culture model developed in (1). Duct genes were expressed in dedifferentiated, but not in

differentiated hepatocytes, consistent with a role for dedifferentiation in promoting reprogramming.

As hepatocytes lose their characteristic epithelial morphology during dedifferentiation, lineage tracing was required to confirm that bile duct genes were activated in hepatocytes rather than a contaminating population. Genetic lineage labelling is not available in rat, but dedifferentiated hepatocytes were identifiable by their expression of the hepatocyte-specific enzyme UDP-galactose transporter (UGT).

3. Identify the intrinsic and extrinsic factors that control reprogramming, including transcription factors, chromatin-level regulators and signalling components.

   Hepatocyte dedifferentiation and activation of ductal markers correlated with repression of C/EBPα and induction of Sox9. However dedifferentiation is a complex process involving up or downregulation of numerous genes. Therefore to demonstrate a causal relationship between changes in C/EBPα and Sox9 expression and reprogramming, adenoviral vectors were employed to overexpress these factors in dedifferentiated and differentiated hepatocytes. C/EBPα and Sox9 were shown to be related by reciprocal inhibition and to promote hepatic and biliary differentiation respectively.

   The epigenetic mechanisms underlying reprogramming were initially investigated at the global level. However as dedifferentiation and duct gene activation involve regulation of specific sets of genes, chromatin immunoprecipitation was established to analyse chromatin structure at individual loci. Characterisation of the extracellular signalling molecules that mediate induction of duct genes was possible only by a candidate approach, as the medium used to promote hepatocyte dedifferentiation is undefined.

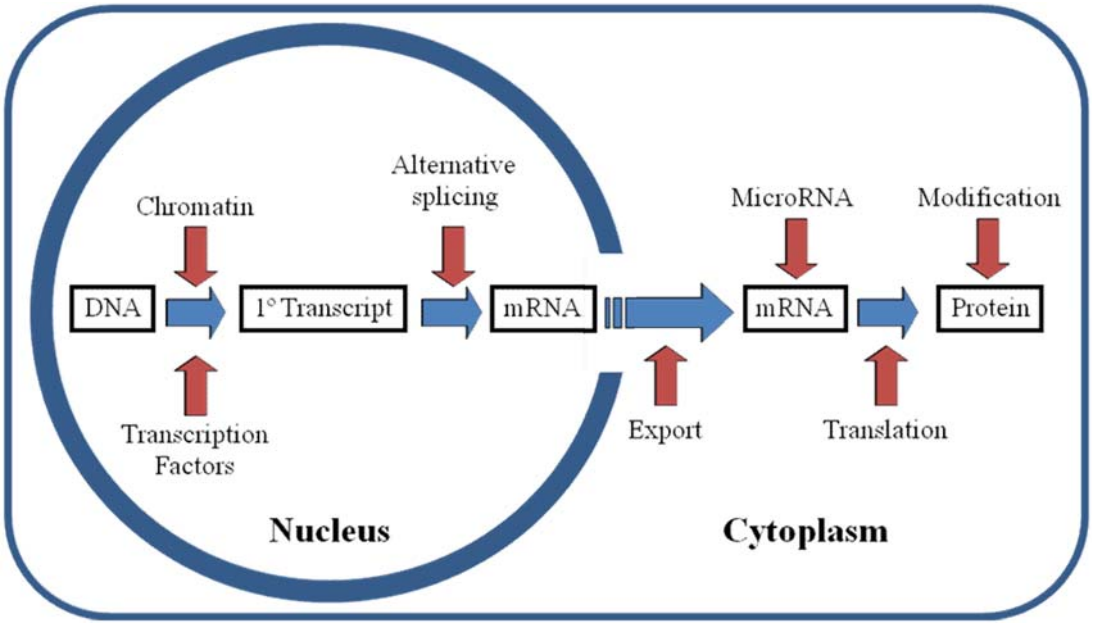

Figure 1.1: Mechanisms of differential gene expression. Specialised cell types arise by differential expression of the same genome. Control of gene expression occurs at numerous different levels including: Gene transcription, RNA processing, translation and post-translational protein modification. Adapted from (Orphanides and Reinberg 2002).

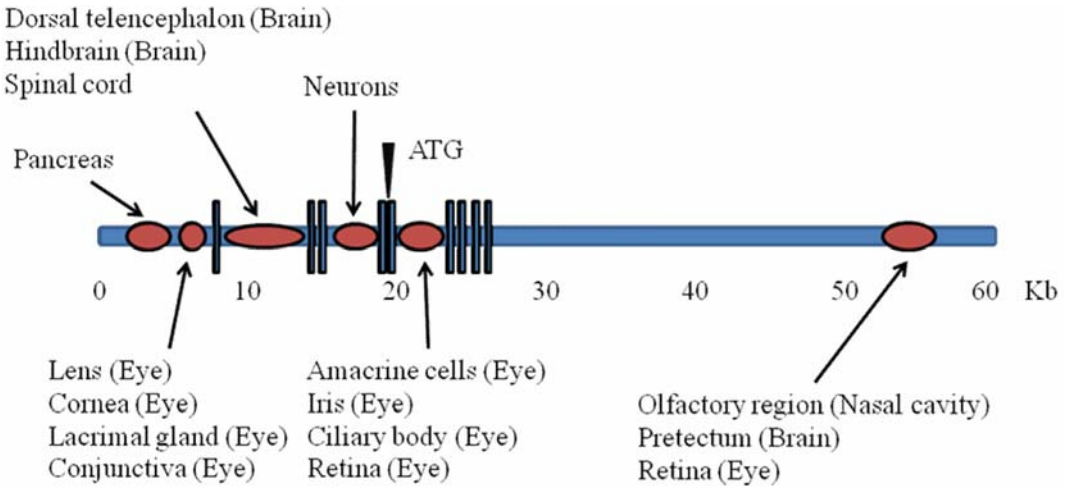

Figure 1.2: Regulation of *Pax6* by enhancers. *Pax6* expression is regulated in space and time by at least 6 upstream and downstream enhancers. Adapted from (Morgan 2004).

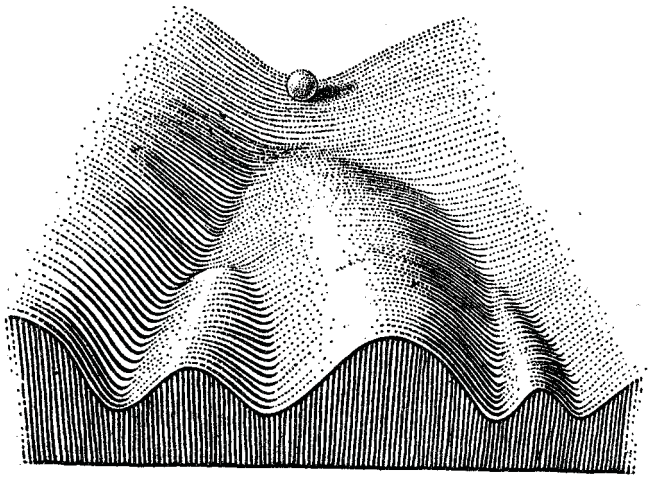

Figure 1.3: The irreversible nature of differentiation. Differentiation can be illustrated as a ball rolling down hill through a series of valleys. Where the valleys bifurcate, the ball travels in one of two possible directions, and is increasingly committed to a single fate. The slope of the landscape makes each decision irreversible (Hochedlinger and Plath 2009). Illustration by (Waddington 1957).

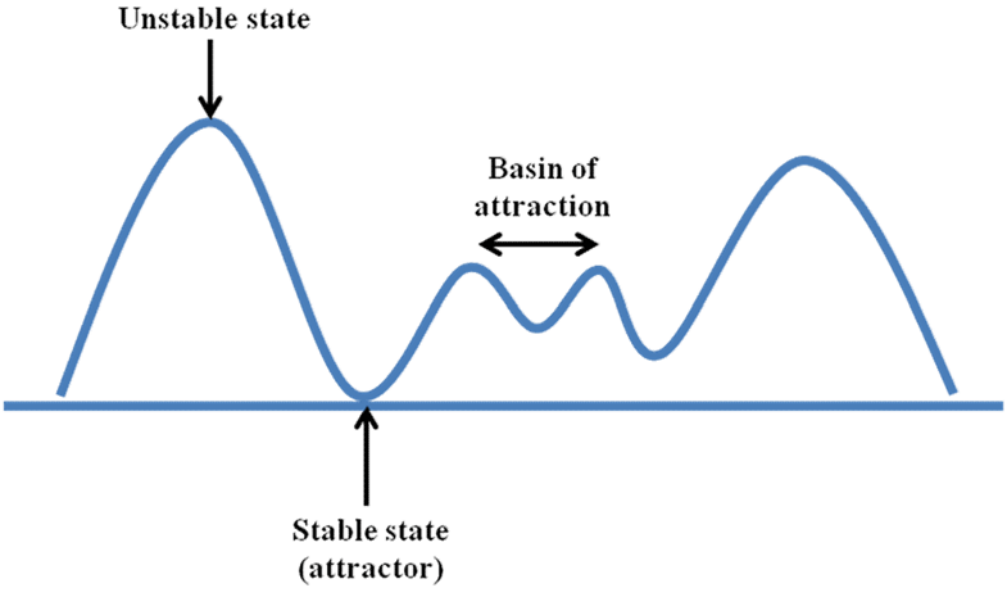

Figure 1.4: An epigenetic landscape. An epigenetic landscape is a quasi potential energy surface embedded in an N-dimensional state space that represents all possible states of a gene regulatory network. Elevation and stability are inversely correlated so that stable states, known as attractors, are depicted at the bottom of valleys, and unstable states are represented as hills. A basin of attraction is the set of initial states that will flow to the same attractor over time. Adapted from (Huang 2009).

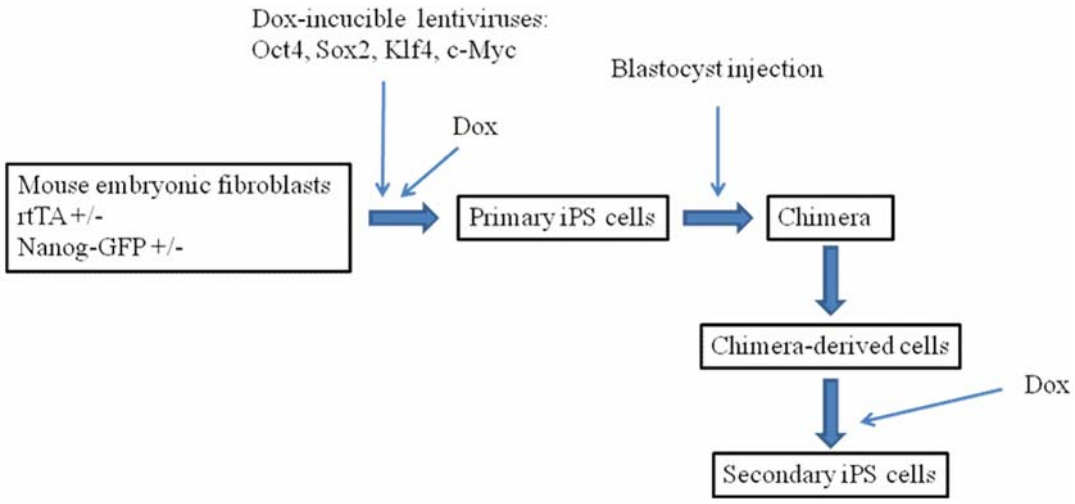

Figure 1.5: Derivation of secondary iPS cells. Clonal populations of cells in primary iPS-derived chimeric mice carry the retroviral insertions that generated primary iPS cells. Reactivation of these retroviruses results in generation of secondary iPS cells. Adapted from (Hanna *et al.* 2008)

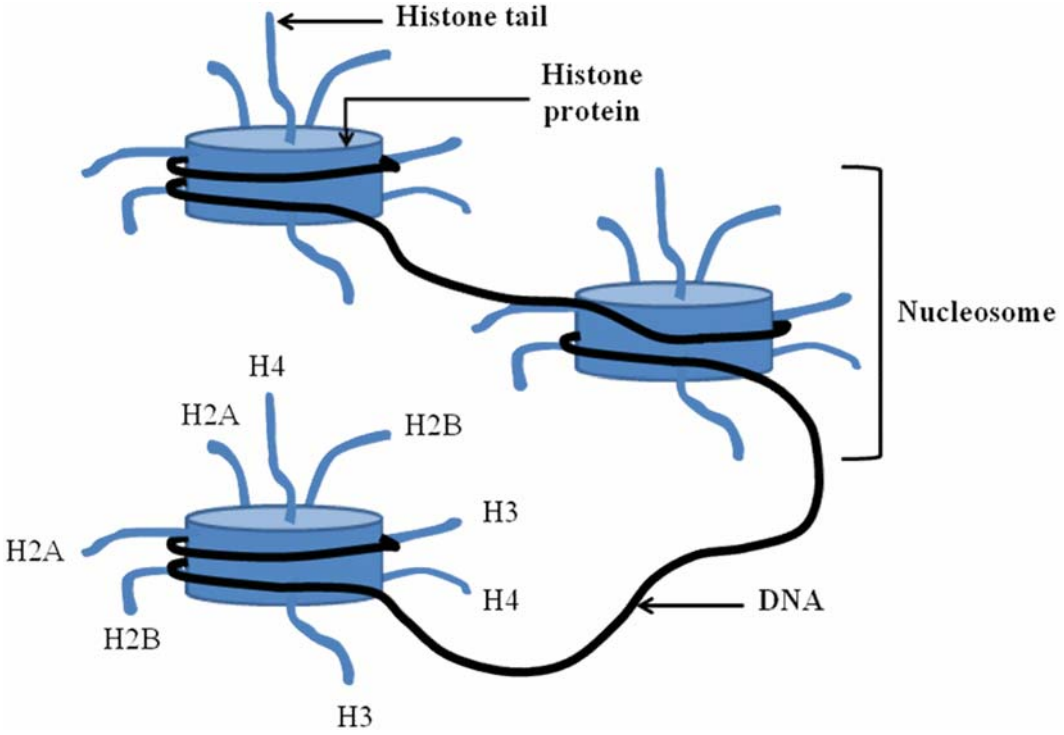

Figure 1.6: Lower order chromatin structure. The fundamental structural unit of chromatin is the nucleosome. A nucleosome consists of an octamer of core histone proteins (two copies of Histone H2A (H2A), H2B, H3 and H4) encircled by 146bp of DNA. Iterated series of nucleosomes resemble "beads on a string", which are in turn compacted several thousand fold into undefined higher order structures. Adapted from (Ruthenburg *et al.* 2007).

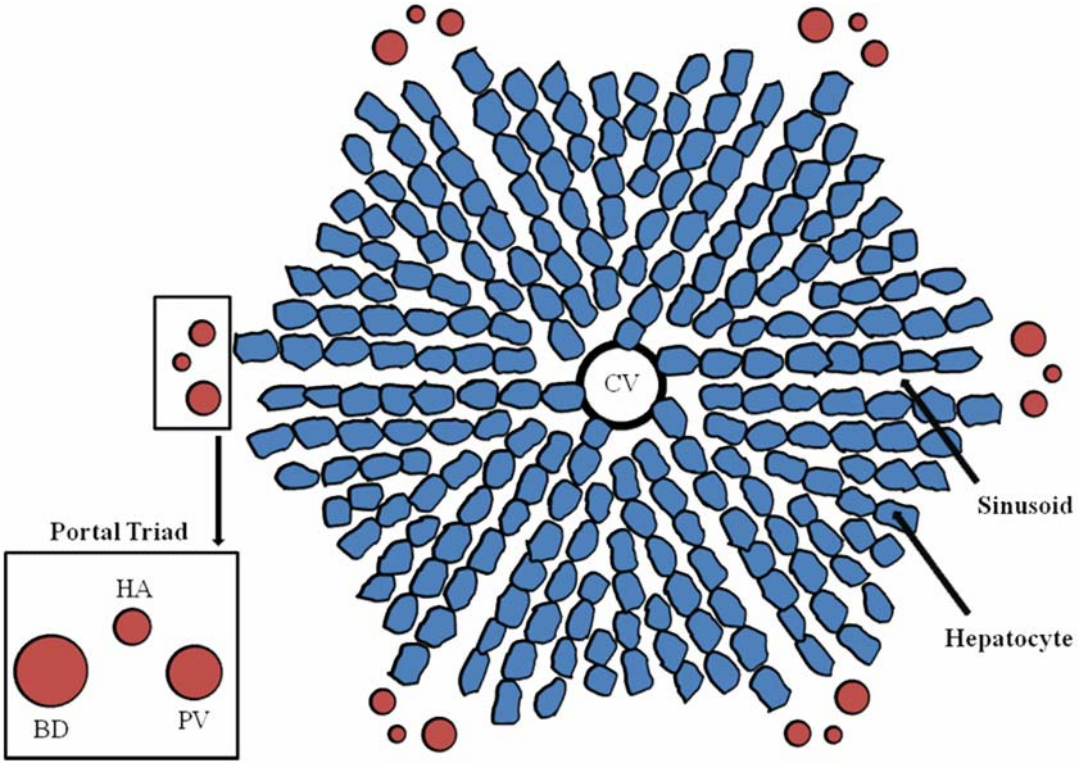

Figure 1.7: A liver lobule. The liver lobule is the architectural subunit of the liver. It is composed of cords of hepatocytes separated by sinusoidal capillaries that radiate towards the central vein (CV). Each corner of the lobule is marked by a portal triad, which consists of a single branch of bile duct (BD) network, hepatic artery (HA) and portal vein (PV). Adapted from (Burke and Tosh 2006)

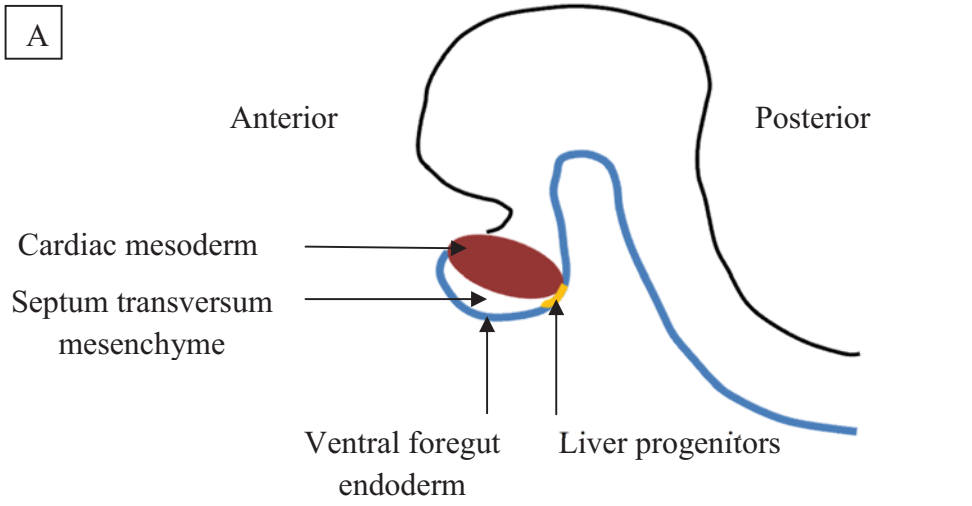
A
Anterior
Posterior
Cardiac mesoderm
Septum transversum mesenchyme
Ventral foregut endoderm
Liver progenitors

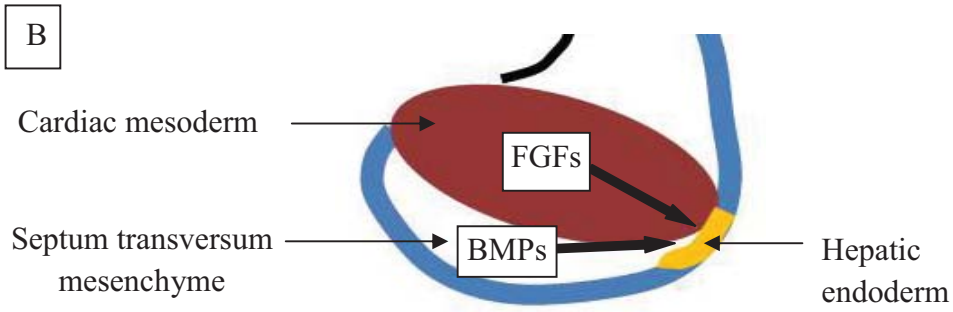
B
Cardiac mesoderm
FGFs
Septum transversum mesenchyme
BMPs
Hepatic endoderm

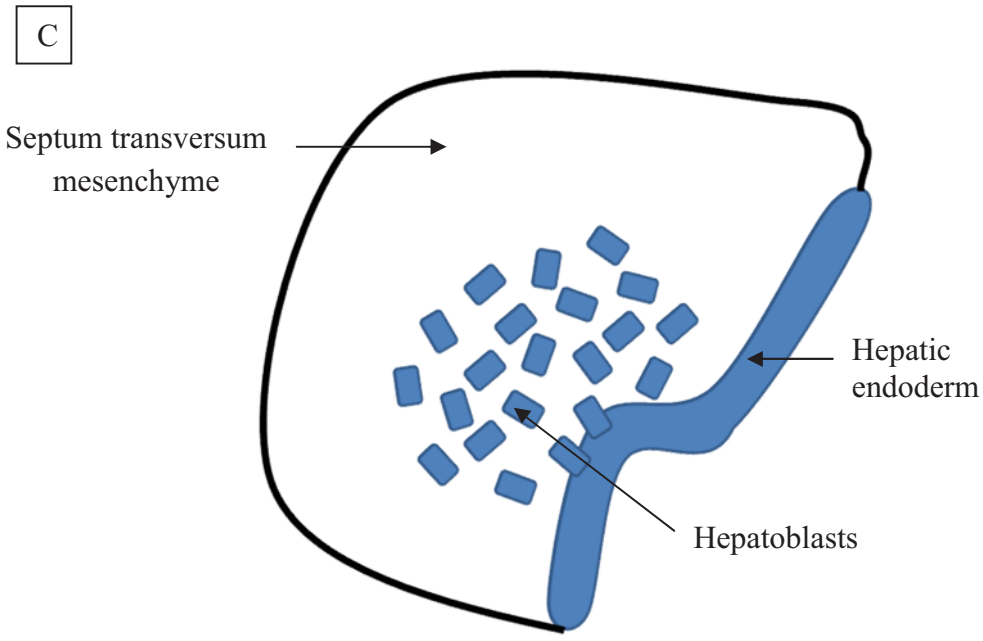
C
Septum transversum mesenchyme
Hepatic endoderm
Hepatoblasts

Figure 1.8: Embryonic development of the liver. A: Lateral view of the anterior portion of a mouse embryo at e8.25. The liver is specified from the ventral foregut endoderm. **B: Liver specification.** Liver specification requires a combination of FGF signalling from the cardiac mesoderm and BMP signalling from the septum transversum mesenchyme (Jung *et al.* 1999) (Rossi *et al.* 2001). **C: Liver bud stage.** Following specification, a diverticulum forms from the foregut. Hepatoblasts proliferate and invade the septum transversum mesenchyme. Figure adapted from (Zaret 2008) and (Zaret 2002).

Chapter 2
Materials and Methods

2A MATERIALS

2A.1 General laboratory chemicals

$CaCl_2$, dithiothreitol (DTT), ethylenediaminetetraacetic acid (EDTA), formaldehyde, D-glucose, glycine, 4-(2-Hydroxyethyl)piperazine-1-ethanesulfonic acid (HEPES), KCl, $MgCl_2$, $NaHCO_3$, phenol/chloroform/isoamyl alcohol, 0.5% phenol red, sodium acetate, sodium deoxycholate, sodium dodecyl sulfate (SDS), Triton X-100, Tween-20 were obtained from Sigma-Aldrich (Gillingham, UK). CsCl, chloroform, ethanol, glycerol, isopropanol, methanol, NaCl, paraformaldehyde (PFA) and Tris Base were supplied by Fisher Scientific (Loughborough, UK). LiCl was from VWR International (Lutterworth, UK). Phosphate buffered saline (PBS) was obtained from Autogen Bioclear (Nottingham, UK). Electrophoresis grade agarose was supplied by Invitrogen (Paisley, UK).

2A.2 Laboratory Equipment

Jencons Spectrafuge 24D (VWR International), Mistral 1000 (MSE, London, UK) and L-80 (Beckman, High Wycombe, UK) centrifuges were used for routine benchtop centrifugation, tissue culture centrifugation, and ultracentrifugation respectively. A Digital Sonifier (Branson, Slough, UK) was required for sonication. DNA and RNA concentrations were measured in UVette® disposable cuvettes (Eppendorf, Cambridge, UK) with an Eppendorf BioPhotometer spectrophotometer. A Spectra Rainbow Thermo microplate spectrophotometer (Tecan, Reading, UK) was used to measure protein concentration. Cells in culture were observed with a DM*IRB* inverted microscope (Leica, Milton Keynes, UK). A DMRB microscope (Leica) was used for all other fluorescence and brightfield microscopy.

2A.3 Cell culture reagents and media

Table 2.1: Stock solutions for cell culture media

Medium component	Stock concentration	Supplier
Gamma irradiated foetal bovine serum (FBS)		Gibco (Invitrogen) 10106
Heat inactivated FBS (for HEK293 medium only)		Sigma F9665
Penicillin,Streptomycin	5000U/ml, 5000U/ml	Lonza (Slough, UK)
Fungizone	250µg/ml	Gibco
Gentamycin	10mg/ml	Gibco
L-glutamine	200mM in 0.85% NaCl	Lonza
Keratinocyte serum-free medium (KSFM) supplements	2.5µg human recombinant EGF and 25mg bovine pituitary extract for use in 500mls medium	Gibco
Dexamethasone	1mM in 100% ethanol	Sigma

Table 2.2: Composition of cell culture media

Cell type	Medium	Composition
Hepatocytes	Attachment	William's Medium E (Sigma W4128), 10% (v/v) FBS, 2mM L-glutamine, 50U/ml penicillin, 50U/ml streptomycin
Hepatocytes	KdS*	KSFM (Gibco 17005), 2mM L-glutamine, 50U/ml penicillin, 50U/ml streptomycin, 1µg/ml fungizone, 50µg/ml gentamycin, 50µg/ml bovine pituitary gland extract, 5ng/ml human recombinant EGF, 10nM dexamethasone
Hepatocytes	DS	Dulbecco's Modified Eagle's Medium (DMEM) (Sigma D5546), 10% (v/v) FBS, 2mM L-glutamine, 50U/ml penicillin, 50U/ml streptomycin, 1µg/ml fungizone, 50µg/ml gentamycin, 50µg/ml bovine pituitary gland extract, 5ng/ml human recombinant EGF
Skin fibroblasts		DMEM (Sigma D5546), 10% (v/v) FBS, 2mM L-glutamine, 50U/ml penicillin, 50U/ml streptomycin, 1µg/ml fungizone, 50µg/ml gentamycin
HEK293s		DMEM with 4.5g/L glucose (Gibco 41966), 10% (v/v) FBS, 50U/ml penicillin, 50U/ml streptomycin, 1µg/ml fungizone

***** KdS medium contains 10nM dexamethasone and is a modified version of KDS medium, described by Li *et al*. (2007), which contains 1µM dexamethasone.

2A.4 Adenoviruses

Table 2.3: Adenoviral vectors

Virus	Construct	Source
Ad-C/EBPα	Ad-CMV-C/EBPα	Vector Biolabs (Philadelphia, USA)
Ad-GFP	Ad-RSV-GFP	Emma Regardsoe, University of Oxford, UK
Ad-LAP	Ad-LAP	Hiroshi Sakaue, Kobe University, Japan
Ad-Sox9	Ad-CMV-Sox9-IRES-eGFP	Shifaan Thowfeequ, University of Bath, UK Plasmid from Neil Hanley, University of Southampton, UK

CMV=cytomegalovirus; RSV= rous sarcoma virus; IRES=internal ribosome entry site; eGFP=enhanced GFP

2A.5 Signalling factors and small molecules

Table 2.4: Stock and working concentrations of signalling factors and small molecules

Compound	Stock concentration	Working concentration	Supplier
ActivinA (recombinant, human)	1µM (1µg/38.5µl)	10ng/ml	Peprotech (London, UK)
Jagged1	100µg/ml	10ng/ml	R&D systems (Abingdon, UK)
DAPT	25mM	25µM	Calbiochem (Merck Chemicals, Nottingham, UK)
Anti-TGFβ	1mg/ml	15µg/ml	R&D systems (AB-100-NA)
5-azacytidine	500µM	10µM	Sigma-Aldrich
TSA	5mM	10µM	Sigma-Aldrich
Sox9 siRNA	100µM	1µM	Dharmacon (Lafayette, USA)

DAPT= N-[N-(3,5-difluorophenacetyl)-l-alanyl]-S-phenylglycine t-butyl ester

2A.6 Immunocytochemistry and immunohistochemistry

Table 2.5: Primary antibodies for immunocytochemistry and immunohistochemistry

Antibody	Raised in	Supplier (Catalogue number)	Dilution
C/EBPα	Rabbit	Santa Cruz (Heidelberg, Germany) (sc-61)	1:50
C/EBPβ	Rabbit	Santa Cruz (sc-150)	1:50
Cps1	Rabbit	Abcam (Cambridge, UK) (ab45956)	1:100
Gck	Rabbit	Santa Cruz (sc-7908)	1:50
PH3	Rabbit	Upstate (Millipore, Watford, UK) (06570)	1:100
Sox9	Rabbit	Chemicon (Millipore, Watford, UK) (AB5535)	1:100 for immunocytochemistry; 1:50 for immunohistochemistry
UGT	Sheep	Cypex (Dundee, Scotland) (CYP601)	1:200
Vimentin	Mouse	Sigma (V6630)	1:100
H3Ac	Rabbit	Upstate (06-599)	1:100
H3K4me2	Rabbit	Abcam (ab7766)	1:100
H3K9me2	Mouse	Abcam (ab1220)	1:100

Table 2.6: Secondary antibodies for immunocytochemistry

Antibody	Conjugate	Raised in	Supplier	Dilution
Anti-mouse IgG	Alexa Fluor® 488	Goat	Invitrogen	1:300
Anti-rabbit IgG	Alexa Fluor® 488	Goat	Invitrogen	1:300
Anti-rabbit IgG	Alexa Fluor® 546	Goat	Invitrogen	1:300
Anti-sheep IgG	Texas Red	Rabbit	Vector Laboratories (Peterborough, UK)	1:200

2A.7 Western blotting

Table 2.7: Primary antibodies for western blotting

Antibody	Raised in	Supplier (Catalogue number)	Dilution
Brg1	Mouse	Santa Cruz (sc-17796)	1:1000
Brm	Goat	Santa Cruz (sc-6450)	1:1000
C/EBPα	Rabbit	Santa Cruz (sc-61)	1:1000
LaminB1	Goat	Santa Cruz (sc-30264)	1:1000
Sox9	Rabbit	Chemicon (AB5535)	1:1000

Table 2.8: Secondary antibodies for western blotting

Antibody	Conjugate	Raised in	Supplier	Dilution
Anti-rabbit IgG	HRP	Goat	Vector Laboratories	1:1000
Anti-goat IgG	HRP	Donkey	Santa Cruz	1:1000
Anti-mouse IgG	HRP	Horse	Vector Laboratories	1:1000

2A.8 Reverse Transcription-Polymerase Chain Reaction (RT-PCR)

Primers were designed using Primer3 software (Rozen and Skaletsky 2000) and synthesised by Eurofins MWG Operon (Ebersberg, Germany)

Table 2.9: Primers for semi-quantitative RT-PCR

Gene	Forward primer (5' to 3')	Reverse primer (5' to 3')	Annealing temp. (◦C)
AFP	AAC AAG TAT GGA TTC TCA GG	ATT GAT GCT CTC TTT GTC TG	56
β-actin	TCC GTA AAG ACC TCT ATG CC	AAA GCC ATG CCA AAT GTC TC	56
Ck19	GAG CTG GAG GTG AAG ATT CG	TCA AAC TTG GTC CGG AAG TC	56
Cps1	CGT CCA AGA TTC CTT GGT GT	ATG GAA GAG AGG CTG GGA TT	56
Cx43	TCT TCA TGC TGG TGG TGT C	TAA CCA GCT TGT ACC CAG G	56
Hes1	CAA CAC GAC ACC GGA CAA ACC	AGT GCG CAC CTC GGT GTT AAC	56

HNF1β	TCA TGG CCA TTG CAC AGA G	CAC CAT TGC AGA TGG GAA CC	56
HNF4	CTC AAC TCA TCC AAC AGC C	AAG CAC TTC TTG AGC CTG C	56
HNF6	GAT CAA TAC CAA AGA GGT GG	TTG GAC GTC TGT GAA GAC C	60
Jagged 1	TCC AGC CTC CAG CCA GTG AA	GGA AGG CTC ACA GGC TAT GT	56
Liv Gck	GAG CCC AGT TGT TGA CTC TG	TTG TCT TCA CGC TCC ACT GC	56
Notch 2	TTT GCT GTC GGA AGA CGA CC	GCC CAT GTT GTC CTG GGC GT	56
Osteopontin	TGA GAC TGG CAG TGG TTT GC	CTG CTT CTG AGA TGG GTC AG	56
Pdx1	TCG CTG GGA ACG CTG GAA C	CTT TGG TGG ATT TCA TCC ACG	56
Sox9	CAA GAC TCT GGG CAA GCT CTG	TCT GCT TGC CCA TTC TTC AC	56
C/EBPα	GCC AAG AAG TCG GTG GAC* AAG AAC	CGG TCA TTG TCA CTG GTC AAC TCC	56
C/EBPβ	ACA AGC TGA GCG ACG AGT AC	ACA GCT GCT CCA CCT TCT TC	56
HNF3β	GTC AGG AGC ACA AGC GAG	TGT GAT GAT GTT GCT GCT CG	56
Ck7	ACT TGC TGG CAC CTC TGA GT	GCT GCT CTT GGC TGA CTT CT	56

*=Single base pair mismatch with rat sequence

Table 2.10: Primers for quantitative polymerase chain reaction (PCR)

Gene	**Forward primer (5' to 3')**	**Reverse primer (5' to 3')**	**Annealing temp. (◦C)**
Sox9	TTG CCA ACC CTG ATG ACT GC	AGT TGT CGC TCC CAC TGA AG	56

2A.9 Sox9 short interfering RNA (siRNA)

Rat Sox9 Accell® SMARTpool® siRNA (Dharmacon, Lafayette, USA) targets the following sequences: CAAGUAGCCCUGGUUUCGU, GGUCCAGGAACUUUUCUUU, GUGGGAGCGACAACUUUAC, GAGCGAGGAAGAUAAAUUC.

2B METHODS

2B.1 Isolation of rat primary hepatocytes

2B.1.1 Animal husbandry

Rats were kept at 25°C, on a 12:12h light-dark cycle and given *ad libitum* access to food and water. Animal procedures were conducted according to UK Home Office regulations.

2B.1.2 Liver perfusion and disassociation

Primary rat hepatocytes were isolated using a two-step collagenase perfusion protocol modified from a method previously described by Tosh *et al*. (1988). Male albino Wistar rats weighing 270-300g were anaesthetised with 4.5% isofluorane (Baxter Healthcare, Newbury, UK) in oxygen, administered at 1500ml/minute. Once the animal was fully anaesthetised, as judged by absence of the pedal reflex, anaesthesia was maintained with 3% isofluorane delivered via a face mask. The rat was placed on a tray with ventral side up and the abdominal fur was disinfected with 70% ethanol. A U-shaped incision was made extending from the lower abdomen to either side of the rib cage. The skin was folded back over the chest, and the intestine laterally displaced to expose the portal vein. To facilitate cannulation of the portal vein, a match stick was inserted underneath, and adipose tissue adhering to the vein was removed using curved forceps. A cotton suture was tied loosely around the vessel and an 18GA cannula (BD Biosciences, Oxford, UK) was inserted distal to the suture. The inner metal stylet of the cannula was removed, allowing blood to flow into the cannula before it was secured by tightening the suture firmly. The abdominal blood vessels (and spinal cord) were cut, providing an outlet for the perfusate during the initial stages of perfusion and causing death of the animal by exsanguination. The cannula was connected to the perfusion pump, which was filled in advance with perfusion buffer 1 [10mM HEPES, 5mM D-glucose, 300μM EDTA, 0.001% phenol red in calcium-free Dulbecco's PBS (Lonza 17-512), pH7.4] prewarmed to 39°C, and set at a flow rate of 25mls/minute. The thoracic cavity was

then opened and the inferior vena cava cut as rapidly as possible. The abdominal vessels were clamped with Spencer-Well's artery forceps, thereby directing the flow of buffer from the portal vein and liver lobes into the thoracic cavity via the vena cava. When the liver had been perfused with 250mls buffer 1, the perfusion pump apparatus was filled with pre-warmed perfusion buffer 2 [30mM HEPES, 5mM D-glucose, 1mM $CaCl_2$, 0.001% phenol red] supplemented with 0.25mg/ml type II collagenase (Worthington Biochemical Corporation, supplied by Lorne Laboratories, Reading, UK; CLS-2). Perfusion was continued for approximately 8 minutes, depending on the activity of the collagenase (Tosh *et al.* 1988).

Following perfusion, the liver was removed from the animal and dissociated in perfusion buffer 2 (without collagenase) using curved forceps. The resulting cell suspension was filtered through a 30μm mesh (Sefar, Bury, UK) to separate partially digested liver and biliary tissue. Dead cells and non-hepatocyte contaminants were removed by three rounds of serial differential centrifugation at 50*g* for 2 minutes. The first centrifugation step was in perfusion buffer 2 and the latter two in attachment medium (*Table 2.2*). To further improve the percentage viability of the final hepatocyte population, cells were sometimes filtered again through a 30μm mesh and spun down at 50*g* for 2 minutes. Finally, the hepatocytes were seeded in attachment medium into Nunc vented plastic tissue culture dishes (Fisher Scientific). The cells were allowed to attach for 5-6 hours at 37°C in 5% (v/v) CO_2, before the medium was changed to KdS or DS (*Table 2.2*).

2B.1.3 Hepatocyte culture

Hepatocytes were cultured at 37°C in 5% (v/v) CO_2. To maintain the cells in a differentiated state, they were cultured in KdS medium. Alternatively, DS medium was used to promote dedifferentiation. The medium was routinely changed every 48 hours.

2B.2 Isolation and culture of rat skin fibroblasts

Rat skin fibroblasts (RSFs) were grown from the dorsal skin of adult rats. Hair and adipose tissue were removed with bent forceps and the remaining material washed in

PBS. The tissue was dissected into 3mm x 3mm pieces and cultured in RSF medium in tissue culture dishes. A glass coverslip was placed on top of the skin to aid attachment. Fibroblasts grew out from the tissue within 7 days, and were split into 75cm^2 tissue culture flasks (Greiner, Stonehouse, UK) after 2 weeks. The cells were passaged as for HEK293 cells (see 2B3.1), except that RSFs were trypsinised for 10 minutes at 37°C. Fibroblasts were passaged a total of three times before use to increase the homogeneity of the cell population.

2B.3 Adenovirus amplification

2B.3.1 HEK293 culture

HEK293 cells were cultured at 37°C in 5% (v/v) CO_2 in a humidified incubator until 70-80% confluent. To passage the cells, they were washed briefly with PBS and trypsinised with 5mls of 0.5% trypsin-EDTA (Invitrogen) for 3 minutes at 37°C. The trypsin was inactivated with an equal volume of HEK293 medium and the cell suspension was centrifuged at 1000rpm for 4 minutes. The resulting supernatant was discarded and the cell pellet resuspended in 1ml HEK293 medium. Cells were then re-seeded at a ratio of 1:10. If longterm storage was required, the cell pellet was instead resuspended in 1ml freezing medium [10% (v/v) dimethylsulfoxide (DMSO) (Sigma) in FBS] and transferred to a cryovial. The cells were frozen slowly in an isopropanol freezing chamber at -80°C overnight and then moved to liquid nitrogen. To revive the cells, they were thawed rapidly in a 37°C waterbath and resuspended in 10mls HEK293 medium. The cell suspension was centrifuged at 1000rpm for 4 minutes, the supernatant discarded and the pellet resuspended in 1ml medium. The cells were then seeded into a 75cm^2 tissue culture flask (Greiner) containing HEK293 medium, which was replaced the following day and every 48 hours thereafter.

2B.3.2 Prestock

Three T75 flasks of HEK293s were grown to 70% confluence, and infected with 10µl, 1µl or 0.1µl of purified virus. One flask was selected for further use, based on the degree of cytopathic effect, which optimally results in 50% cell detachment

within 2-4 days. The cells were harvested by shaking the flask and centrifuging the cell suspension at 1000rpm for 4 minutes. The supernatant was discarded and the cell pellet was resuspended in 1ml HEK293 medium. In order to release the virus, the cells were rapidly freeze-thawed four times, freezing in a dry ice/ absolute ethanol bath and thawing in a 37°C water bath.

2B.3.3 Further amplification

To establish optimal conditions for further amplification of the virus, three Corning T225 flasks (Fisher Scientific, UK) of 70% confluent HEK293s were infected with 125µl, 12.5µl or 2µl of prestock. An ideal volume of prestock results in 50% cell detachment within 2-4 days. Eight T225 flasks of 70% confluent HEK293s were infected with the optimal quantity of prestock and harvested 2-4 days later. Cells were harvested by gently shaking the flask and centrifuging the cell suspension at 2000rpm for 10 minutes. After discarding the supernatant, the pellet was resuspended in 5mls 100mM Tris-HCl, pH8. The cells were lysed by four cycles of rapid freeze-thawing and debris was spun out at 2000rpm for 5 minutes. The supernatant was collected into a 10ml syringe and mixed with 0.6 volumes of CsCl saturated 100mM Tris HCl, pH 8.0. The solution was then divided between two Beckman centrifuge tubes, which were filled to the neck with balance solution [one volume 100mM Tris.HCl:0.6 volumes CsCl saturated Tris.HCl] and heat-sealed. The tubes were centrifuged at 65000rpm for at least four hours at 22ºC in an L-80 ultracentrifuge (Beckman). During centrifugation, the virus accumulates as a horizontal white band approximately half way down the tubes. To extract the bands, each tube was placed vertically in a retort stand and a 25G needle was inserted in the top. The virus was collected into a 2ml syringe through a second 25G needle inserted just below the band. It was then expelled into a new Beckman centrifuge tube, which was filled to the neck with balance solution. The tube was heat-sealed and centrifuged at 65000rpm overnight at 22°C. The resulting virus band was extracted as before in as small a volume as possible and injected into a Pierce Gamma Irradiated Slide-A-Lyzer™ Dialysis Cassette (0.5ml-3ml) (Thermo Fisher Scientific, Cramlington, UK). Air was removed from the cassette, which was then attached to a float and incubated in 1 litre of cold dialysis buffer [10mM Tris.HCl pH 7.5, 1mM $MgCl_2$, 135mM NaCl] for six hours at 4°C, stirring continuously. The buffer was

refreshed and incubation continued overnight. To extract the virus from the cassette, the cassette was pierced with a 25GA needle, and the virus collected into a 2ml syringe through 25GA needle inserted into an opposing corner. The virus was filtered though a 0.22µm filter and aliquoted on wet ice, before being frozen on dry ice. Virus stocks were stored at -80°C.

2B.3.4 Titration

For virus titration, HEK293s were grown in a Nunc 12-well plate (Fisher Scientific) until just confluent. The purified virus was serially diluted in DMEM to make 10^{-2}, 10^{-3}, 10^{-4}, 10^{-5}, 10^{-6} and 10^{-7} dilutions. 100µl of each dilution was added to a separate well of the 12-well plate, the latter 5 dilutions in duplicate. After incubating for 48 hours at 37°C, the medium was aspirated from the plate, which was then air-dried for 5 minutes in a safety cabinet. The cells were fixed with ice-cold methanol for 10 minutes at -20°C and blocked in 2% blocking buffer (Roche, Burgess Hill, UK 11096176001) at 4°C overnight. An Adeno-X™ Rapid Titer Kit (Clontech, Saint-Germain-en-Laye, France) was used to estimate the titre of the virus by immunostaining for the viral hexon protein. Positive cells were detected with a 3,3'-diaminobenzidine (DAB) Peroxidase Substrate Kit (Vector SK-4100), which was used according to the manufacturer's instructions. The titre in infectious units/ml was calculated as: N x (573/0.1) x dilution factor, where N is the mean number of positive cells in ten fields counted under 20X magnification (and 10X eyepiece), 573 is the number of fields per well and 0.1ml is the volume of virus added to each well. Counts were made at the dilution factor that resulted in 5-50 positive cells per field.

2B.3.5 Adenovirus infections

Adenoviral infection of KdS hepatocytes was carried out in KdS medium supplemented with 10% FBS to support cell viability. The cells were incubated with Ad-Sox9 at multiplicity of infection (MOI) of 2 for 1 hour at 37°C, and then rinsed with PBS before being transferred back to unsupplemented KdS medium. Dedifferentiated hepatocytes were infected with Ad-LAP at an MOI of 20 in DS medium for 1 hour at 37°C. Ad-C/EBPα infection of DS cells required an MOI of 200 and overnight incubation at 37°C. In addition, 5µg/ml dextran was added to the medium to improve infection efficiency. Rat skin fibroblasts were infected with Ad-

Sox9 at an MOI of 5 and incubated overnight at 37°C in the presence of 5µg/ml dextran. All virus experiments were controlled with Ad-GFP, with infections conducted under the conditions used for the virus of interest.

2B.4 Immunocytochemistry

Hepatocytes and rat skin fibroblasts grown on coverslips were fixed in 4% (w/v) paraformaldehyde, pH7.4 for 20 minutes at room temperature, ice cold methanol for 10 minutes at -20°C (For Cps1 immunostaining) or ice cold 1:1 acetone:methanol for 10 minutes at -20°C (For vimentin immunostaining). The cells were permeabilised in 0.1% (v/v) Triton X-100 in PBS for 20 minutes at room temperature and then blocked in 2% (w/v) blocking buffer (Roche) for 1-2 hours. Primary antibodies were diluted in 2% blocking buffer, and incubated on the coverslips overnight at 4°C. After 3 x 15 minute washes in PBS, the samples were incubated with fluorochrome-conjugated secondary antibodies diluted in 2% blocking buffer for 2 hours in the dark at room temperature. Cells were kept in the dark for the remainder of the experiment. Excess antibody was removed by 3 x 15 minute washes in PBS and the nuclei were stained by incubation in 500ng/ml 4,6-diamidino-2-phenylindole dihydrochloride (DAPI) (Sigma) for 10 minutes at room temperature. Coverslips were rinsed briefly three times in PBS and mounted on Fisherbrand microscope slides with Gel Mount™ mounting medium (Sigma).

2B.5 Immunohistochemistry

Adult rat liver was fixed in 4% (w/v) PFA overnight at 4°C and processed sequentially through the following: PBS, NaCl, 50% ethanol, 70% ethanol, 90% ethanol, 100% ethanol, 100% ethanol, Histoclear, Histoclear, wax, wax and wax for one hour each in a Leica TP 1020 tissue processor. The tissue was embedded in paraffin wax at a Leica EG 1160 embedding station and sectioned using a Leica RM 2155 microtome into 4µm ribbons that were mounted on Fisherbrand microscope slides.

For immunostaining, sections were dewaxed and rehydrated by sequential incubation in Histoclear (I) and Histoclear (II) (Fisher Scientific) for 7 minutes each, then 100%, 100%, 95%, 90%, 70% and 50% ethanol for 1 minute each. The tissue was permeabilised in 0.5% (v/v) Triton X-100 in PBS for 30 minutes at room temperature. For antigen retrieval, sections were incubated in 1X EDTA heat-induced epitope retrieval buffer (Fisher Scientific) in distilled water for 30 minutes at 90°C and then cooled to room temperature. Endogenous peroxidases were quenched using Dako EnVision peroxidise block (Dako EnVision+ System-HRP (DAB) K4011; Dako, Ely, UK) according to the manufacturer's instructions. The sections were blocked in 2% blocking buffer (Roche) for 1 hour at room temperature and then incubated with anti-Sox9 antibody diluted in 2% blocking buffer overnight at 4°C. Following 3 x 10 minute washes in PBS, the specimens were covered in a peroxidase labelled secondary antibody (Dako EnVision) for 30 minutes at room temperature. Positive tissue was visualised by incubation in a DAB substrate-chromogen solution (Dako EnVision). The sections were counterstained with 0.2% Light Green in 95% ethanol for 45 seconds and then dehydrated by sequential incubation in two baths of 100% ethanol for 1 minute each, and Histoclear (I) and Histoclear (II) for 2 minutes each. Slides were mounted in DPX.

2B.6 Western blotting

2B.6.1 Nuclear Extraction

Two 10cm dishes of primary rat hepatocytes were scraped on ice in 1ml ice cold cytosolic extraction buffer [20mM HEPES, 10mM KCl, 1mM EDTA, 10% glycerol, pH7.9 plus protease inhibitor cocktail (4-(2-aminoethyl)benzenesulfonyl fluoride (AEBSF), pepstatinA, E-64, bestatin, leupeptin, and aprotinin, Sigma P8340)]. To ensure efficient disruption of plasma membranes, the lysate was incubated for 30 minutes at 4°C on a rotator and then pulled 10 times through a 27G needle. Nuclei were collected by centrifugation at 16300*g* at 4°C for 5 minutes, and washed three times by repeated resuspension in 500µl cytosolic extraction buffer and centrifugation. The final pellet was resuspended in 200µl ice cold nuclear extraction buffer [20mM HEPES, 10mM KCl, 400mM NaCl, 1mM EDTA, 20% glycerol

pH7.9 plus protease inhibitor cocktail] and incubated for 1 hour at 4°C on a rotator to lyse the nuclei. Samples were then centrifuged at 16300*g* for 15 minutes at 4°C, and the supernatant retained as the nuclear fraction.

2B.6.2 Protein quantification

The protein concentration of nuclear extracts was determined using the Bio-Rad protein assay (Bio-Rad, Hemel Hempstead, UK), which is based on Bradford assay chemistry. Diluted samples or bovine serum albumin (Sigma) standards were mixed with 5X Bio-Rad reagent and incubated at room temperature for 5 minutes. The final concentrations of the standards were 0, 2, 5, 10 and 20µg/µl. Each sample and standard was aliquoted in triplicate into a 96-well plate, and the absorbance read at 595nm on a microplate spectrophotometer (Tecan).

2B.6.3 Electrophoresis, blotting and detection

Normalised protein samples were mixed with an equal volume of 2X sample buffer [125mM Tris-HCl, pH6.8, 4% SDS, 20% glycerol, 0.2M DTT, 0.02% bromophenol blue] and denatured at 100°C for 5 minutes. 10µg of sample was loaded onto a 5% or 10% Tris-HCl Criterion™ Precast Gel (BioRad) alongside a Precision Plus Dual-Colour standard (Biorad) and subjected to electrophoresis at 100V in running buffer [25mM Tris, 192mM glycine, 0.1% SDS]. The protein was wet transferred onto a Immun-Blot™ polyvinylidene fluoride (PVDF) 0.2µm membrane (Bio-Rad) for 2 hours at 200mA in transfer buffer [25mM Tris, 192mM glycine, 20% methanol]. Blots were stained with Ponceau S [0.6% (w/v) Ponceau S (Sigma), 2.8% acetic acid] to visualise the protein and then blocked in 5% (w/v) skimmed milk (Marvel) in PBS-T [0.1% Tween-20 in PBS] overnight at 4°C. The membranes were exposed to primary antibody diluted in 3% milk in PBS-T for 2 hours at room temperature. After 3 x 15 minute washes in PBS-T, blots were incubated with a horse radish peroxidase (HRP)-conjugated secondary antibody diluted in 3% milk in PBS-T for 1 hour at room temperature. The membranes were then washed in PBS-T for 3 x 15 minutes and covered in ECL detection reagent (GE Healthcare, Chalfont St Giles, UK) for 5 minutes at room temperature. Bound secondary antibody was detected by ECL chemiluminescence (GE Healthcare), which was visualised by autoradiography on MIDSCI Classic Blue Autoradiography film BX (Cole-Parmer, London, UK).

2B.7 RT-PCR

2B.7.1 RNA extraction and DNase I treatment

Total RNA was extracted using TRI REAGENT™ (Sigma) according to the manufacturer's instructions. The final pellets were dissolved in diethylpyrocarbonate (DEPC)-treated water [0.0001% (v/v) DEPC (Sigma)] and the concentration of each sample determined using a spectrophotometer (Eppendorf). To remove genomic DNA contamination, 5µg of RNA was treated with 0.2U/µl of Ambion RNase-free DNase I (Applied Biosytems, Warrington, UK) for 30 minutes at 37˚C. The DNase was inactivated by a further incubation at 65˚C for 10 minutes.

2B.7.2 Reverse transcription

The concentration of DNase I-treated RNA was measured by spectrophotometry. 2µg was incubated with 1µl of 500µg/ml Oligo$(dT)_{12\text{-}18}$ primer (Invitrogen) and 1µl of 10mM dNTP mix (Invitrogen) in a total volume of 12µl for 5 minutes at 65˚C. Complementary DNA was synthesised by adding 4µl of 5X First-Stand buffer, 2µl of 0.1M DTT and 1µl of 200U/µl Superscript™ II Reverse Transcriptase (all Invitrogen), and incubating the reaction for 52 minutes at 42˚C. The enzyme was inactivated by heating to 70˚C for 15 minutes.

2B.7.3 Semi-quantitative Polymerase Chain Reaction

Approximately 100ng of cDNA was mixed with primers and 2X ReddyMix™ PCR Master Mix (1.5mM $MgCl_2$) with KCl buffer (Fisher Scientific) to give the following final concentrations: 500nM forward primer, 500nM reverse primer and 1X master mix. Amplification was conducted in a thermal cycler under the following conditions: Initial denaturation 94˚C for 5 minutes; PCR (22-30 cycles) denaturation 94˚C for 60 seconds, annealing 56˚C (or 60˚C for *Hnf6*) for 60 seconds, elongation 72˚C for 60 seconds; Final extension 72˚C for 5 minutes. PCR products were run on a 2% agarose gel.

2B.8 Chromatin Immunoprecipitation (ChIP) and Real-time PCR

2B.8.1 Chromatin immunoprecipitation

The ChIP protocol was based on that described by Chakrabarti *et al*. (2002). Three 10cm plates of primary rat hepatocytes were cross-linked with 0.2% (v/v) formaldehyde in culture medium for 10 minutes at room temperature. To stop the fixation, glycine was added to a final concentration of 0.125M and the plates incubated at room temperature for a further 5 minutes. Cells were washed twice in PBS and suspended in 0.6ml lysis buffer [50mM Tris-HCl, pH8.1, 1% Triton X-100, 0.1% deoxycholate, 150mM NaCl, 5mM EDTA plus protease inhibitor cocktail (Sigma P8340)]. The chromatin was sheared to an average size of 500bp by 10 x 5 second pulses of sonication on ice using a Beckford Sonifier with microtip at an amplitude of 60%. Cell debris was removed by centrifugation at 13300rpm for 20 minutes at 4˚C. To check the effectiveness of shearing, 100µl of the supernatant was incubated at 65˚C to reverse the cross-links. RNA was degraded by adding 200µg/ml RNaseA (Sigma) and incubating at 37˚C for 30 minutes. Protein was then digested as described below and 30µl of the test sample was run on a 1% agarose gel with DNA molecular weight standards. The size range of the fragments was visualised with ethidium bromide staining. 50µl of the test sample was used to establish the DNA concentration by adding 450µl of ChIP lysis buffer and conducting phenol-chloroform extraction and ethanol precipitation as described below. For immunoprecipitation, 25µg of sheared chromatin was diluted to 1ml in ice cold lysis buffer containing protease inhibitors. The sample was incubated with 40µl of protein A-agarose beads (Santa Cruz) for 3 hours at 4˚C, then centifuged at 5000rpm for 5 minutes to remove protein bound non-specifically to the beads. 5µg of antibody or normal serum (Sigma) was added to the supernatant and incubated overnight at 4˚C. Immuno complexes were collected with 40µl protein A-agarose beads, which were incubated with the sample for 3 hours at 4˚C in the presence of 20µg/ml herring sperm DNA (Sigma), and then pelleted by centrifugation at 5000rpm for 5 minutes. The beads were washed consecutively with 1ml lysis buffer, lysis buffer plus 500mM NaCl, lysis buffer plus 0.25M LiCl and Tris/EDTA [10mM Tris, 1mM EDTA]. To elute DNA and protein, the beads were incubated in 250µl elution buffer [0.1M $NaHCO_3$ with 1% SDS and 20µg/ml herring sperm DNA] for 20 minutes at

room temperature and then centrifuged at 5000rpm for 5 minutes. The elution step was repeated and the two supernatants pooled. Formaldehyde cross-linking was reversed by incubation at 65°C for 4 hours before protein cleavage by 40µg/ml proteinase K (Sigma) at 42°C for 1 hour. DNA was extracted by addition of an equal volume of phenol/chloroform/isoamyl alcohol, centrifugation at 13300rpm for 5 minutes and removal of the upper aqueous phase to a new tube. The extraction was repeated and DNA was precipitated by addition of 1/10 volume 3M sodium acetate pH5.2 and 2.5 volumes 100% ethanol, and incubation overnight at -20°C. The sample was centrifuged at 13300rpm for 20 minutes at 4°C to pellet the DNA, which was then washed in 1ml 70% ethanol. After re-centrifugation at 13300rpm for 20 minutes at 4°C, the supernatant was decanted and the pellet air-dried at room temperature. The DNA pellets were finally dissolved in 100µl Tris/EDTA pH8 (Chakrabarti *et al.* 2002).

2B.8.2 Quantitative Polymerase Chain Reaction

ChIP experiments were quantified by SYBR Green real-time PCR. 1µl of sample was combined with primers and 2X Takara SYBR® *Premix Ex Taq*™ (Lonza, Wokingham, UK) to give final concentrations of 0.2µM forward primer, 0.2µM reverse primer and 1X master mix. The reaction mixture was transferred to LightCycler® capillaries (Roche) and briefly centrifuged. A LightCycler® 1.5 (Roche) was used to perform Shuttle PCR under the following conditions: Initial denaturation 95°C 10 seconds 20°C/second; PCR (40 cycles) denaturation 95°C 5 seconds 20°C/second, annealing/extension 60°C 20 seconds 20°C/second. All samples were analysed in duplicate, and the experiment repeated in triplicate. Following amplification, melting curve analysis was conducted using the following parameters: 95°C 0 seconds 20°C/second, 65°C 15 seconds 20°C/second, 95°C 0 seconds 0.1°C/second.

2B.8.3 Data analysis

The relative amount of Sox9 promoter in the immunoprecipitate was calculated using the ΔC_T method. Mean threshold cycle ($\bar{C}_T$) numbers were derived from C_T values supplied by the LightCycler® 1.5 (Roche) software. $\bar{C}_T$ values for 2% input

samples were adjusted to reflect sample dilution by subtracting $\log_2 50$. The $\bar{C}_T$ value for immunoprecipitated samples ($\bar{C}_T$(*Output*)) was then normalised against the $\bar{C}_T$ value for the appropriate input sample ($\bar{C}_T$(*Input*)) by subtracting $\bar{C}_T$(*Output*) from $\bar{C}_T$(*Input*). Fold differences were calculated as $2^{(\bar{C}_T(Input)-\bar{C}_T(Output))}$. To express these values as % input, they were multiplied by 100. Data analysis assumed that amplification was 100% efficient, that is exponential with base 2. A negligible amount of Sox9 promoter was amplified from serum control immunoprecipitates.

2B.9 Sox9 siRNA

To knockdown Sox9 in dedifferentiated hepatocytes, the cells were treated with Accell® SMARTpool® siRNA (Dharmacon) targeted against rat Sox9, a mixture of 4 siRNAs that can be delivered in the absence of transfection reagent. DS hepatocytes were transferred to Accell® siRNA delivery medium (Dharmacon) containing 1μM siRNA on day 1. On day 4, the cells were either harvested, or returned to DS medium (without siRNA) and harvested on day 6 or day 8.

2B.10 Nuclear Area

The nuclear area of KdS and DS hepatocytes was calculated using DAPI staining in conjuction with ImageJ software (http://rsbweb.nih.gov/ij/).

2B.11 Images

Images of cells in culture were collected on a DM*IRB* microscope (Leica) with a SPOT™ digital camera. A DMRB microscope (Leica) and Nikon digital camera were used to collect all other fluorescent and brightfield images. Figures were assembled in Photoshop 7.0.1.

Chapter 3
Characterisation of differentiated and dedifferentiated hepatocytes

3.1 BACKGROUND

Primary rat hepatocytes cultured *in vitro* are a useful model for studies of xenobiotic metabolism, liver disease and regeneration. However the duration of these experiments has been limited by the fact that isolated hepatocytes progressively lose their characteristic gene expression pattern, function, and morphology. This process, termed dedifferentiation, reflects reduced expression of liver-enriched transcription factors, which in turn is a result of disrupted cell-cell and cell-matrix interactions (Elaut *et al.* 2006). Li *et al*. (2007) described a KSFM-based medium, KDS, that maintains the differentiation state of hepatocytes during long-term culture. Cells grown in KDS continue to express liver transcription factors, serum proteins and enzymes involved in ammonia detoxification and phase I and II metabolism. Hepatic functions such as ureagenesis, glycogen synthesis and xenobiotic metabolism are also preserved (Li *et al.* 2007).

The use of KDS medium allows differentiated and dedifferentiated hepatocytes to be directly compared, providing an opportunity to investigate the effect of dedifferentiation on the efficiency of hepatocyte to ductal reprogramming. In the analyses that follow, primary hepatocytes were cultured in a differentiated or dedifferentiated state, and the expression of hepatic and ductal genes was investigated at the messenger RNA (mRNA) and protein levels. The relationship between dedifferentiated hepatocytes and hepatoblasts was also considered, both in terms of gene expression and proliferation.

3.2 RESULTS

3.2.1 Isolation and culture of primary rat hepatocytes

Primary rat hepatocytes were isolated by two-step collagenase perfusion. Viable cells, which can be identified by their refractile appearance and well-defined nuclei, comprised approximately 80% of the population. Freshly isolated hepatocytes were depolarised due to disruption of cell-cell and cell-matrix interactions, and were therefore spherical in shape (*Figure 3.1*). On occasion, they also exhibited reversible cell-surface blebbing. However following 5-6 hours in attachment medium, the cells attached to the substratum and started to flatten out, gradually acquiring a characteristic cuboidal morphology. Bile canaliculi, a feature of well-differentiated and repolarised hepatocytes, appeared at the apical poles of adjacent cells within 12 hours.

After 12 hours in attachment medium, hepatocytes were cultured until day 5 in either KdS medium or DS medium. Cells in KdS medium maintained their epithelial characteristics throughout the culture period, but DS medium promoted progressive acquisition of an elongated, fibroblast-like morphology (*Figure 3.1*). Consistent with these observations, immunostaining on day 5 of culture showed that DS cells, but not KdS cells, induced expression of the intermediate filament protein vimentin, a mesenchymal marker (*Figure 3.2*).

3.2.2 KdS medium maintains the hepatocyte phenotype

24 hours after isolation, hepatocytes cultured in KdS medium expressed an array of hepatic genes that together define the phenotype of terminally differentiated cells. Transcripts encoding carbamoyl phosphate synthetase 1 (Cps1), a urea cycle enzyme, and the liver-specific isoform of glucokinase (Gck), a glucose metabolising enzyme, were both readily detectable by RT-PCR. *Cebpα* and *cebpβ*, which encode liver-enriched transcription factors, were also transcribed. The expression level of all

four markers was maintained after culture in KdS medium for at least five days, and was comparable to that in freshly isolated cells (*Figure 3.3*). Immunostaining showed that at the 24 hour timepoint Cps1, Gck, C/EBPα and C/EBPβ were highly expressed at the protein level as well as the mRNA level. There was some reduction in the quantity of each protein over a five day culture period, but the hepatocyte phenotype was broadly sustained (*Figures 3.5* and *3.6*).

3.2.3 DS medium promotes dedifferentiation

Hepatocytes cultured in DS medium inactivated *cps1* and *gck*, and downregulated *cebpα* after only 24 hours (*Figure 3.3*). By the five day time-point, expression of Cps1 and Gck also appeared to be substantially reduced at the protein level (*Figure 3.5*). However the weak signals observed by immunostaining for Gck may in part reflect the fact that the nuclei of dedifferentiated cells were larger than those of differentiated cells. Downregulation of C/EBPα protein was observed by immunostaining (*Figure 3.6*), but was much more marked in data obtained by western blotting (*Figure 3.8*). This discrepancy may be due to antibody cross-reaction.

Although *cebpα* is rapidly downregulated in DS medium, RT-PCR analysis shows that *cebpβ*, *hnf1β*, *foxa2*, *hnf4α* and *hnf6* transcripts are as abundant after five days of dedifferentiation as they are in freshly isolated cells (*Figure 3.4*). Immunostaining for C/EBPβ, in contrast, suggests that there is some downregulation of the protein (*Figure 3.6*). Together, these results show that while KdS medium maintains hepatocytes in a differentiated state, DS medium promotes inactivation of a subset of hepatic genes, a process referred to as dedifferentiation.

3.2.4 Dedifferentiated hepatocytes induce expression of duct genes

Dedifferentiated hepatocytes not only downregulated hepatic genes, but also induced ductal genes. Indeed *sox9*, which encodes a transcription factor that regulates duct development, was rapidly induced within 24 hours of DS culture, and progressively

upregulated thereafter (*Figure 3.7*). Sox9 protein was not detectable by western blotting until day 3 but was abundant on day 5 (*Figure 3.8*), when it was also evident by immunostaining (*Figure 3.9*). Low level mRNA and protein expression was sometimes found in KdS-cultured cells on day 5, perhaps indicating incipient dedifferentiation, but was never present on day one. Like Sox9, the early duct gene *osteopontin* was expressed in DS cells after one day of dedifferentiation, followed on day 3 by expression of the intermediate filament gene *ck7*. *Ck19* mRNA was also detectable in DS cells from day 3, although small amounts were sometimes amplified from day 5 KdS cells. Finally, *cx43*, which encodes a gap junction protein, was expressed in differentiated hepatocytes, but was further upregulated during dedifferentiation (*Figure 3.7*).

3.2.5 Duct-like cells are derived from differentiated hepatocytes

The adult liver is composed of hepatocytes, biliary epithelial cells, endothelial cells, stellate cells and Kupffer cells. Non-hepatocyte cell types should be eliminated by differential centrifugation during the hepatocyte isolation procedure. However the induction of duct genes in DS cultures could have occurred in a non-hepatocyte population, or simply have reflected proliferation of contaminating duct cells. In order to distinguish these possibilities, the hepatocyte lineage was traced by immunostaining for the hepatocyte-specific enzyme UGT, which was still immunodetectable after five days of dedifferentiation. UGT and Sox9 were extensively coexpressed in DS cells, demonstrating that duct genes were induced in dedifferentiated hepatocytes. Furthermore, some cells that coexpressed UGT and Sox9 were also binucleate, a characteristic of hepatocytes (*Figure 3.10*).

3.2.6 Hepatocyte reprogramming does not occur via a hepatoblast intermediate

Both hepatocytes and intrahepatic duct cells are derived from bipotential hepatoblasts (Tanimizu and Miyajima 2004) (Suzuki *et al.* 2008) (Strick-Marchand and Weiss 2002). Reprogramming of hepatocytes to duct-like cells could therefore involve three phases: Downregulation of liver genes, regression to a hepatoblast-like

intermediate, and activation of the duct gene expression profile. However RT-PCR analysis showed that *afp*, which is expressed specifically in hepatoblasts, was not transcribed in DS cells (*Figure 3.11*). Furthermore, as discussed above, Sox9 was induced in cells that coexpressed the hepatocyte marker UGT. Dedifferentiated hepatocytes therefore remained distinct from hepatoblasts, although they could reexpress hepatocyte genes (see chapter 4, *Figure 4.7*), activate ductal genes (*Figure 3.7*) and reenter the cell cycle (*Figure 3.12*). This suggests that loss of liver gene expression alone was sufficient to allow expression of duct genes in dedifferentiated hepatocytes.

3.2.7 Dedifferentiated hepatocytes reenter the cell cycle

In vivo, hepatocytes are quiescent, and immunostaining for the mitosis marker phospho-histone H3 (PH3) showed that isolated cells cultured in KdS medium remained arrested. In contrast, at least some dedifferentiated hepatocytes reentered the cell cycle (*Figure 3.12*).

3.2.8 Dedifferentiated hepatocytes do not express pancreatic genes

Expression of duct genes in dedifferentiated hepatocytes could represent specific activation of the ductal program, or more general transcriptional promiscuity. Intrahepatic biliary epithelial cells and hepatocytes are more closely developmentally related to each other than is either to the pancreas. Therefore RT-PCR analysis of *pdx1*, a master regulator of pancreas development, was used to test for a broader lineage-inappropriate transcription of endodermal genes. Pdx1 was not expressed in dedifferentiating hepatocytes (as determined at 30 cycles of PCR), implying that transcriptional activation may be restricted to ductal genes (*Figure 3.13*).

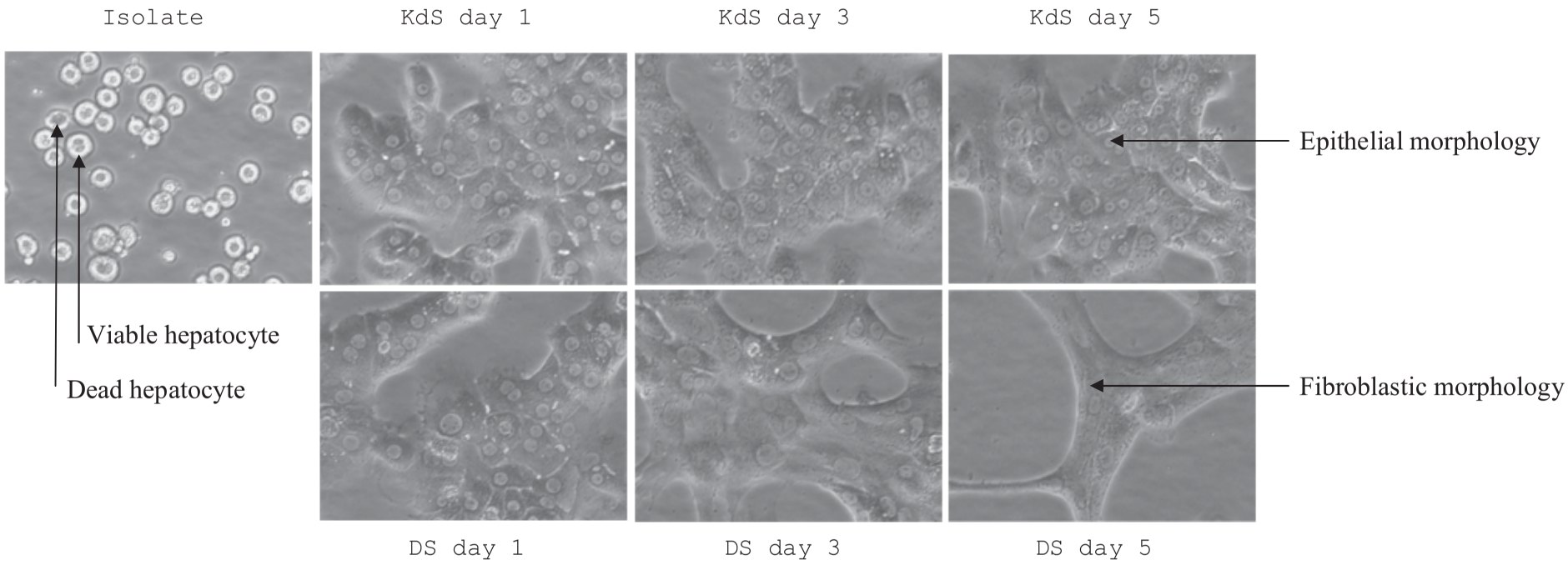

Figure 3.1: Phase contrast images of differentiated and dedifferentiated hepatocytes. Hepatocytes cultured in KdS medium maintain a characteristic polygonal morphology, while cells cultured in DS medium become elongated and fibroblast-like. Abbreviation: Freshly isolated hepatocytes (Isolate)

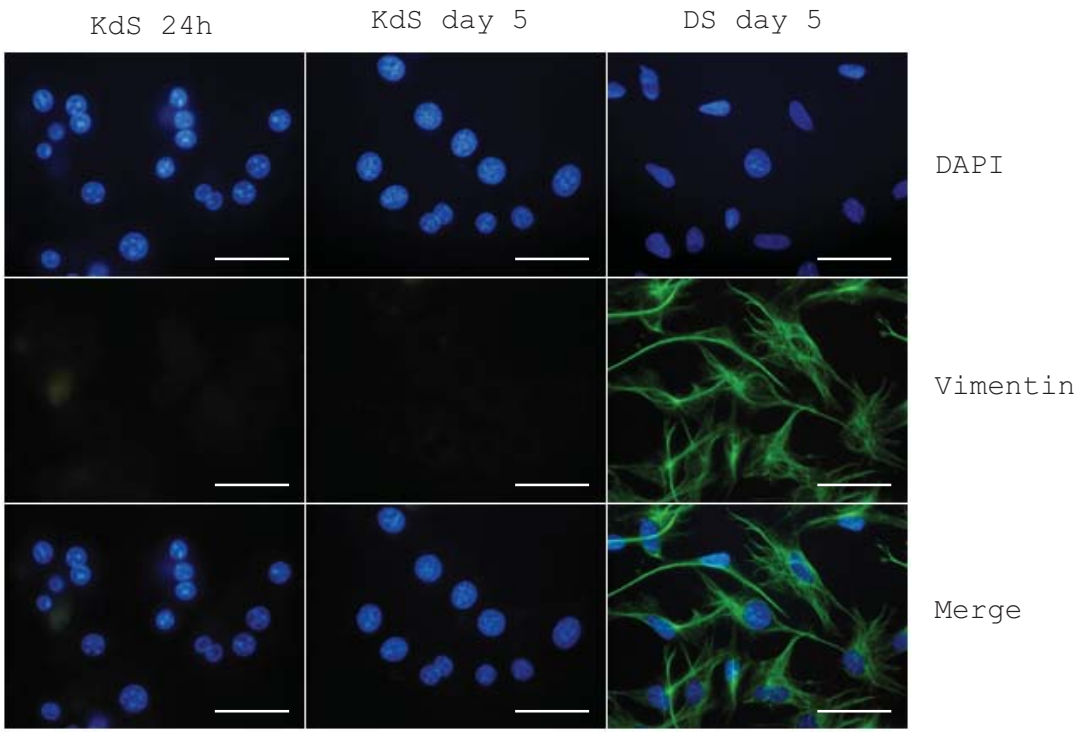

Figure 3.2: Dedifferentiated hepatocytes express vimentin. Hepatocytes cultured in KdS medium for 24 hours or 5 days, or in DS medium for 5 days were immunostained for vimentin (green) and counterstained with DAPI (blue). A cytoplasmic array of vimentin filaments is present in dedifferentiated hepatocytes, but not in differentiated hepatocytes. Scale bar represents 50μm.

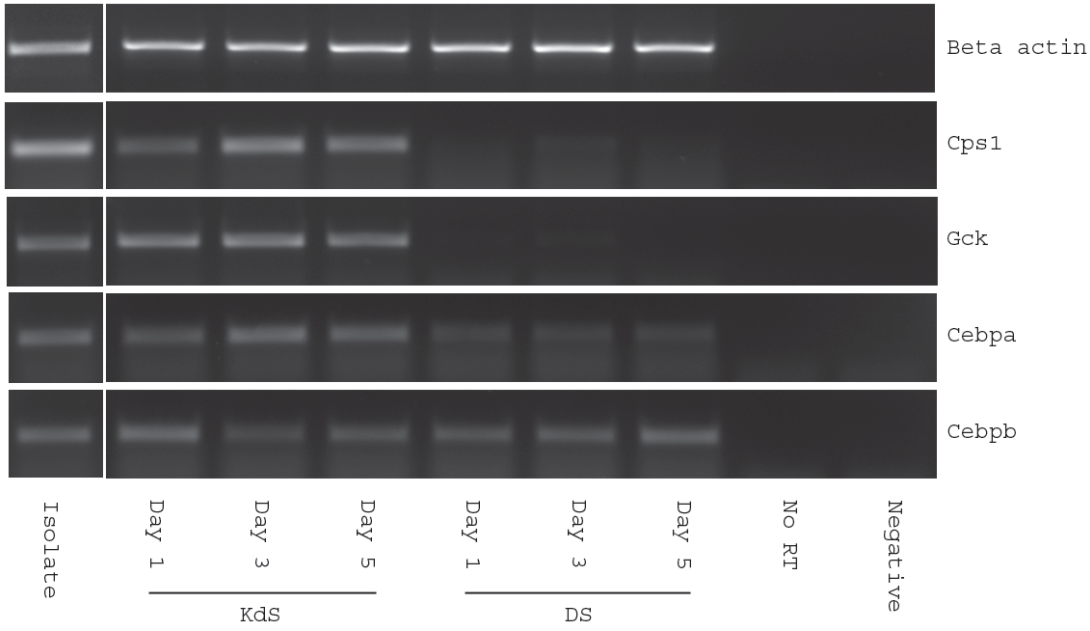

Figure 3.3: Hepatic genes are downregulated in dedifferentiated hepatocytes. Hepatocytes were cultured in KdS or DS medium and total RNA was extracted on day 1, 3 or 5. 5µg RNA was DNase-treated, of which 2µg was reverse transcribed. 100ng of cDNA was amplified by PCR using specific primers. In differentiated hepatocytes (KdS), liver gene expression is maintained. Dedifferentiated hepatocytes (DS) downregulate transcription of *cps1*, *gck* and c*ebpα*, but maintain *cebpβ* expression. Controls include a no reverse transcriptase (RT) reaction and a negative control reaction (negative) that did not contain sample. Cycle numbers: *Beta-actin*, 22; *cps1*, 23; *gck*, 28; *cebpα*, 28; *cebpβ*, 28.

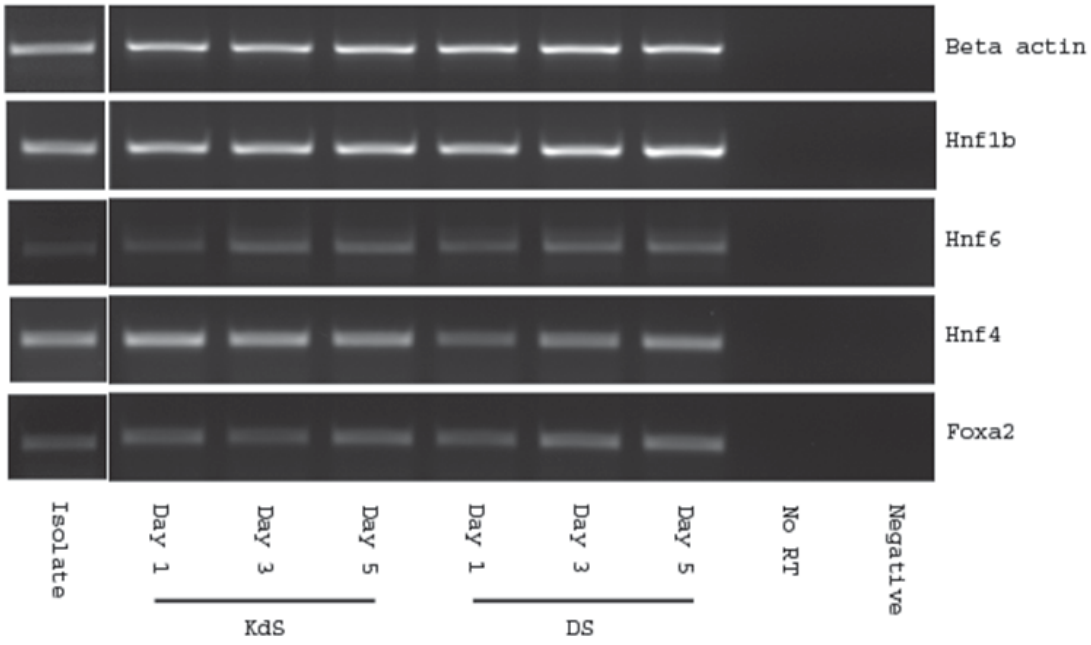

Figure 3.4: Dedifferentiated hepatocytes maintain expression of some core liver-enriched transcription factors. Hepatocytes were cultured in KdS or DS medium and total RNA was extracted on day 1, 3 or 5. 5µg RNA was DNase-treated, of which 2µg was reverse transcribed. 100ng of cDNA was amplified by PCR using specific primers. Expression of *hnf1b*, *hnf6*, *hnf4* and *foxa2* is maintained in both differentiated and dedifferentiated hepatocytes. Cycle numbers: *Beta actin*, 22; *hnf1β*, 30; *hnf6*, 28; *hnf4*, 25; *foxa2*, 28.

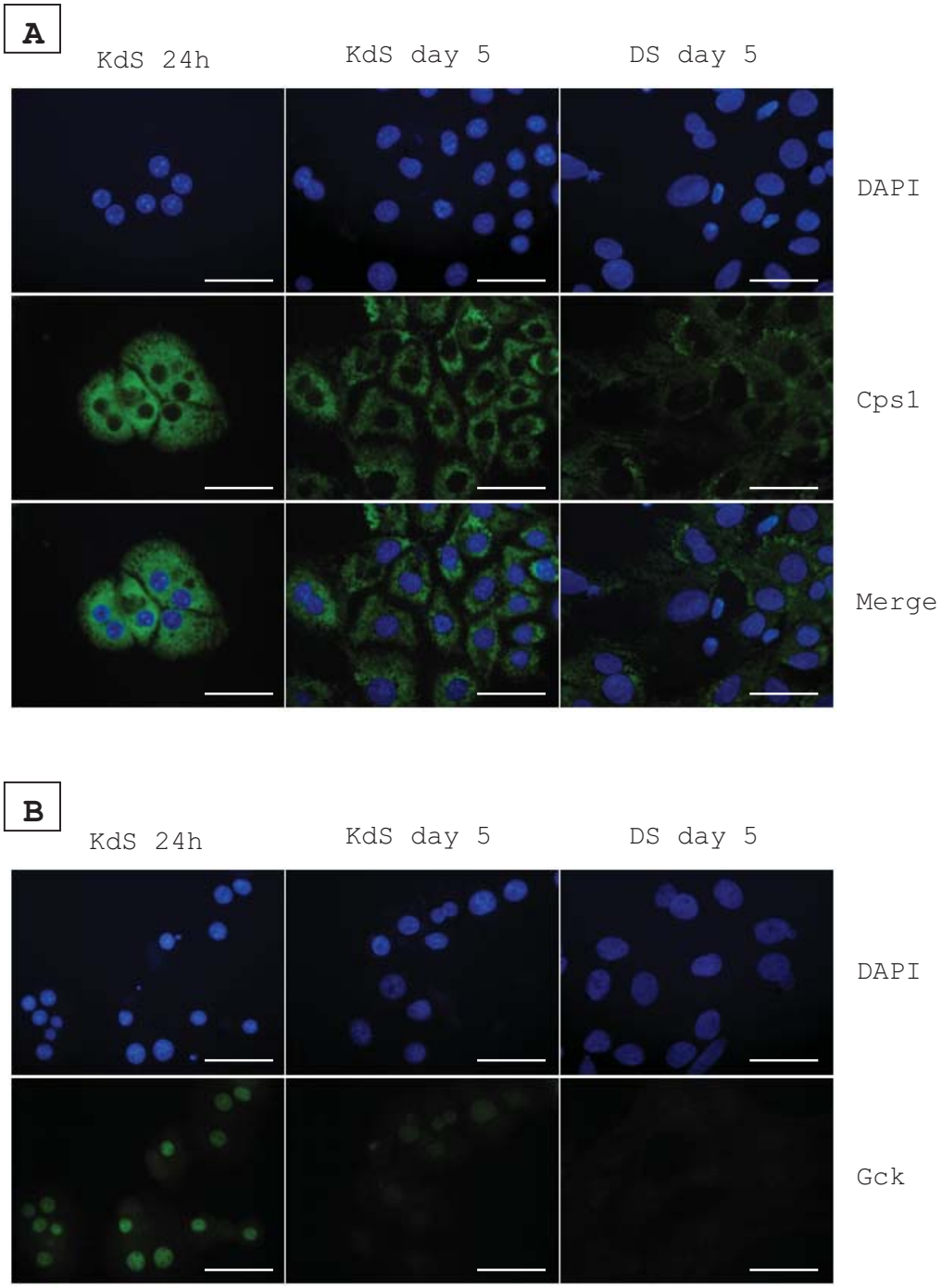

Figure 3.5: Cps1 and Gck are downregulated in dedifferentiated hepatocytes. Hepatocytes cultured in KdS medium for 24 hours or 5 days, or in DS medium for 5 days were immunostained for Cps1 (green) (A) or Gck (green) (B) and counterstained with DAPI (blue). Both markers are suppressed in dedifferentiated cells. Although Gck expression in day 5 KdS cells is reduced in comparison to 24 hour cultures, it remains higher than in day 5 DS cells. Note however that the larger nuclei characteristic of dedifferentiated hepatocytes may exaggerate Gck downregulation. Scale bar represents 50μm.

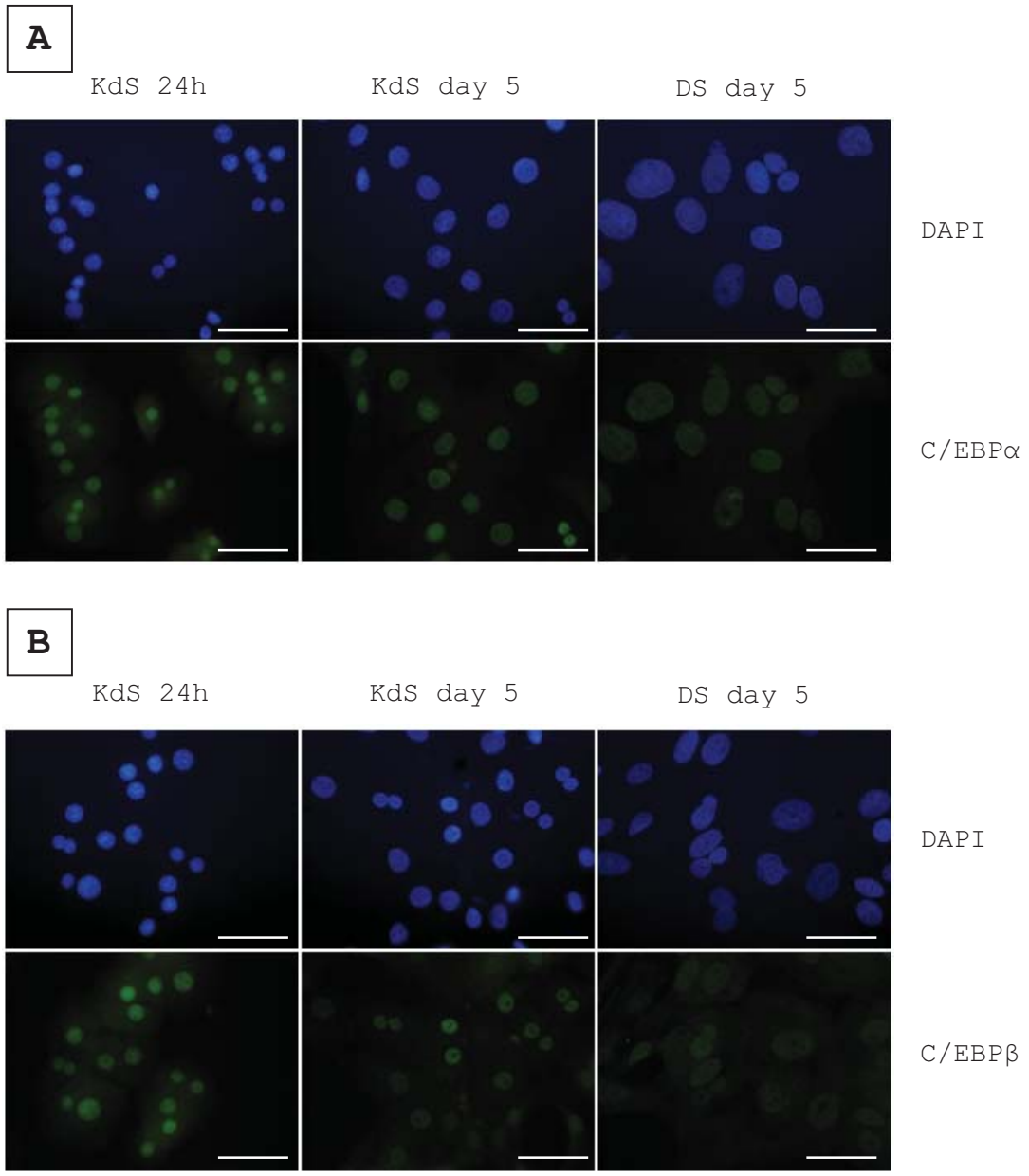

Figure 3.6: Hepatocyte dedifferentiation is characterised by repression of C/EBPα and C/EBPβ. Hepatocytes cultured in KdS medium for 24 hours or 5 days, or in DS medium for 5 days were immunostained for C/EBPα (green) (A) or C/EBPβ (green) (B) and counterstained with DAPI (blue). Both transcription factors are depleted in dedifferentiated cells compared to differentiated cells. Note, however, the potentially confounding effect of a dedifferentiation-associated increase in nuclear size. Scale bar represents 50μm.

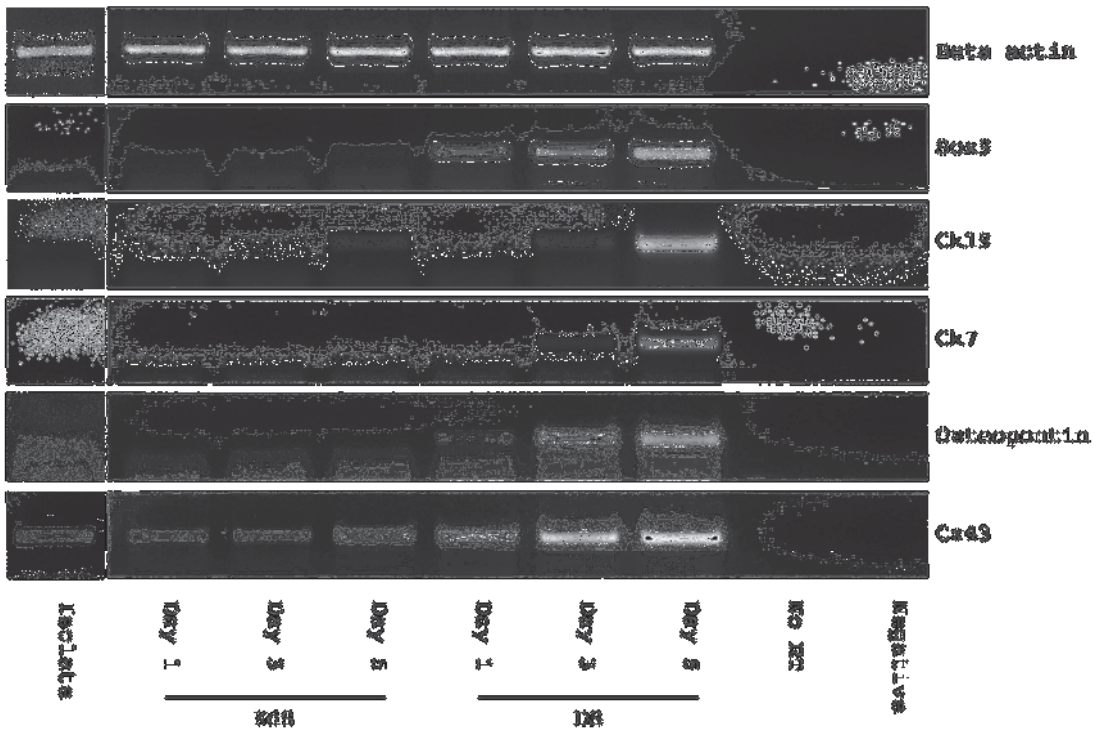

Figure 3.7: Dedifferentiated hepatocytes induce expression of ductal genes. Hepatocytes were cultured in KdS or DS medium and total RNA was extracted on day 1, 3 or 5. 5µg RNA was DNase-treated, of which 2µg was reverse transcribed. 100ng of cDNA was amplified by PCR using specific primers. The ductal genes *sox9*, *ck19*, *ck7*, *osteopontin* and *cx43* were activated in dedifferentiated, but not in differentiated cells. Cycle numbers: *Beta actin*, 22; *sox9*, 30; *ck19*, 30; *ck7*, 30; *osteopontin*, 25; *cx43*, 30.

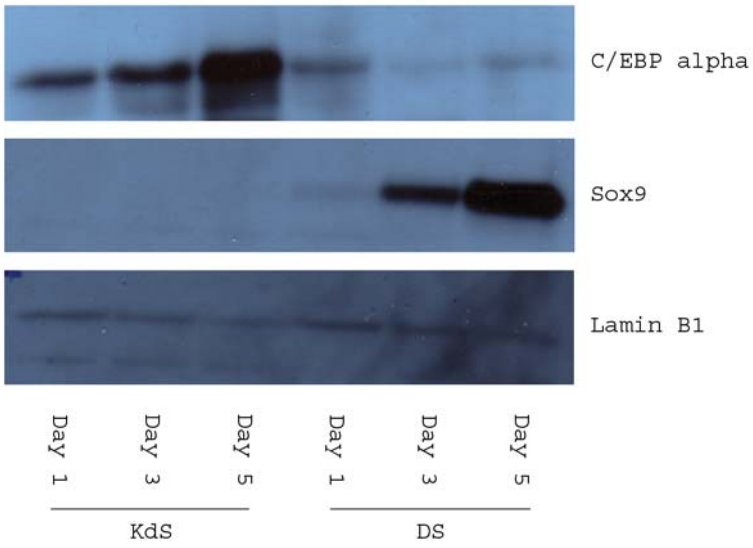

Figure 3.8: Downregulation of C/EBPα precedes expression of Sox9. Nuclear extracts were prepared from hepatocytes cultured for 1, 3 or 5 days in either KdS or DS medium. 10µg of each sample was separated by electrophoresis on a 10% Tris-HCl gel and blotted onto a PVDF membrane. Blots were probed with primary antibodies against C/EBPα, Sox9 or LaminB1 and then with HRP-conjugated secondary antibodies. The signal was detected by ECL chemiluminescence. During dedifferentiation, loss of C/EBPα occurs prior to the onset of Sox9 expression.

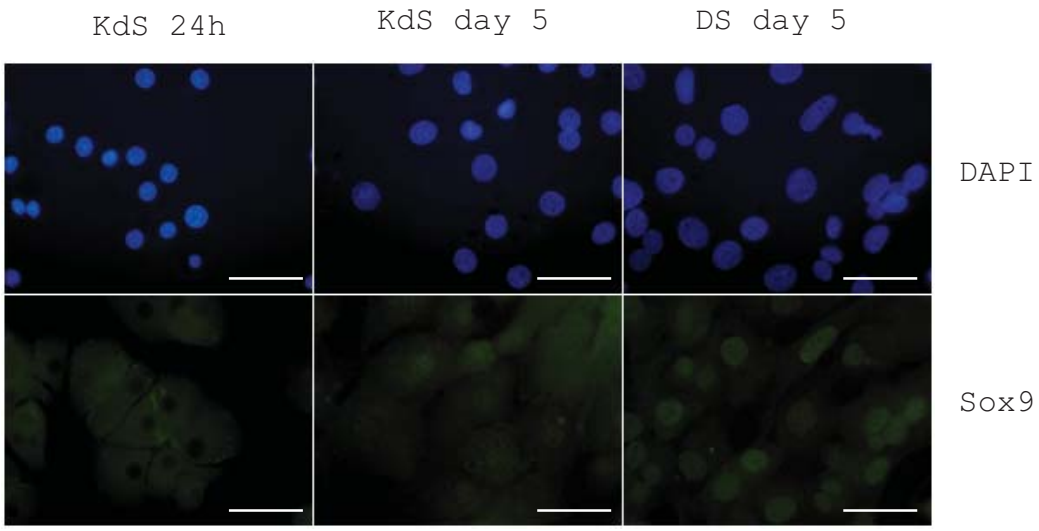

Figure 3.9: Sox9 is highly expressed in dedifferentiated hepatocytes. Hepatocytes cultured in KdS medium for 24 hours or 5 days, or in DS medium for 5 days were immunostained for Sox9 (green) and counterstained with DAPI (blue). KdS cells are Sox9-negative after 24 hours. By 5 days, some Sox9 is present in differentiated hepatocytes, but much greater expression is observed in dedifferentiated cells. Scale bar represents 50µm.

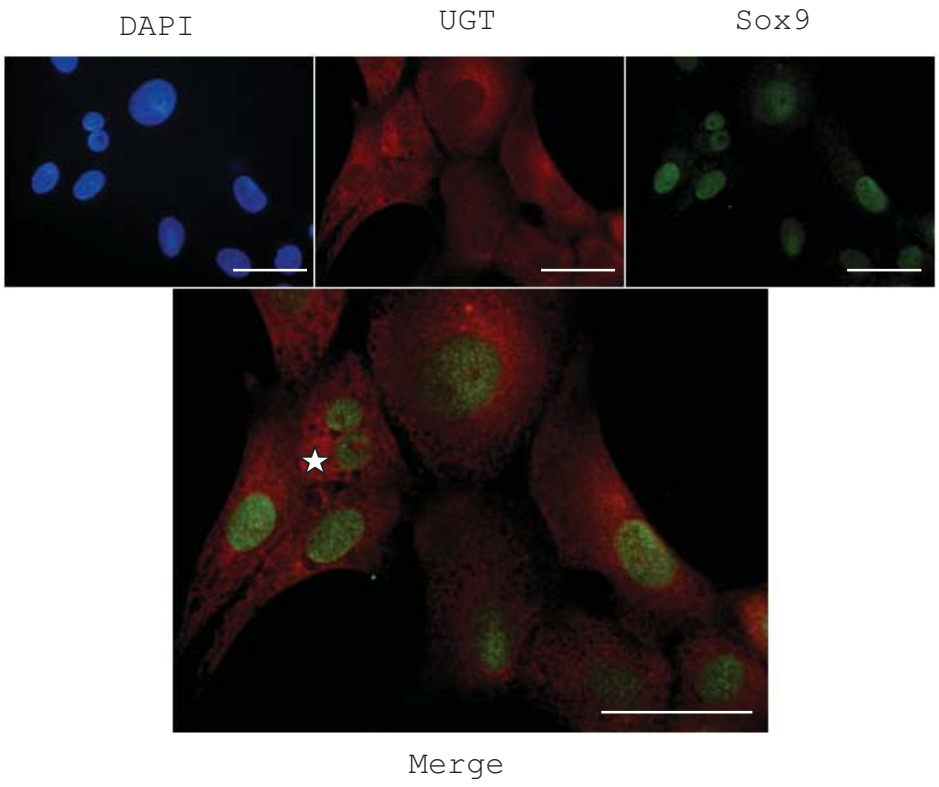

Figure 3.10: Sox9 is induced in dedifferentiated hepatocytes. Hepatocytes cultured for 5 days in DS medium were immunostained for Sox9 (green) and UGT (red) and counterstained with DAPI (blue). Sox9 and UGT are extensively coexpressed, often in binucleate cells (star). Scale bar represents 50µm.

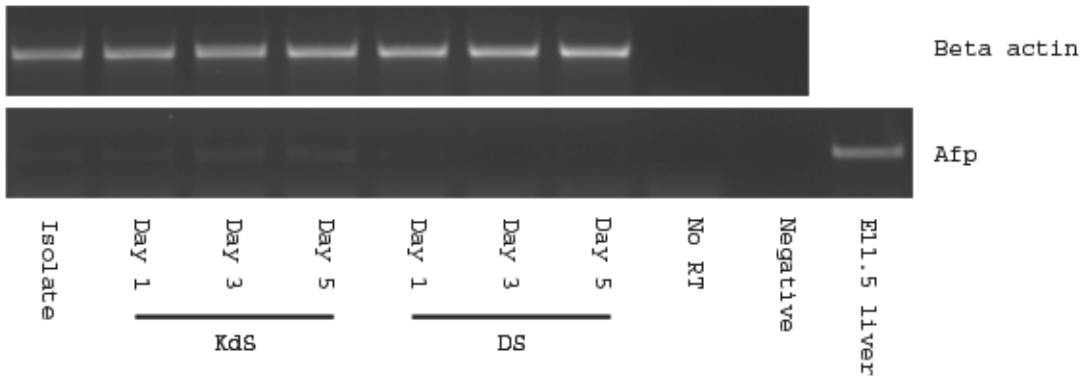

Figure 3.11: Reprogramming does not occur via a hepatoblast-like intermediate. Hepatocytes were cultured in KdS or DS medium and total RNA was extracted on day 1, 3 or 5. 5µg RNA was DNase-treated, of which 2µg was reverse transcribed. 100ng of cDNA was amplified by PCR using specific primers. The hepatoblast-specific gene *afp* is not induced during dedifferentiation. Cycle number: 30.

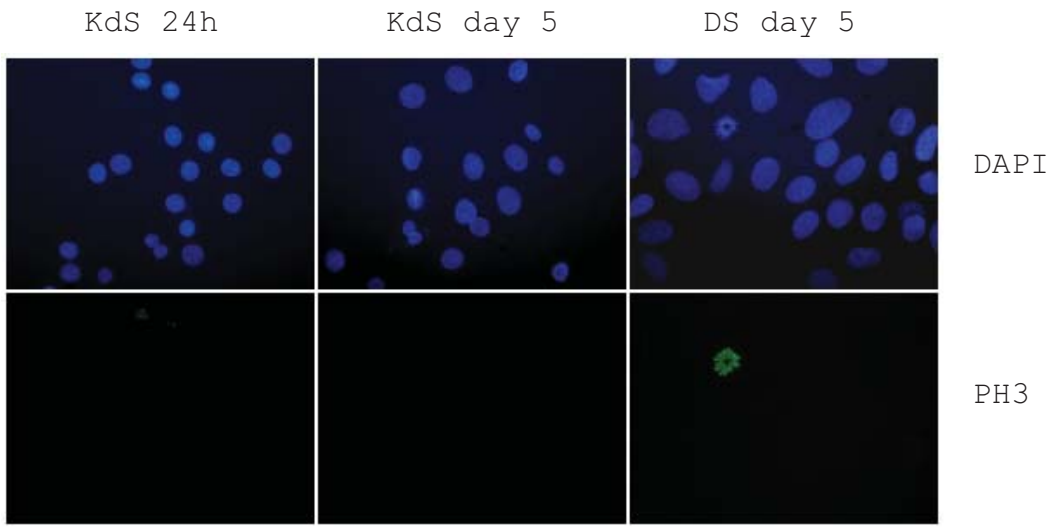

Figure 3.12: Hepatocytes reenter the cell cycle during dedifferentiation. Hepatocytes cultured in KdS medium for 24 hours or 5 days, or in DS medium for 5 days were immunostained for phospho-histone H3 (PH3) (green) and counterstained with DAPI (blue). Occasional DS hepatocytes, but not KdS hepatocytes are immunopositive. At least some dedifferentiated cells therefore undergo mitosis, while differentiated cells are quiescent.

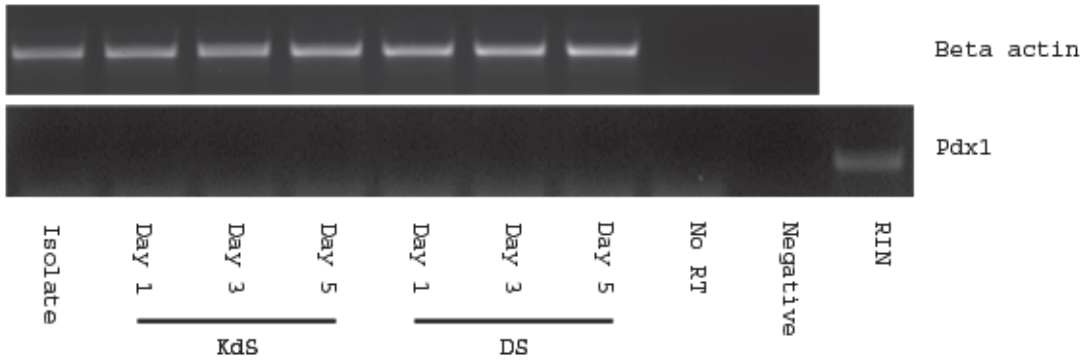

Figure 3.13: Dedifferentiated hepatocytes do not induce pancreatic genes. Hepatocytes were cultured in KdS or DS medium and total RNA was extracted on day 1, 3 or 5. 5µg RNA was DNase-treated, of which 2µg was reverse transcribed. 100ng of cDNA was amplified by PCR using specific primers. *Pdx1* is not expressed in dedifferentiated hepatocytes. Cycle number: 30

3.3 DISCUSSION

3.3.1 Induction of ductal genes in hepatocytes

Dedifferentiation of hepatocytes cultured in DS medium occurs concurrently with duct gene induction. Hepatocytic activation of ductal markers has previously been described by Nishikawa *et al*. (2005), who analysed gene expression in aggregates of primary rat hepatocytes embedded in a collagen gel matrix. In this environment, *ck19*, *ck20*, and *jagged1* (*jag1*) are induced, and branching morphogenesis is observed in the presence of insulin and epidermal growth factor (EGF). Following long-term culture, albumin expression is downregulated and ductular structures surrounded by a basement membrane are formed (Nishikawa *et al.* 2005). Induction of ductal genes precedes downregulation of albumin, but analysis of *cebpα*, *cps1* and *gck* expression is not reported. It is therefore not clear whether hepatocyte dedifferentiation is required in this system for acquisition of the ductal phenotype. Furthermore, as the authors did not conduct a lineage tracing analysis, it remains possible that the observed upregulation of ductal genes reflects selective expansion of contaminating duct cells, rather than reprogramming of hepatocytes.

3.3.2 Gene induction in dedifferentiated hepatocytes reflects developmental relatedness

Sox9 is expressed in both intrahepatic and extrahepatic bile ducts (Eberhard *et al.* 2008), but the two tissues have very different developmental origins. Intrahepatic BECs are derived from bipotential hepatoblasts, which also give rise to hepatocytes (Tanimizu and Miyajima 2004) (Suzuki *et al.* 2008) (Strick-Marchand and Weiss 2002). In contrast, extrahepatic BECs, like the gall bladder, cystic duct and common duct, share a $Sox17^{+}Pdx1^{+}$ progenitor with the ventral pancreas (Spence *et al.* 2009). Given that hepatocytes have a closer developmental relationship to intrahepatic than

to extrahepatic BECs, it is likely that dedifferentiated hepatocytes more closely resemble intrahepatic BECs.

The importance of developmental relationship is illustrated by the fact that reprogramming is much more efficient between related than unrelated cell types. Zhou *et al*., (2008), for example, showed that adenovirus-mediated missexpression of Ngn3, Pdx1 and MafA in pancreatic exocrine cells converts more than 20% of infected cells to insulin-positive beta-like cells. However insulin is not induced in skeletal muscle or fibroblasts expressing the same transcription factor combination (Zhou *et al.* 2008). In addition to being efficient, exocrine to beta-cell reprogramming also occurs relatively fast. While generation of insulin-expressing cells from human embryonic stem cells takes approximately two weeks (D'Amour *et al.* 2006), insulin positive cells are detectable in exocrine pancreas three days after infection (Zhou *et al.* 2008).

The substantial influence of developmental relationship on the efficiency of reprogramming may explain why dedifferentiated hepatocytes induce expression of duct genes, but not of pancreatic genes. Liver and ventral pancreas are specified from a bipotential precursor population in the ventral foregut endoderm (Deutsch *et al.* 2001). Pancreatic cells are therefore more distantly related to hepatocytes than intrahepatic BECs, which share a more derived progenitor.

3.3.3 Expression of many liver-enriched transcription factors is maintained during dedifferentiation

Hnf1β, *foxa2*, *hnf4α* and *hnf6* are all C/EBPα targets, both during embryonic development and in adult hepatocytes. However while *cebpα* is rapidly downregulated during hepatocyte dedifferentiation, expression of *hnf1β*, *foxa2*, *hnf4α* and *hnf6* is maintained. This robustness may stem from the fact that in adult hepatocytes, the proteins encoded by the latter four genes cooperate with HNF1α and liver receptor homolog 1 (LRH1) to form a highly cross-regulatory network. Expression of each gene in the network depends not only on a single factor, but on

combinatorial action of a subset of the other five regulators, thus generating a system that remains robust in the absence of any one factor (Kyrmizi *et al.* 2006).

Conditional inactivation of *hnf4α* in adult hepatocytes (*Alb-Cre*; *hnf4α* $^{loxP/loxP}$), like loss of C/EBPα during dedifferentiation, has only a minimal effect on expression of the other core transcription factors (Kyrmizi *et al.* 2006). This again reflects the self-stabilising nature of the core transcription factor network. However deletion of *hnf4α* in embryonic liver (*Alfp-Cre*; *Hnf4*$^{loxP/loxP}$) results in substantially altered promoter occupancy and reduced transcription factor expression. During development, the core hepatic transcription factors are organised in a simple hierarchical system that is progressively replaced by more complex crossregulatory interactions. The stability of the transcription factor network therefore correlates with its complexity (Kyrmizi *et al.* 2006).

Although C/EBPα occupies the promoter of *hnf1α*, *hnf1β*, *foxa2 hnf6* and *lrh1*, and the enhancer of *hnf4α*, its own promoter is not bound by any of the core transcription factors (Kyrmizi *et al.* 2006). This absence of stabilising cross-regulatory interactions may make transcription of *Cebpα* vulnerable to external perturbations, and therefore explain why the gene is selectively downregulated during hepatocyte dedifferentiation.

3.3.4 C/EBPα couples hepatocyte-specific gene expression and cell cycle exit

Repression of *Cebpα* during hepatocyte dedifferentiation is likely to underlie downregulation of the C/EBPα targets *Cps1* (Christoffels *et al.* 1998) and *Gck* (Inoue et al. 2004). However loss of C/EBPα may also explain the proliferation of dedifferentiated cells. In *cebpα*$^{-/-}$ livers, *c-jun* and *c-Myc* are induced, and the frequency of proliferating cell nuclear antigen (PCNA) positive cells is increased in comparison to wildtype controls (Flodby *et al.* 1996). Furthermore, primary hepatocytes isolated from *cebpα*$^{-/-}$ livers divide more rapidly than wildtype cells (Soriano *et al.* 1998). Coupling of lineage-specific transcription and cell-cycle exit by C/EBPα has previously been described in the interfollicular epidermis. In this context, commitment of basal keratinocytes to spinous layer fate depends on the

DNA binding activity of C/EBPα, while suppression of basal cell proliferation relies on protein-protein interaction between C/EBPα and E2F (Lopez *et al.* 2009).

3.3.5 Mitosis may facilitate reprogramming of dedifferentiated hepatocytes

Although conversion of exocrine cells to beta cell-like cells can occur in the absence of cell division (Zhou *et al.* 2008), it may be that proliferation facilitates reprogramming (Egli *et al.* 2008). Consistent with this idea, Martinez-Balbas *et al*. (1995) showed that transcription factors are transiently displaced from mitotic chromosomes, perhaps providing a "window of opportunity" in which a new gene expression pattern can be established (Martinez-Balbas *et al.* 1995). Heterochromatin protein 1 (HP1), a chromodomain protein that mediates gene silencing, is also disassociated from chromatin in dividing cells. During mitosis, the kinase AuroraB phosphorylates histone H3 at serine 10 and thereby prevents HP1 binding to it's target, H3K9me3 (Hirota *et al.* 2005). This in turn may provide an opportunity to reactivate repressed genes.

3.3.6 Hepatocyte dedifferentiation resembles an epithelial-mesenchymal transition

As they dedifferentiate, hepatocytes in DS medium acquire a fibroblast-like morphology, induce expression of the intermediate filament protein vimentin, and may reenter the cell cycle. Dedifferentiation therefore exhibits some of the features that define epithelial-mesenchyme transition (EMT). Further shared characters were identified by Godoy *et al*. (2010), who observed that dedifferentiating hepatocytes also induce the EMT markers snail1, matrix metallopeptidase 9 (MMP9) and MMP14 and downregulate the tight-junction proteins claudin1 and occludin. However expression of the epithelial marker E-cadherin is not lost and there is no upregulation of the other EMT-promoting transcription factors snail2 and zinc finger E-box binding homeobox 2 (Zeb2) (Godoy *et al.* 2010).

3.3.7 Summary

KdS medium maintains the phenotype of primary rat hepatocytes. However hepatocytes cultured in DS medium dedifferentiate, rapidly downregulating *cebpα* and a subset of liver-specific genes. Notably, dedifferentiated hepatocytes also induce expression of ductal genes, including *sox9*, and therefore provide a useful *in vitro* model of cell reprogramming. Conversion of hepatocytes to duct-like cells occurs by activation of ductal genes in dedifferentiated hepatocytes rather than by a two-step process involving regression to a hepatoblast-like intermediate.

Chapter 4

The molecular mechanism of hepatocyte reprogramming

4.1 BACKGROUND

Reprogramming of differentiated cells is usually achieved experimentally by expressing the transcription factors that regulate embryonic development of one tissue type in adult cells of a different tissue type. For example, a combination of Pdx1, Ngn3 and MafA can convert pancreatic exocrine cells to insulin-secreting β-cells (Zhou *et al.* 2008). Pdx1 is required for morphogenesis and differentiation of the pancreas and is also expressed in adult β-cells (Jonsson *et al.* 1994; Ahlgren *et al.* 1996; Offield *et al.* 1996). Ngn3, which is expressed only during development, specifies endocrine precursors (Gradwohl *et al.* 2000), and MafA is necessary for insulin secretion in response to glucose (Zhang *et al.* 2005).

As cellular reprogramming relies on recapitulation of development, reprogramming of hepatocytes to duct-like cells may involve activation of transcription factors expressed in embryonic intrahepatic bile ducts (IHBDs). Sox9 is the earliest specific marker of intrahepatic biliary differentiation and is therefore a candidate regulator of ductal gene expression in hepatocytes (Antoniou *et al.* 2009). Development of murine IHBDs begins with the appearance of a single layered ring of Sox9-expressing cells around branches of the portal vein. Focal areas of the ring become bilayered, giving rise to asymmetrical ductal structures that are lined on the portal side by biliary cells and on the parenchymal side by hepatoblasts. As morphogenesis proceeds, the hepatoblasts differentiate into BECs to form symmetrical, Sox9-positive bile ducts (Antoniou *et al.* 2009).

In Sox9 deficient livers (*Alfp-Cre*; *sox9*$^{fl/fl}$), maturation of asymmetrical ductal structures to symmetrical ducts is delayed. This is associated with persistent expression of C/EBPα on both the portal and parenchymal sides of the primitive ducts, and with abnormal expression of TGFβ receptor II (Antoniou *et al.* 2009). The phenotype of Sox9 mutants suggests that Sox9 plays a role in regulating biliary differentiation during embryonic development. Reactivation of Sox9 in dedifferentiated hepatocytes may therefore drive induction of their duct-like gene expression profile.

4.2 RESULTS

4.2.1 Sox9 is expressed in intrahepatic bile ducts but not in hepatocytes

The transcription factor Sox9 regulates development of murine intrahepatic bile ducts (Antoniou *et al.* 2009), and was induced in dedifferentiating rat hepatocytes after only 24 hours of culture (see chapter 3, *Figure 3.8*). It may therefore mediate dedifferentiation-associated activation of downstream ductal genes such as *ck19* and *osteopontin*. This idea is consistent with Sox9 immunohistochemistry in adult liver, which showed that Sox9 is expressed specifically in intrahepatic bile ducts, and not in hepatocytes (*Figure 4.1*).

4.2.2. Sox9 activates ductal genes in differentiated hepatocytes

To further investigate the potential of Sox9 to activate ductal genes, differentiated hepatocytes maintained in KdS medium were infected on day 1 with an adenoviral vector expressing either Sox9 (Ad-Sox9) or GFP (Ad-GFP). By day 5, RT-PCR analysis of Ad-Sox9 infected cells identified induction of *ck19* and *osteopontin* and upregulation of *cx43* (*Figure 4.2*). However the lack of ductal gene expression on day 3, despite accumulation of exogenous Sox9 mRNA, suggests that the activation of duct genes may be indirect. Furthermore, ectopic expression of Sox9 was not sufficient to activate *ck7* in differentiated hepatocytes (*Figure 4.2*), although the latter is induced in dedifferentiated cells (see chapter 3, *Figure 3.8*).

4.2.3 Sox9 represses hepatic markers in differentiated hepatocytes

Reprogramming of hepatocytes to duct-like cells involves repression of hepatic genes as well as activation of ductal genes. The effect of ectopic Sox9 on hepatic gene transcription was therefore investigated by RT-PCR. By day 3, differentiated hepatocytes infected with Ad-Sox9 downregulated expression of *cebpα*, *cebpβ* and

gck. Repression of these genes was maintained on day 5, by which time some downregulation of *cps1* was also observed (*Figure 4.3*). Thus in addition to activating the duct gene expression profile, Sox9 contributes to suppression of the liver phenotype. The latter activity may primarily reflect repression of *cebpα*, which is upstream of *cps1* and *gck*.

4.2.4 C/EBPα represses ductal genes in dedifferentiated hepatocytes

C/EBPα, unlike other liver-enriched transcription factors, was rapidly downregulated during hepatocyte dedifferentiation (*Figure 3.3*). In order to establish whether repression of C/EBPα is a necessary prerequisite for induction of duct genes, dedifferentiating hepatocytes were infected on day 1 with Ad-*cebpα* or Ad-*GFP*. Restoration of C/EBPα expression repressed transcription of *sox9*, *ck19* and *osteopontin* by day 3, and repression persisted on day 5. However the effect on *cx43* expression was negligible (*Figure 4.5*). Downregulation of C/EBPα is therefore required for expression of a subset of duct genes, perhaps because it inactivates *sox9*, which is in turn necessary for duct induction. C/EBPα-mediated repression of *sox9* is particularly interesting given that Sox9 negatively regulates *cebpα*.

4.2.5 C/EBPβ represses duct genes in dedifferentiated hepatocytes

C/EBPα and C/EBPβ can act redundantly in many aspects of liver differentiation (Chen *et al.* 2000), so the ability of the two proteins to repress transcription of duct genes was compared. Dedifferentiated hepatocytes were infected on day 1 with an adenovirus expressing LAP, an isoform of C/EBPβ that acts as a transcriptional activator (Ramji and Foka 2002), or with Ad-*GFP*. Like C/EBPα, LAP suppressed expression of *sox9*, *ck19* and *osteopontin* but not of *cx43* (*Figure 4.6*). During hepatocyte dedifferentiation, duct genes were induced despite continued *cebpβ* expression (*Figure 3.3*). This suggests either than physiological levels of C/EBPβ are insufficient to compensate for downregulation of C/EBPα, or that C/EBPβ is inactivated posttranscriptionally.

4.2.6 C/EBPα restores some hepatic gene expression in dedifferentiated hepatocytes

Downregulation of C/EBPα during hepatocyte dedifferentiation was accompanied by repression of its targets *cps1* and *gck* (*Figure 3.3*). Analysis of DS cells infected with Ad-*cebpa* showed that exogenous C/EBPα partially rescued *cps1* expression on days 3 and 5, but that *gck* remained inactive (*Figure 4.4*). Complete reactivation of the liver gene expression program in dedifferentiated cells may require additional liver-enriched transcription factors or extracellular signals such as glucocorticoids.

4.2.7 Dedifferentiation and induction of duct genes are reversible

In order to establish whether reprogramming of hepatocytes to duct-like cells can be reversed, hepatocytes were cultured for three days in DS medium, and then transferred to KdS medium until day 5 or day 7. Control cells were left in DS for the duration of the experiment. Figure 4.7 shows that in cells switched from DS to KdS medium, expression of *cebpα*, *cps1* and *gck* was restored to levels characteristic of freshly isolated hepatocytes by day 5. Conversely, expression of *sox9* and *ck19* was dramatically reduced in switched cells compared to DS cells, and *osteopontin* and *cx43* were also repressed (*Figure 4.7*). The opposing response of hepatocyte and ductal genes to the change in culture conditions indicates that the hepatic and ductal gene expression may be mutually exclusive. This in turn may reflect the antagonistic interaction of C/EBPα and Sox9.

4.2.8 Sox9 can induce *ck19* in primary fibroblasts

Some hepatic transcription factors, such as HNF6 and HNF1β, are also expressed in IHBDs (*Figure 3.*4) and so may facilitate Sox9-mediated activation of ductal genes in hepatocytes. To investigate whether Sox9 can also induce duct genes in a developmentally unrelated cell type, primary fibroblasts were isolated from adult rat skin (*Figure 4.8*). The resulting cell population was largely homogenous and uniformly expressed the mesenchymal marker vimentin (*Figure 4.9*). Skin

fibroblasts were also amenable to infection with adenovirus, as demonstrated by immunostaining for Sox9 in Ad-*sox9* infected cells (*Figure 4.10*).

Fibroblasts were passaged three times in order to reduce any contamination by slowly proliferating epithelial cells and then infected overnight with Ad-*sox9*, Ad-*pdx1* or Ad-*GFP*. Two days after infection, *ck19* was activated in cells overexpressing Sox9, but not in control cells. However expression of *hnf1β* was not induced (*Figure 4.11*). Sox9 can therefore drive expression of some duct genes in fibroblasts, but cannot activate the complete duct gene expression program.

4.2.9 Sox9 siRNA was not effective in dedifferentiated hepatocytes

In an attempt to confirm the dependence of duct gene induction on Sox9, dedifferentiated hepatocytes were treated with Sox9 siRNA. However knockdown was not achieved at either the mRNA or protein level (*Figure 4.12*).

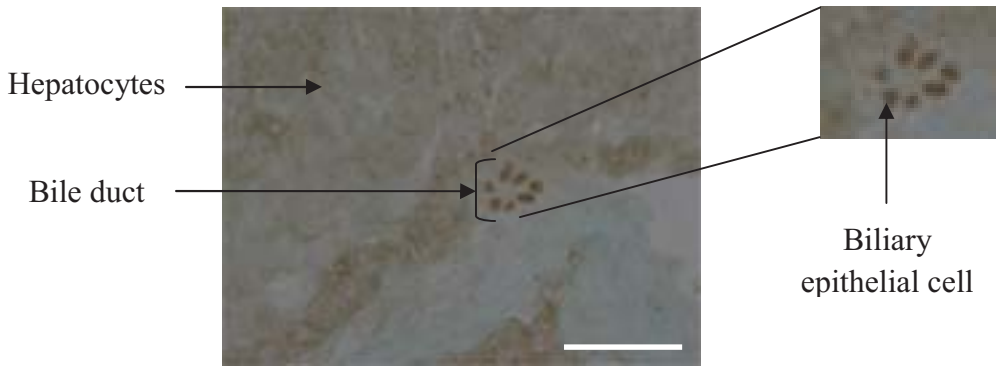

Figure 4.1: Sox9 is specifically expressed in intrahepatic bile ducts. Paraffin-embedded sections of adult rat liver were immunostained with anti-Sox9 and a horseradish peroxidise-conjugated secondary antibody. The signal was detected by DAB staining. Scale bar represents 50μm.

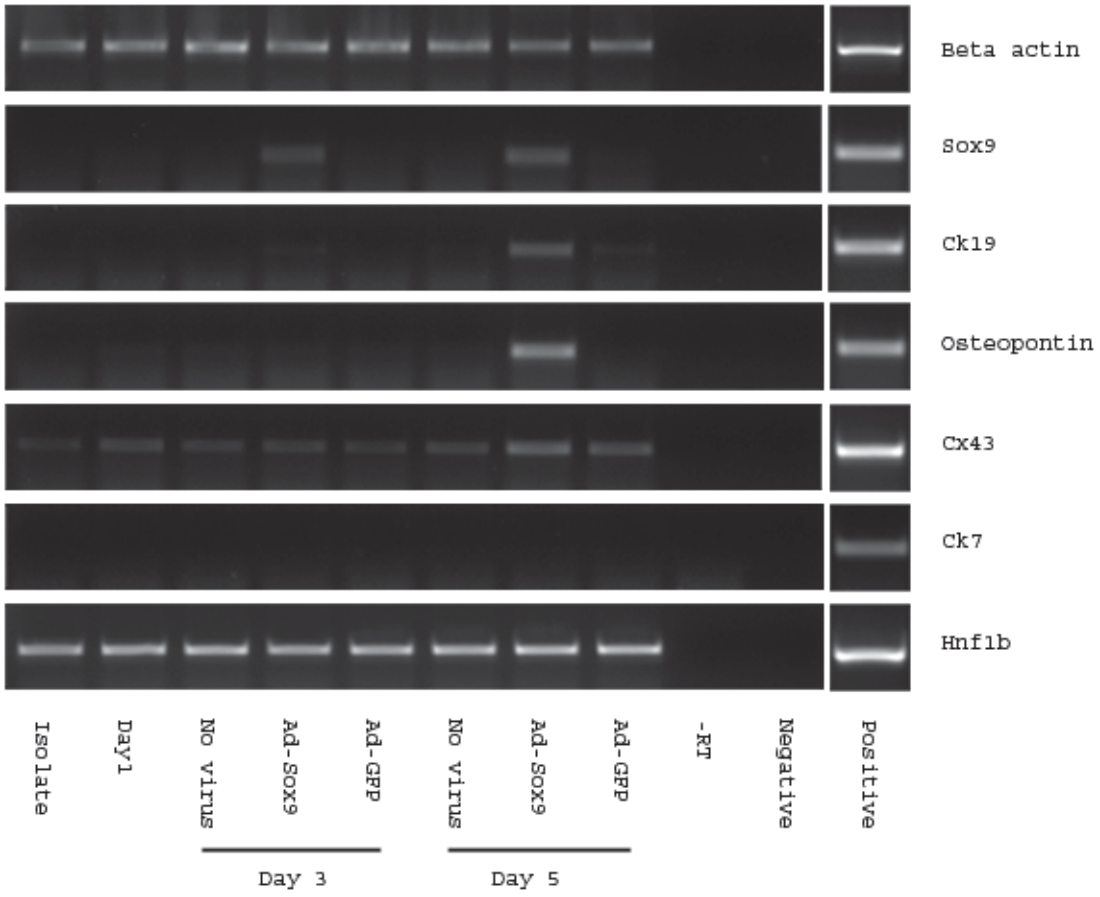

Figure 4.2: Ectopic Sox9 induces duct genes in hepatocytes. Hepatocytes were cultured for 12 hours in KdS medium and then infected with adenovirus. For adenovirus infection, the cells were transferred to KdS medium supplemented with 10% serum, and exposed to Ad-*sox9* (M.O.I. 2) or Ad-*GFP* (M.O.I. 2) for one hour at 37˚C. The medium was then replaced with KdS (without serum). Total RNA was extracted on day 3 or day 5. 5µg of RNA was DNase-treated, of which 2µg was reverse transcribed. 100ng of cDNA was amplified by PCR using specific primers. Ad-*sox9*, but not Ad-*GFP*, induces expression of *ck19* and *osteopontin*, and upregulates *cx43*. *Ck7*, however, is not induced. *Hnf1β* is expressed in control hepatocytes, and is not affected by ectopic Sox9. Controls include freshly isolated hepatocytes (Isolate), Day 5 DS hepatocytes (Positive), and reactions without reverse transcriptase (-RT) or without sample (Negative). Cycle numbers: *Beta actin*, 22; *sox9*, 28; *ck19*, 30; *osteopontin*, 30; *cx43*, 30; *ck7*, 30; *hnf1β*, 30.

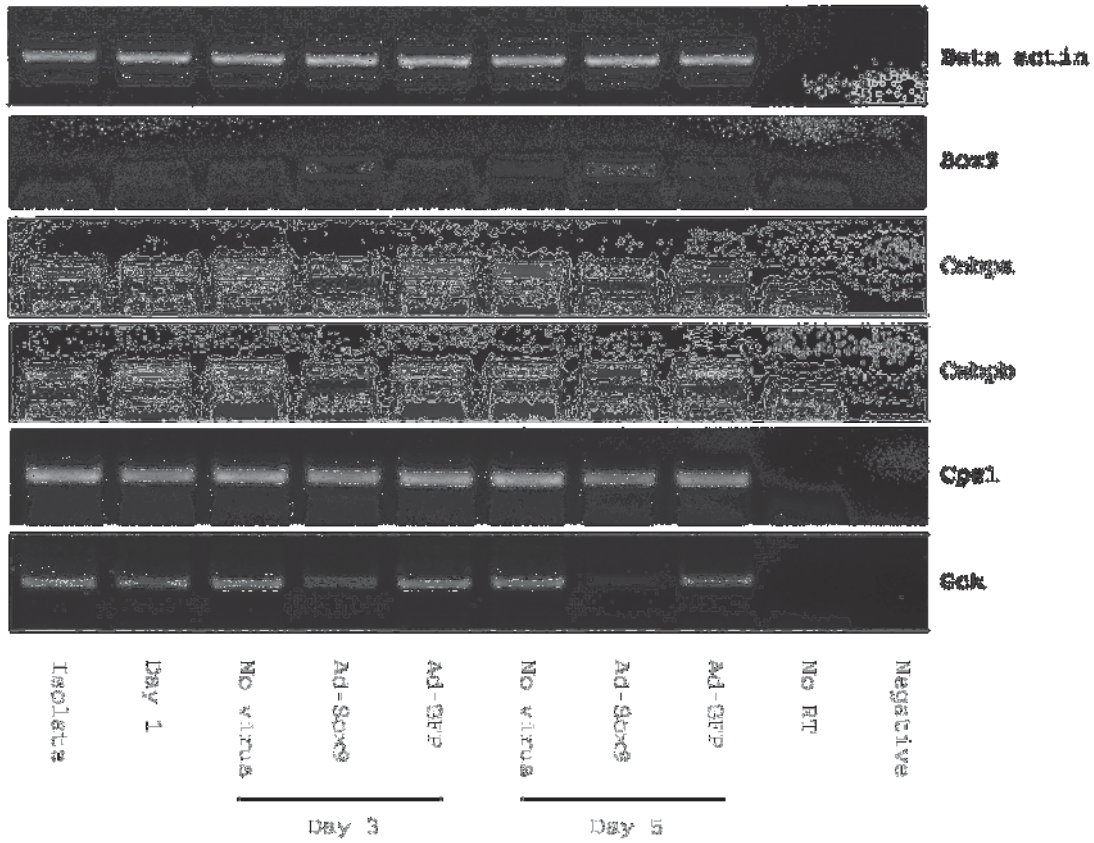

Figure 4.3: Sox9 represses expression of *cebpα* and other hepatic genes in hepatocytes. Day 1 KdS hepatocytes were incubated with Ad-*sox9* (M.O.I. 2) or Ad-*GFP* (M.O.I. 2) for one hour at 37°C. For the duration of the incubation, the cells were maintained in KdS medium supplemented with 10% serum. Total RNA was extracted on day 3 or day 5. 5µg of RNA was DNase-treated, of which 2µg was reverse transcribed. 100ng of cDNA was amplified by PCR using specific primers. Ad-*sox9*, but not Ad-*GFP*, represses expression of *cebpα*, *cebpβ* and *gck*. *Cps1* expression, in contrast, is unaltered. Cycle numbers: *Beta actin*, 22; *sox9*, 28; *cebpα*, 28; *cebpβ*, 28; *cps1*, 27; *gck*, 27.

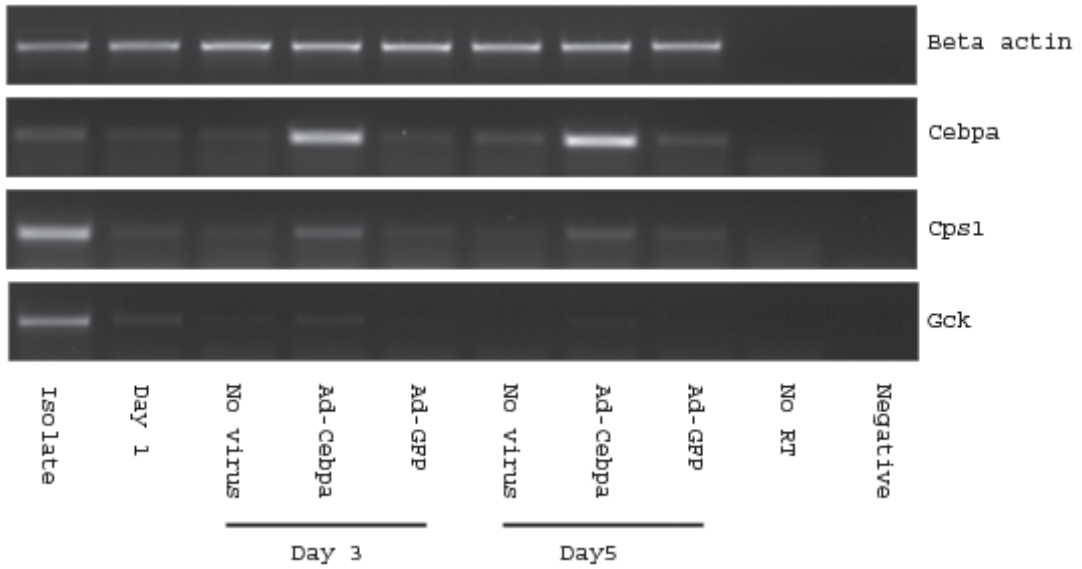

Figure 4.4: C/EBPα partially restores liver gene expression in dedifferentiating hepatocytes. Day 1 DS hepatocytes were incubated overnight with Ad-*cebpα* (M.O.I . 200) or Ad-*GFP* (M.O.I. 200) in the presence of 5µg/ml dextran. Total RNA was extracted on day 3 or day 5. 5µg of RNA was DNase-treated, of which 2µg was reverse transcribed. 100ng of cDNA was amplified by PCR using specific primers. Adenovirus-mediated expression of C/EBPα in dedifferentiating cells partially restores expression of *cps1*, and to a lesser extent *gck*. Ad-*GFP* has no effect. Cycle numbers: *Beta actin*, 22; *cebpα*, 28; *cps1*, 25; *gck*, 30.

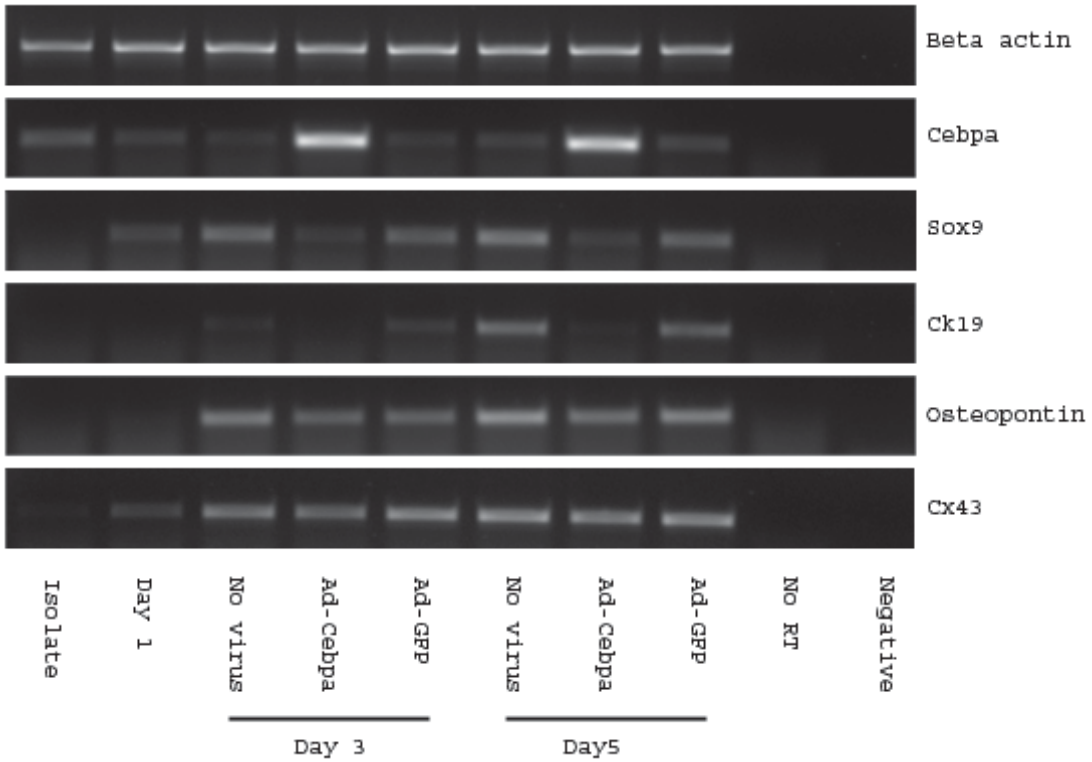

Figure 4.5: C/EBPα represses induction of *sox9* and *ck19* in dedifferentiating hepatocytes. Day 1 DS hepatocytes were incubated overnight with Ad-*cebpα* (M.O.I . 200) or Ad-*GFP* (M.O.I. 200) in the presence of 5µg/ml dextran. Total RNA was extracted on day 3 or day 5. 5µg of RNA was DNase-treated, of which 2µg was reverse transcribed. 100ng of cDNA was amplified by PCR using specific primers. Adenovirus-mediated expression of C/EBPα, but not of GFP, represses the induction of *sox9* and *ck19* in dedifferentiating cells. Cycle numbers: *Beta actin*, 22; *cebpα*, 28; *sox9*, 27; *ck19*, 27; *osteopontin*, 25; *cx43*, 27.

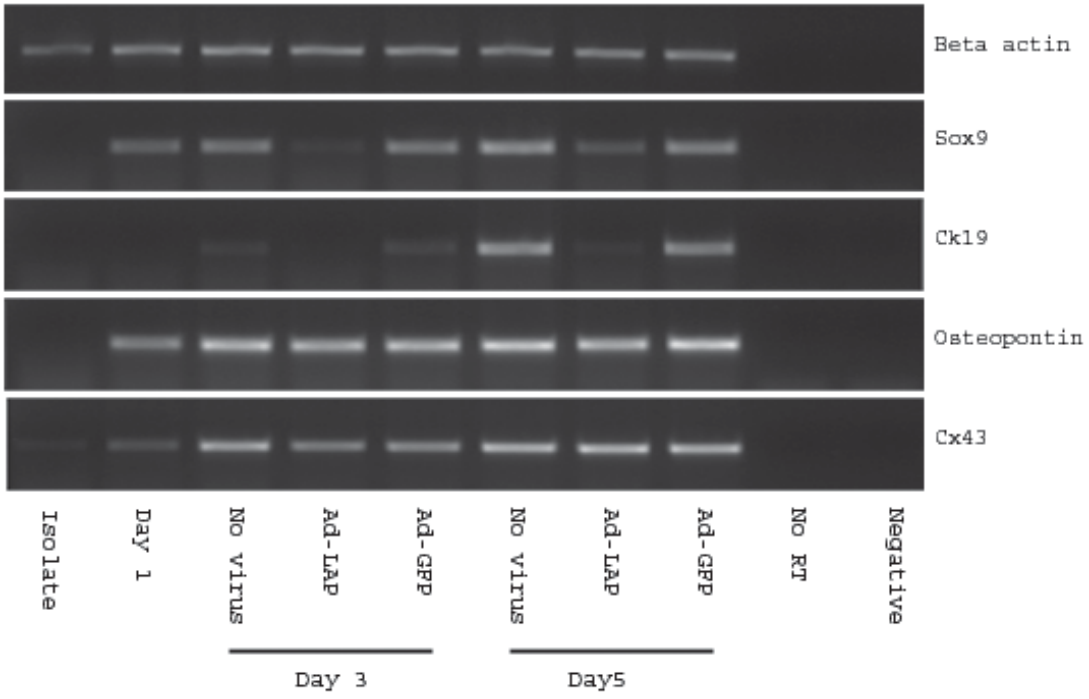

Figure 4.6: C/EBPβ represses induction of *sox9* and *ck19* in dedifferentiating hepatocytes. Day 1 DS hepatocytes were incubated overnight with Ad-*LAP* (M.O.I . 20) or Ad-*GFP* (M.O.I. 20). Total RNA was extracted on day 3 or day 5. 5µg of RNA was DNase-treated, of which 2µg was reverse transcribed. 100ng of cDNA was amplified by PCR using specific primers. Adenovirus-mediated expression of C/EBPβ, but not of GFP, represses the induction of *sox9* and *ck19* in dedifferentiating cells. Cycle numbers: *Beta actin*, 22; *sox9*, 27; *ck19*, 27; *osteopontin*, 25; *cx43*, 27.

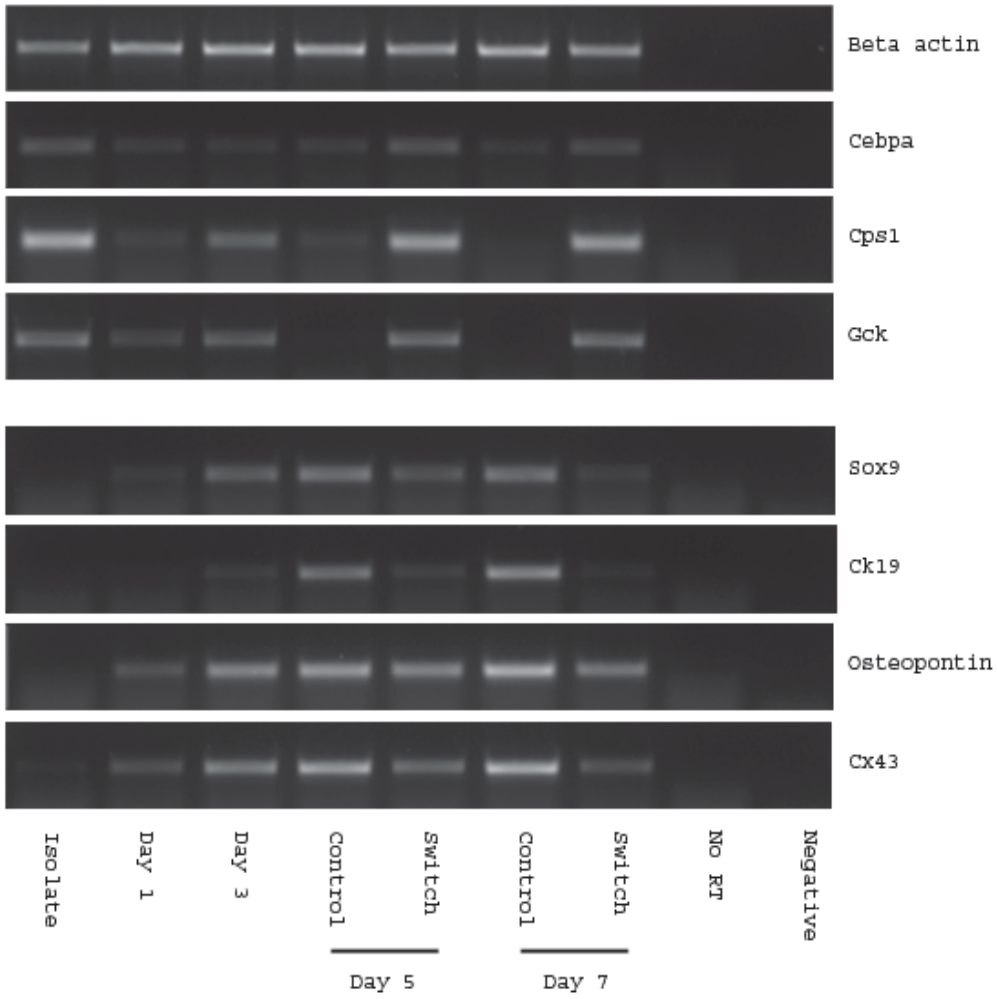

Figure 4.7: Dedifferentiation and induction of duct genes are both reversible. Hepatocytes were cultured in DS medium for 3 days and then transferred to KdS medium, while control cells remained in DS medium. Total RNA was extracted on day 5 or day 7 and 5µg was DNase-treated. 2µg of DNase-treated RNA was reverse transcribed and the resulting cDNA was amplified by PCR using specific primers. KdS medium restores expression of hepatic genes in dedifferentiated hepatocytes. Conversely, expression of ductal genes is repressed. Cycle numbers: *Beta actin*, 22; *cebpα*, 28; *cps1*, 25; *gck*, 30; *sox9*, 27; *ck19*, 27; *osteopontin*, 27; *cx43*, 27.

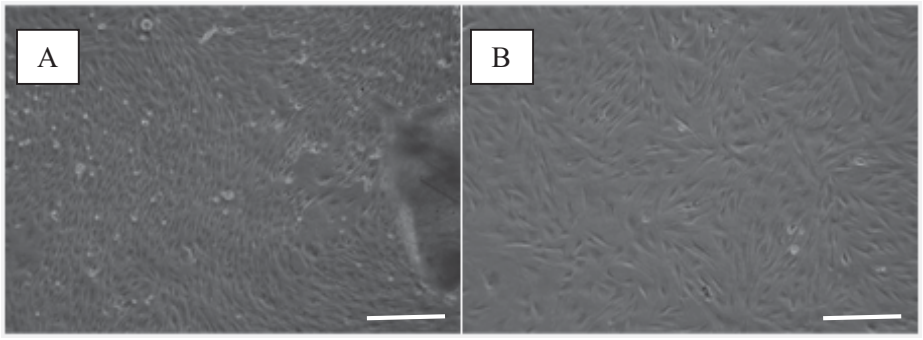

Figure 4.8: Primary fibroblasts derived from adult rat skin. Phase contrast images of primary fibroblasts (A) growing out from adult rat skin after two weeks in culture (scale bar represents 300μm) and (B) after splitting (scale bar represents150μm).

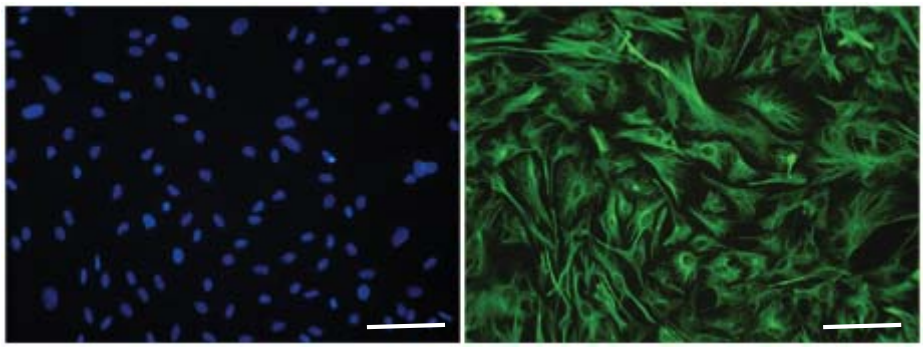

Figure 4.9: Primary fibroblasts uniformly express vimentin. Passage three fibroblasts were immunostained for vimentin (green), a mesenchymal marker, and counterstained with DAPI (blue). Vimentin expression is homogeneous. Scale bar represents 100μm.

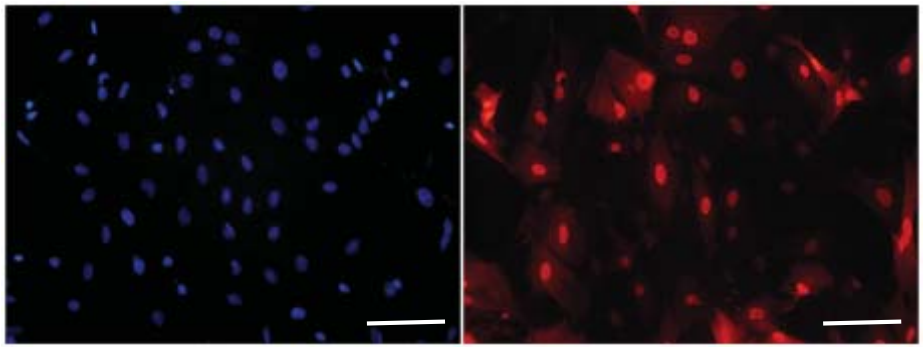

Figure 4.10: Primary fibroblasts are amenable to adenovirus infection. Passage three fibroblasts were incubated overnight with Ad-*sox9* (M.O.I. 5) in the presence of 5μg/ml dextran. After 48 hours, the cells were immunostained for Sox9 (red) and counterstained with DAPI (blue). Substantial adenovirus-mediated Sox9 expression is visible in almost all cells. Scale bar represents 100μm.

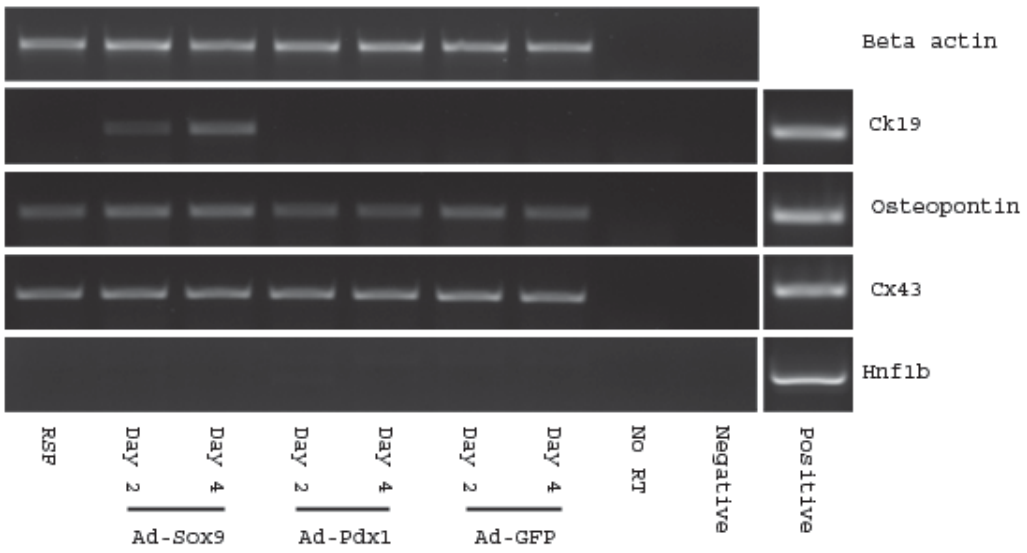

Figure 4.11: Sox9 induces *ck19* expression in primary fibroblasts. Passage three rat skin fibroblasts (RSF) were incubated overnight with Ad-*sox9* (M.O.I. 5), Ad-*pdx1* (M.O.I. 5) or Ad-*GFP* (M.O.I. 5) in the presence of 5µg/ml dextran. Total RNA was extracted after two or four days. 5µg of RNA was DNase-treated, of which 2µg was reverse transcribed. 100ng of cDNA was amplified by PCR using specific primers. Adenovirus-mediated overexpression of Sox9, but not of Pdx1 or GFP, induces *ck19* expression in primary fibroblasts. *Osteopontin* and *cx43* are already expressed in control cells. Cycle numbers: *Beta actin*, 22; *ck19*, 30; *osteopontin*, 30; *cx43*, 30; *hnf1β*, 30.

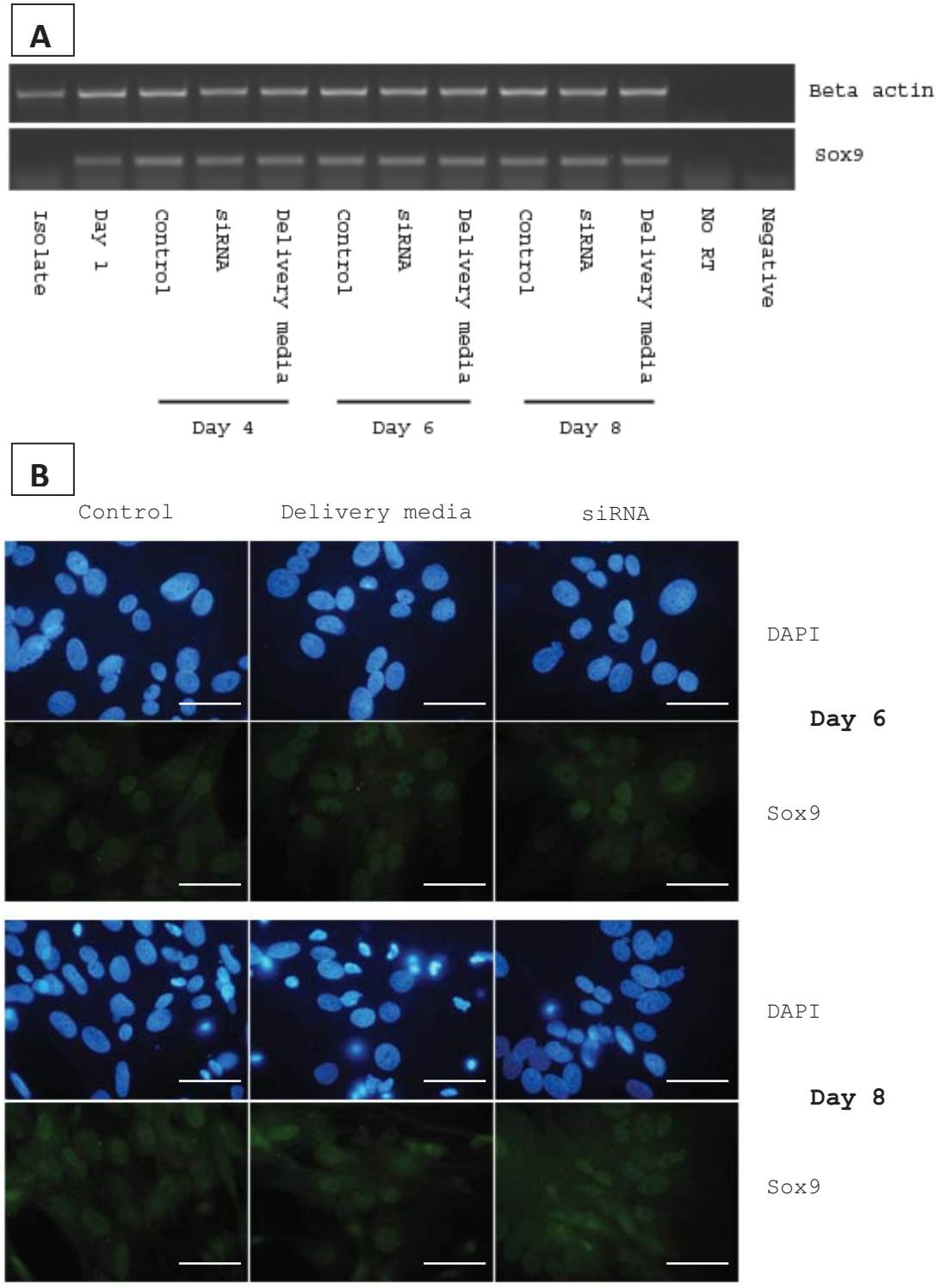

Figure 4.12: Sox9 siRNA does not cause knockdown at the mRNA or protein level. Day 1 DS hepatocytes were transferred either to siRNA delivery medium, or to delivery medium containing Sox9 siRNA. On day 4, the delivery medium and siRNA were removed and replaced with DS medium. Cells were harvested either immediately or on day 6 or day 8. RT-PCR (A) and immunostaining (B) show that there is no knockdown of Sox9 at the mRNA or protein level. Cycle numbers: *Beta actin*, 22; *sox9*, 26. Scale bar represents 50µm.

4.3 DISCUSSION

4.3.1 C/EBPα is required to maintain lineage commitment in adult hepatocytes

C/EBPα, in contrast to HNF1β, Foxa2, HNF4 and HNF6, is rapidly downregulated during hepatocyte dedifferentiation. This occurs concurrently with inhibition of *cps1* and *gck*, both C/EBPα targets (*Figure 3.3*, *Figure 3.4*). However loss of C/EBPα activity not only promotes dedifferentiation, it is also a necessary prerequisite for the induction of duct genes. When C/EBPα is reexpressed in dedifferentiating cells, expression of *sox9* is inhibited. *Osteopontin* and *ck19* are also repressed, likely as a consequence of reduced *sox9* expression. C/EBPα therefore has two separate activities. First, it transcriptionally activates liver-specific targets genes; and second, it maintains lineage commitment in adult hepatocytes by repressing *sox9*. HNF6 and C/EBPα are required for segregation of the hepatobiliary lineages during development (Clotman *et al.* 2005; Yamasaki *et al.* 2006), but a role in lineage commitment of adult cells has not previously been described for any other liver-enriched transcription factor.

There are several additional examples of transcription factors that maintain lineage commitment. In pro-B cells, the transcription factor Pax5 maintains both B-lymphoid gene expression and lineage commitment, echoing the role played by C/EBPα in hepatocytes. Mikkola *et al*. (2002) identified this dual function by conditionally deleting *pax5* in committed pro-B cells sorted from the bone marrow of *CreED-30*; $pax5^{flox/flox}$ mice. *CreED-30*; $pax5^{flox/flox}$ animals express a Cre recombinase fusion protein specifically in B lymphocytes, which deletes the floxed *pax5* locus upon activation by 4-hydroxytamoxifen. *Pax5* deleted pro-B cells ($pax5^{\Delta/\Delta}$) downregulate Pax5-dependent B-lymphocyte genes such as *CD19*, and in addition reacquire multilineage potential. In the presence of the myeloid cytokine M-CSF, for example, *in vitro*-cultured $pax5^{\Delta/\Delta}$ pro-B cells differentiate into macrophages. Furthermore, $pax5^{\Delta/\Delta}$ pro-B cells injected into T-cell deficient mice can fully reconstitute T cell development, despite being unable to generate B-cells (Mikkola *et al.* 2002).

FoxL2 is a further example of a transcription factor required to maintain lineage commitment in adult cells. In R26CreERT2; *foxl2*$^{flox/flox}$ mice, which ubiquitously induce Cre recombinase activity in response to tamoxifen, deletion of *foxl2* causes transdifferentiation of granulosa cells (somatic cells that support the oocytes), to male-specific Sertoli cells. *Foxl2* ablation is immediately followed by induction of Sox9, which is necessary and sufficient for testis differentiation. Therefore FoxL2 is required to block Sox9-mediated differentiation of Sertoli cells in adult granulosa cells (Uhlenhaut *et al.* 2009). FoxL2 represses *sox9* directly by binding to a *cis*-regulatory element that mediates testis-specific expression (TESCO) (Sekido and Lovell-Badge 2008).

The activities of C/EBPα, Pax5 and FoxL2 prove that maintenance of lineage commitment in adult cells is an active process requiring continuous repression of alternative transcriptional programs by cell type-specific transcription factors. As a direct consequence, lineage commitment is reversible; even terminally differentiated cells, in the absence of a single transcription factor, can induce lineage-promiscuous gene expression.

4.3.2 Dedifferentiation facilitates reprogramming because lineage-instructive transcription factors often repress alternative fates.

The observation that C/EBPα-mediated repression of *sox9* maintains lineage commitment in adult hepatocytes explains why dedifferentiation, which involves loss of C/EBPα, results in activation of ductal genes. Bifunctional transcription factors like C/EBPα, Pax5 and FoxL2, which both activate lineage-specific genes and repress conflicting expression programs, are prevalent. Therefore dedifferentiation will often be coupled with loss of lineage commitment, and so may facilitate reprogramming in a range of tissue contexts.

Repression of bifunctional transcription factors that maintain lineage commitment can be achieved by overexpression of a negative regulator, as well as by dedifferentiation. Ectopic expression of Sox9 in differentiated hepatocytes, for example, both activates duct genes and represses C/EBPα (see *figures 4.2* and *4.3*). Similarly, Pax5 is inactivated during C/EBPα-mediated conversion of B cell

precursors to macrophages (Xie *et al.* 2004). In both systems, the silenced endogenous transcription factor functions both to activate genes characteristic of the existing cell fate and repress those associated with the target fate. Thus overexpression of a single transcription factor can replace dedifferentiation in reversing lineage commitment and facilitating reprogramming.

4.3.3 Mutual antagonism of C/EBPα and Sox9 may maintain lineage commitment of both hepatocytes and duct cells

C/EBPα and Sox9 are mutually antagonistic (*Figures 4.3 and 4.5*) and activate cell type-specific genes in hepatocytes and duct cells respectively. The major advantage of this cross-regulatory system is that it allows tight coordination between mutually exclusive transcriptional programs. That is, expression of hepatocyte genes is directly coupled to repression of duct genes, and vice versa. Lineage commitment of hepatocytes and duct cells may therefore depend on the ratio of C/EBPα and Sox9 expression.

4.3.4 Mutual antagonism of C/EBPα and Sox9 may determine hepatoblast fate

Reciprocal repression of C/EBPα and Sox9 is a feature of embryonic liver as well as adult hepatocytes. In wildtype livers, C/EBPα is downregulated in biliary cells by e18.5. However in *Alfp-Cre; sox9*$^{fl/fl}$ animals, C/EBPα persists on both the portal and parenchymal sides of primitive ductal structures (Antoniou *et al.* 2009). Conversely, Sox9 is upregulated in *Alfp-Cre*; *cebpα*$^{fl/fl}$ livers at e12.5 (Z. Burke, unpublished data). Therefore, in addition to maintaining commitment of adult hepatocytes and duct cells, reciprocal repression of C/EBPα and Sox9 may determine the fate of hepatoblasts during embryonic liver development.

Cross-antagonism of lineage-instructive transcription factors is an important developmental mechanism that often underlies binary differentiation of progenitor cells. In haematopoiesis, for example, an antagonistic interaction between PU.1 and GATA1 controls differentiation of myeloerythroid precursors into myeloid and erythroid lineages (Graf and Enver 2009). PU.1 and GATA1 activate the myeloid

and erythroid programs respectively. In addition, however, direct protein-protein interaction allows each factor to repress the transcriptional activity of the other. PU.1 inhibits the erythroid program by binding target-bound GATA1 and organising a repressive complex composed of retinoblastoma protein, the H3K9 methyltransferase suppressor of variegation 3-9 homolog (Suv39h) and HP1 (Rekhtman *et al.* 1999) (Stopka *et al.* 2005). Conversely, binding of GATA1 to PU.1 competitively displaces the PU.1 cofactor c-Jun, thus inhibiting PU.1 activity and repressing myeloid differentiation (Zhang *et al.* 1999) (Nerlov *et al.* 2000).

A parallel of GATA1:PU.1 antagonism may regulate differentiation of vascular smooth muscle and skeletal muscle from multipotent cells of the dorsal somite (dermomyotome) (Lagha *et al.* 2009). The dermomyotome coexpresses Foxc2 and Pax3, which promote smooth muscle and skeletal fate respectively. In the absence of Foxc2, the dorsal aorta is formed, but cells in the position of smooth muscle cells fail to repress Pax3 and do not acquire vascular fate. Conversely, in explant cultures, inhibition of wingless-related (Wnt) signalling results in repression of Pax3 and upregulation of Foxc2, which in turn mediates increased differentiation of vascular smooth muscle at the expense of skeletal muscle. Skeletal muscle differentiation is restored by Foxc2 siRNA, highlighting the importance of the Foxc2:Pax3 ratio in determining progenitor fate (Lagha *et al.* 2009).

4.3.5 Reciprocal antagonism of C/EBPα and Sox9 may explain the liver phenotype of C/EBPα knockout mice

Biliary differentiation is usually confined to periportal hepatoblasts. However in *cebpα* knockout mice, pseudoglandular structures that coexpress hepatocyte and biliary markers develop throughout the liver parenchyma (Yamasaki *et al.* 2006). Yamasaki *et al*. (2006) suggest that this ectopic expression of ductal genes is a result of elevated expression of HNF6 and its target *HNF1β*. However *sox9* is induced in e12.5 *Alfp-Cre*; *cebpα*$^{fl/fl}$ livers compared to *cebpα*$^{fl/fl}$ controls, coinciding with the apprearance of pseudoglandular structures (Z. Burke, unpublished data) (Yamasaki *et al.* 2006). The permissive effect of C/EBPα repression on ductal differentiation may therefore depend primarily on induction of *sox9*.

4.3.6 C/EBPα-mediated repression of *sox9* occurs at the level of transcription

C/EBPα-mediated repression of *sox9* occurs not only in the liver, but also during differentiation of keratinocytes. Lopez *et al*. (2009) investigated the role of C/EBPs in the epidermis by generating conditional mutant mice that lacked epidermal expression of C/EBPα and C/EBPβ. A single intact allele of either *cebpα* or *cebpβ* was sufficient to rescue the mutant phenotype. Therefore mutational analysis of C/EBPα could be achieved by replacing a single conditional *cebpα* allele with either a control knock-in wildtype allele, or alleles carrying mutations that disabled E2F interaction (BRM2), or both DNA binding and E2F interaction (KK). In wildtype epidermis, Sox9 is restricted to hair follicle bulge stem or progenitor cells. However in BRM2 and KK mutants, Sox9 was ectopically expressed by interfollicular keratinocytes in both the basal and suprabasal layers of the epidermis (Lopez *et al.* 2009). The BRM2 mutation affects a non DNA binding residue in the basic region of C/EBPα, suggesting that C/EBPα represses Sox9 through protein-protein interaction. However in dedifferentiated hepatocytes, C/EBPα represses Sox9 at the level of transcription. Consistent with this observation, the 5' upstream region of *sox9* contains predicted C/EBPα binding sites (GCAA) (www.genomatrix.de). It is therefore probable that C/EBPα directly represses the *sox9* promoter, and that this DNA binding activity is impaired in BRM2 mutants.

4.3.7 Summary

C/EBPα and Sox9 activate hepatocyte and duct-specific gene expression respectively, and in addition are mutually antagonistic. The C/EBPα-mediated repression of *sox9* maintains lineage commitment of adult hepatocytes by blocking activation of the ductal program. Therefore dedifferentiation, which involves downregulation of C/EBPα, promotes reprogramming of hepatocytes to duct-like cells. Mutual antagonism of lineage-activating transcription factors is found in a range of tissue contexts, suggesting that dedifferentiation may commonly facilitate interconversion of differentiated cell types.

Chapter 5
The role of chromatin and extracellular signalling in hepatocyte reprogramming

5.1 BACKGROUND

Differential gene expression during development is partly controlled by extracellular signalling molecules that bind to receptors in the plasma membrane of target cells. Information is transmitted from the bound receptor to the nucleus by signal transduction cascades, which function primarily to activate specific transcription factors (Lodish 2004). Expression of *sox9* in dedifferentiated hepatocytes is regulated endogenously by C/EBPα. However exogenous signalling molecules are also likely to contribute to gene activation, and may do so via other transcription factors. TGFβ, for example, upregulates Sox9 in a hepatoblast cell line derived from e14.5 livers (Bipotential mouse embryonic liver cells (BMEL) (Strick-Marchand and Weiss 2002)). This is associated with repression of the hepatoblast markers HNF4, albumin, apolipoprotein AII and transthyretin, and also with induction of osteopontin, an early ductal marker (Antoniou *et al.* 2009). *In vivo*, TGFβ2 and TGFβ3 bind to ductal plate cells, and later to cells on the parenchymal side, but not the portal side, of asymmetrical primitive ductal structures. TGFβ receptor type II (TGFβRII) is also present only on the parenchymal side of primitive ductal structures, but is absent in mature ducts (Antoniou *et al.* 2009). These data indicate that TGFβ signalling promotes biliary differentiation of hepatoblasts to generate symmetrical ducts lined completely by BECs. In *Alfp-Cre*; *sox9*$^{fl/fl}$ livers, TGFβRII is expressed on both the parenchymal and portal sides of primitive ductal structures, suggesting that Sox9 is both regulated by and regulates TGFβ signalling (Antoniou *et al.* 2009).

Notch signalling has also been implicated in modulation of *sox9* expression and biliary development. Conditional mutation of *recombination signal binding protein for immunoglobulin kappa J region* (*rbpj*), a key Notch effector, in hepatoblasts (*Foxa3-Cre*; *Rbpj*$^{fl/\Delta}$) results in a reduced number of Sox9-positive ductal plate cells at e16.5 and bile ducts at P0. If *rbpj* is inactivated later in development (*Afp-Cre*; *Rbpj*$^{fl/\Delta}$), the ductal plate forms normally, but the number of postnatal bile ducts is reduced (Zong *et al.* 2009). Notch signalling is therefore required for both

acquisition of biliary fate and ductal morphogenesis. Consistent with these loss-of-function analyses, constitutive activation of Notch signalling (*Afp-Cre*; *Rosa*$^{NICD/+}$) gives rise to ectopic Sox9 expression throughout the liver lobules and tubule formation in the liver parenchyma. The *sox9* promoter is bound by the Notch intracellular domain (NICD) in *Afp-Cre*; *Rosa*$^{NICD/+}$ livers, implying that Notch signalling directly activates *sox9* (Zong *et al.* 2009).

Notch not only directs duct development, but also induces ductal markers, including Sox9, in postnatal hepatocytes (*Albumin-CreER*; *Rosa*$^{NICD/+}$). Notch signalling may therefore mediate expression of ductal genes in dedifferentiated hepatocytes by directly activating *sox9* (Zong *et al.* 2009). The following analyses are designed to investigate this possibility and also to establish the contribution of TGFβ signalling to duct gene induction. Given the fundamental importance of chromatin-level mechanisms in controlling cell-type specific gene expression and reprogramming (see *Chapter 1*, *Section 1.7*), the second part of the chapter will address the role of histone modification, nucleosome remodelling and DNA methylation in dedifferentiation and the activation of ductal gene expression.

5.2 RESULTS

5.2.1 Jag1 is upregulated in dedifferentiated hepatocytes

Notch signalling can directly induce *sox9* in postnatal hepatocytes (Zong *et al.* 2009), suggesting that it may also activate duct gene expression during hepatocyte dedifferentiation. Both Notch ligands and their receptors are encoded by gene families, but genetic analysis in mice indicates that the Jag1 ligand and the Notch2 receptor are the most important Notch components in the context of bile duct development (McCright *et al.* 2002). Expression of *jag1* and *notch2* was therefore analysed by RT-PCR in hepatocytes cultured for 1, 3 or 5 days in KdS medium or DS medium (*Figure 5.1*). *Jag1* was upregulated in dedifferentiated cells compared to differentiated cells, implying that reprogramming of hepatocytes may depend on Notch signalling. *Notch2* was equally expressed in differentiated and dedifferentiated hepatocytes.

5.2.2 Exogenous Jag1 and ActivinA may not be biologically active when applied to dedifferentiated hepatocytes

As *sox9* is a target of TGFβ signalling as well as Notch signalling, dedifferentiated hepatocytes were treated on day 1 with 10ng/ml Jag1, 10ng/ml of the TGFβ agonist ActivinA, or a combination of both. RT-PCR analysis of cells harvested on day 3 or day 5 showed that *sox9* expression was not upregulated in response to either factor (*Figure 5.2*). To investigate whether induction of *sox9* could be blocked by antagonising Notch or TGFβ signalling, day 1 dedifferentiated hepatocytes were treated with 25μM DAPT (a gamma-secretase inhibitor), 15μg/ml anti-TGFβ (designed to neutralise the biological activity of TGFβ1, TGFβ1.2, TGFβ2, TGFβ3 and TGFβ5), or a combination of both.. None of these treatments downregulated expression of *hairy and enhancer of split 1* (*hes1*), a known target of Notch and TGFβ signalling, suggesting that DAPT and anti-TGFβ did not modulate signalling under the conditions described (*Figure 5.3*).

5.2.3 Nuclear area increases during dedifferentiation

Signalling cascades and transcription factors regulate gene expression in part by modulating the chromatin environment. When mouse embryonic stem cell nuclei are injected into an amphibian oocyte germinal vesicle, their nuclear volume increases by about 30 times and chromatin is decondensed (Gurdon and Melton 2008). To investigate whether hepatocyte reprogramming similarly relies on large-scale reorganisation of chromatin structure, the nuclei of differentiated and dedifferentiated hepatocytes were DAPI stained and the mean nuclear area for each cell type was calculated using ImageJ software (*Figure 5.4*). Figure 5.4 shows that the nuclei of dedifferentiated cells were significantly larger than those of differentiated cells.

5.2.4 Trichostatin A does not substantially affect hepatocyte reprogramming

Acetylation of H4K16 inhibits formation of compact 30nm chromatin fibres (Shogren-Knaak *et al.* 2006), suggesting that histone acetylation may underlie decompaction of chromatin in dedifferentiated cells. Global histone hyperacetylation can be induced experimentally by the small molecule histone deacetylase inhibitor TSA. Previous studies have shown that TSA maintains expression of C/EBPα in primary rat hepatocytes (Henkens *et al.* 2007) and induces Sox9 expression in human fetal hepatocytes (Hanley *et al.* 2008). Dedifferentiated hepatocytes were treated with 10μM TSA on day 1 and day3, and cells were harvested on day 3 or day 5. RT-PCR analysis showed that TSA had no effect on expression of *cebpα*, *sox9* or downstream duct genes, but did upregulate *cps1* (*Figure 5.5*).

5.2.5 Immunostaining for histone modifications is not informative

To further investigate the mechanism of nuclear decondensation, hepatocytes were cultured for 24 hours or 5 days in KdS medium, or for 5 days in DS medium and immunostained for the histone modifications H3Ac, H3K4me2 and H3K9me2 (*Figure 5.6*). The results are difficult to interpret because the fluorescence was made

more diffuse by the larger nuclei of dedifferentiated cells independently of the abundance of the histone modification.

5.2.6 Optimisation of chromatin immunoprecipitation

Immunostaining can only provide information on histone modification at the level of the whole genome. To investigate dedifferentiation-associated changes in chromatin structure specifically at the *sox9* promoter, ChIP was used. The resolution of ChIP experiments depends on the fragment size of the immunoprecipitated DNA, which is usually in the range 200bp-500bp. The most important determinants of DNA fragment size are the concentration of formaldehyde used in cross-linking and the number of sonication pulses. These parameters were optimised by testing 1%, 0.5% and 0.2% formaldehyde combined with 5, 10, 15 or 20 x 5 second pulses of sonication. In order to achieve 500bp resolution, it was necessary to reduce the amount of formaldehyde used in the cross-linking step from the standard 1% to 0.2% and sonicate the cross-linked material 10 times for 5 seconds at 60% amplitude (*Figure 5.7*). DNA fragments derived from differentiated and dedifferentiated cells were equally sized under these conditions, allowing a direct comparison of the two cell types (*Figure 5.8*). The enrichment of selected histone modifications at the *sox9* promoter was quantified by real-time PCR. Melting curve analysis of the amplification reaction did not show any evidence of non-specific amplification or primer dimer formation (*Figure 5.9*).

5.2.7 Activation of *sox9* in dedifferentiated hepatocytes is not associated with histone modification at the promoter

H3Ac and H3K4me2 correlate with transcriptional activity, while H3K9me2 and H3K27me3 are localised at silent genes (Ruthenburg *et al.* 2007). Enrichment of each of these modifications at the *sox9* promoter was compared in day 5 differentiated and dedifferentiated hepatocytes by ChIP (*Figure 5.10*). Figure 5.10 shows that activation of *sox9* during dedifferentiation does not occur in conjuction with histone modification.

5.2.8 The ratio of Brm to Brg1 changes during reprogramming

As activation of duct genes in dedifferentiated hepatocytes does not appear to require histone modification, reprogramming may instead depend on the activity of chromatin remodellers. To investigate this possibility, nuclear extracts were prepared from hepatocytes cultured in KdS or DS medium for 1, 3 or 5 days, and the abundance of Brm and Brg1 was determined by western blotting (*Figure 5.11*). In comparison to KdS hepatocytes on day 1, Brm expression was reduced in KdS hepatocytes on day 5 and in DS hepatocytes on days 3 and 5. Given that induction of Sox9 is sometimes apparent in day 5 KdS cells (see *Chapter 3*, *section 3.2.4*), downregulation of Brm may correlate with dedifferentiation. Brg1, in contrast, was upregulated in dedifferentiated hepatocytes compared to differentiated hepatocytes.

5.2.9 5-azacytidine may not provoke DNA demethylation in dedifferentiated hepatocytes

DNA methylation is a major mechanism of epigenetic gene repression. The small molecule 5-azacytidine inhibits DNA methyltransferases and was therefore used to test for involvement of DNA methylation in regulating gene expression during hepatocyte reprogramming. Dedifferentiated hepatocytes were treated from day 1 with 10μM 5-azacytidine and harvested for RT-PCR analysis on day 3 or day 5 (*Figure 5.12*). Figure 5.12 shows that 5-azacytidine failed to prevent repression of *cebpα*, or to facilitate activation of *sox9* in hepatocytes. However as 5-azacytidine-mediated demethylation is passive, this lack of activity may have been due to a low rate of proliferation in dedifferentiated hepatocytes.

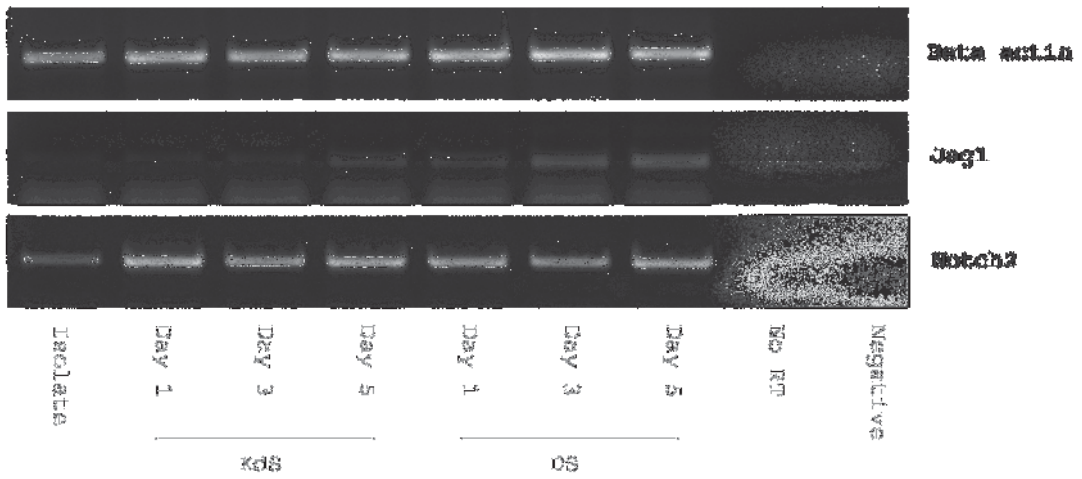

Figure 5.1: *Jag1* is upregulated during hepatocyte dedifferentiation. Hepatocytes were cultured in either KdS medium or DS medium and total RNA was extracted on day 1, 3 or 5. 5µg of RNA was DNase-treated, of which 2µg was reverse transcribed. 100ng of cDNA was amplified by PCR using specific primers. *Jag1*, but not *notch2*, is upregulated in dedifferentiated cells. Controls included freshly isolated hepatocytes (Isolate) and reactions without reverse transcriptase (No RT) or without sample (Negative). Cycle numbers: *Beta actin*, 22; *jag1*, 30; *notch2*, 30.

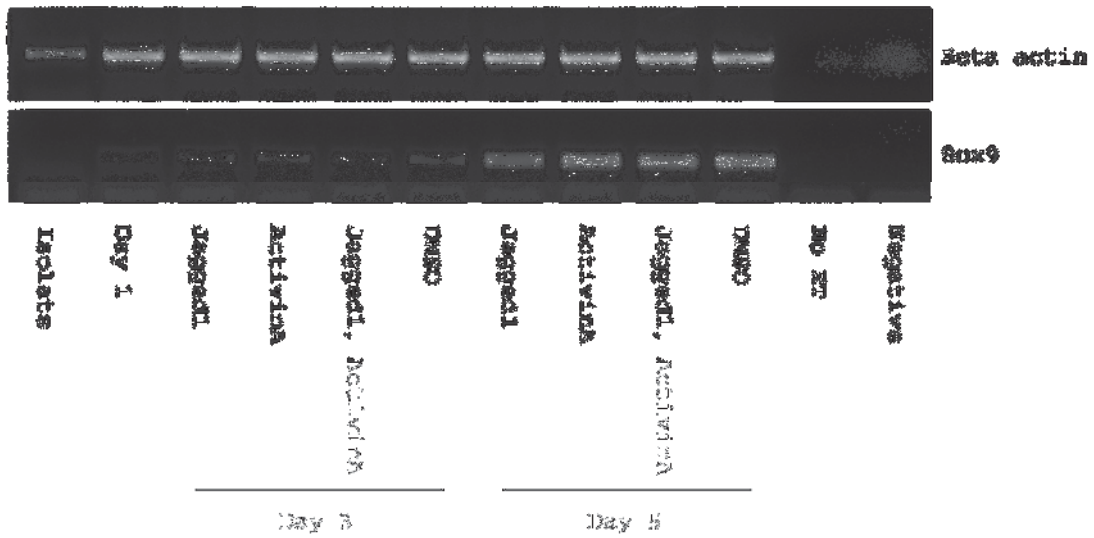

Figure 5.2: Exogenous Jag1 and ActivinA may not be biologically active when applied to dedifferentiated hepatocytes. Hepatocytes were cultured in DS medium, and treated on day 1 with 10ng/ml Jagged1, 10ng/ml ActivinA or both. The signalling molecules were reapplied on day 3, and total RNA was extracted on day 3 or day 5. 5µg of RNA was DNase-treated, of which 2µg was reverse transcribed. 100ng of cDNA was amplified by PCR using specific primers. Jagged1 and ActivinA may not be biologically active when applied to dedifferentiated hepatocytes under these conditions. Cycle numbers: *Beta actin*, 22; *sox9*, 27.

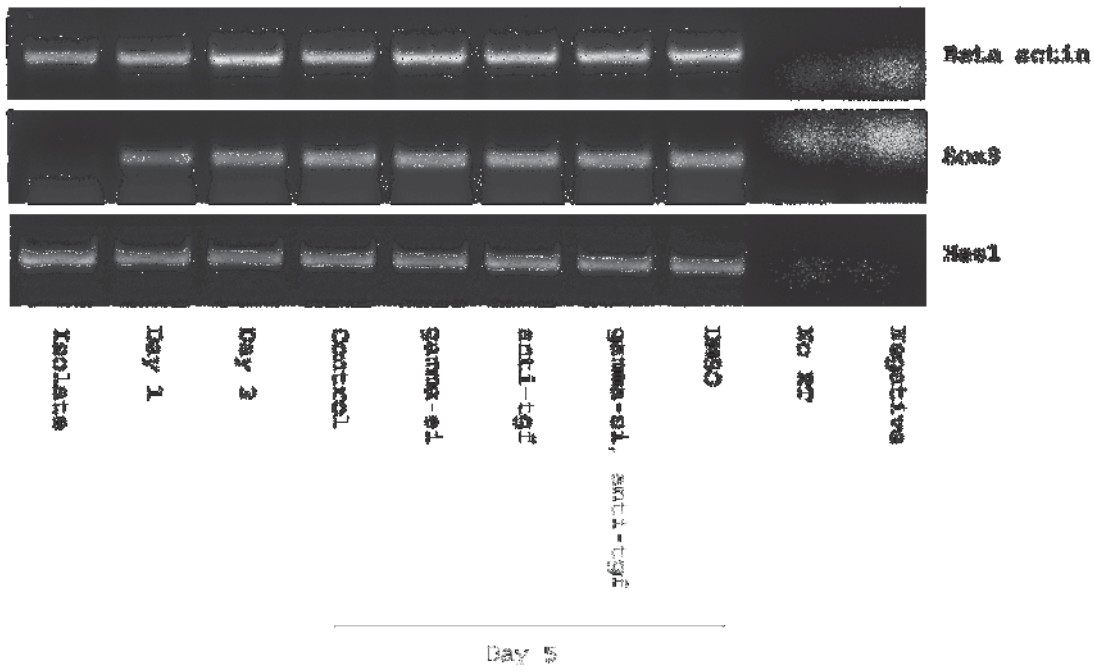

Figure 5.3: DAPT and anti-TGFβ have no biological activity when applied to dedifferentiated hepatocytes. Hepatocytes were cultured in DS medium, and treated on day 1 with 25µm N-[N-(3,5-Difluorophenacetyl-L-alanyl)]-S-phenylglycine *t*-Butyl Ester (DAPT), 15µg/ml anti-TGFβ or both. The signalling antagonists were reapplied on day 3 and total RNA was extracted on day 3 or day 5. 5µg of RNA was DNase-treated, of which 2µg was reverse transcribed. 100ng of cDNA was amplified by PCR using specific primers. Expression of *hes1*, a known target of Notch and TGFβ signalling, is not affected by DAPT or anti-TGFβ, suggesting that neither is active in dedifferentiated hepatocytes under these conditions. Cycle numbers: *Beta actin*, 22; *sox9*, 28; *hes1*, 28.

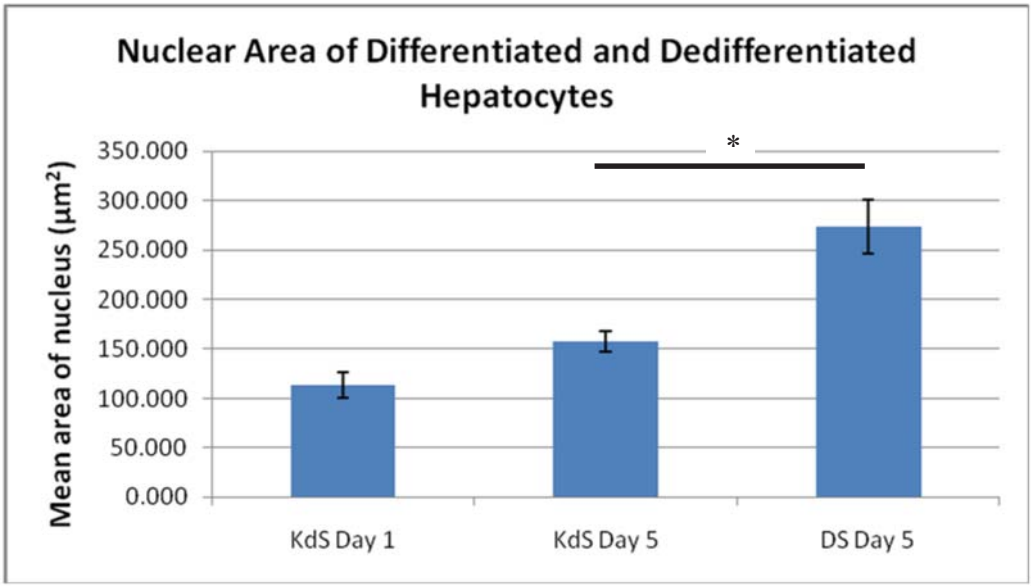

Figure 5.4: The area of hepatocyte nuclei increases during dedifferentiation. Hepatocytes were cultured in KdS medium for 24 hours or 5 days, or in DS medium for 5 days. Nuclei were DAPI stained, and the nuclear area was calculated using ImageJ software. The nuclei of dedifferentiated hepatocytes are significantly larger (T-Test, $p<0.05$) than those of differentiated hepatocytes (*). Error bars represent ± 1 standard error.

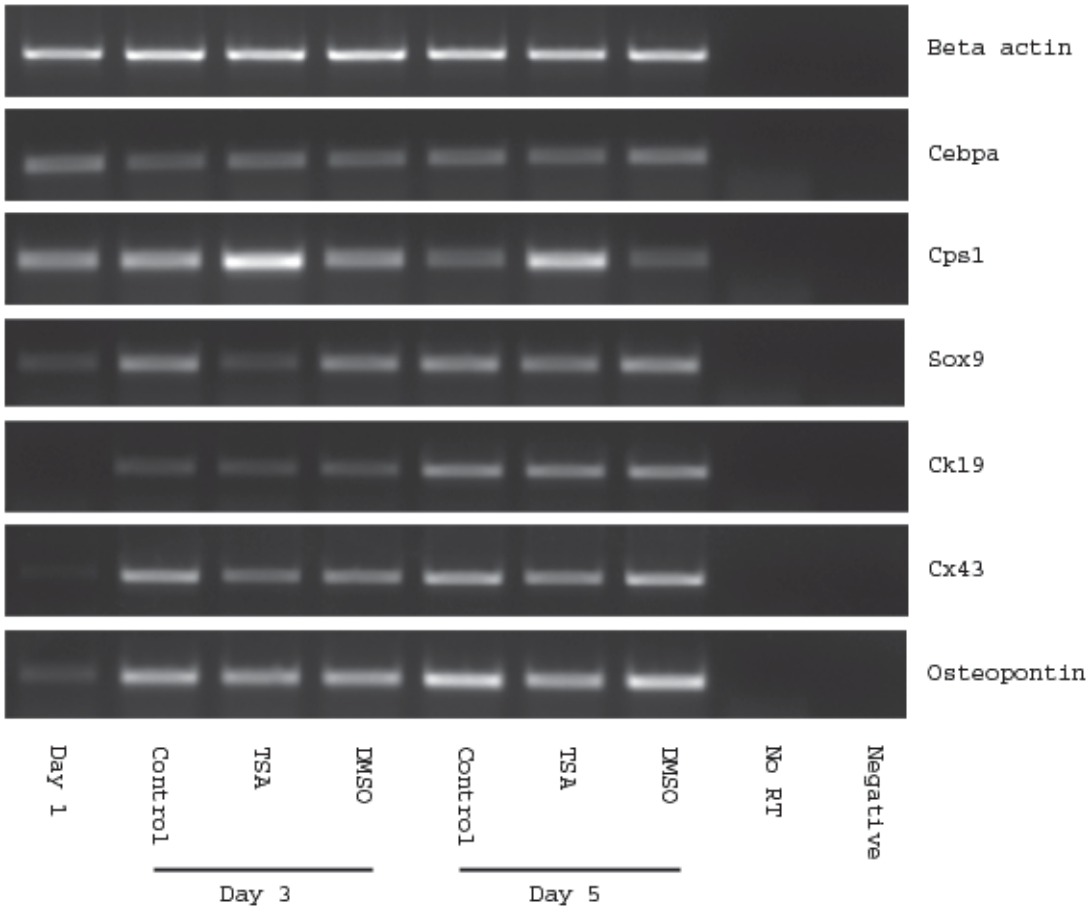

Figure 5.5: TSA upregulates *cps1* in dedifferentiated hepatocytes but has a negligible effect on expression of duct genes. Dedifferentiated hepatocytes were treated on day 1 with 10μM trichostatinA. The compound was reapplied on day 3 and total RNA was extracted on day 3 or day 5. 5μg of RNA was DNase-treated, of which 2μg was reverse transcribed. 100ng of cDNA was amplified by PCR using specific primers. TSA upregulates *cps1* but has a negligible effect on duct gene transcription. Cycle numbers: *Beta actin*, 22; *cebpα*, 30; *cps1*, 30; *sox9*, 27; *ck19*, 27; *cx43*, 27; *osteopontin*, 27.

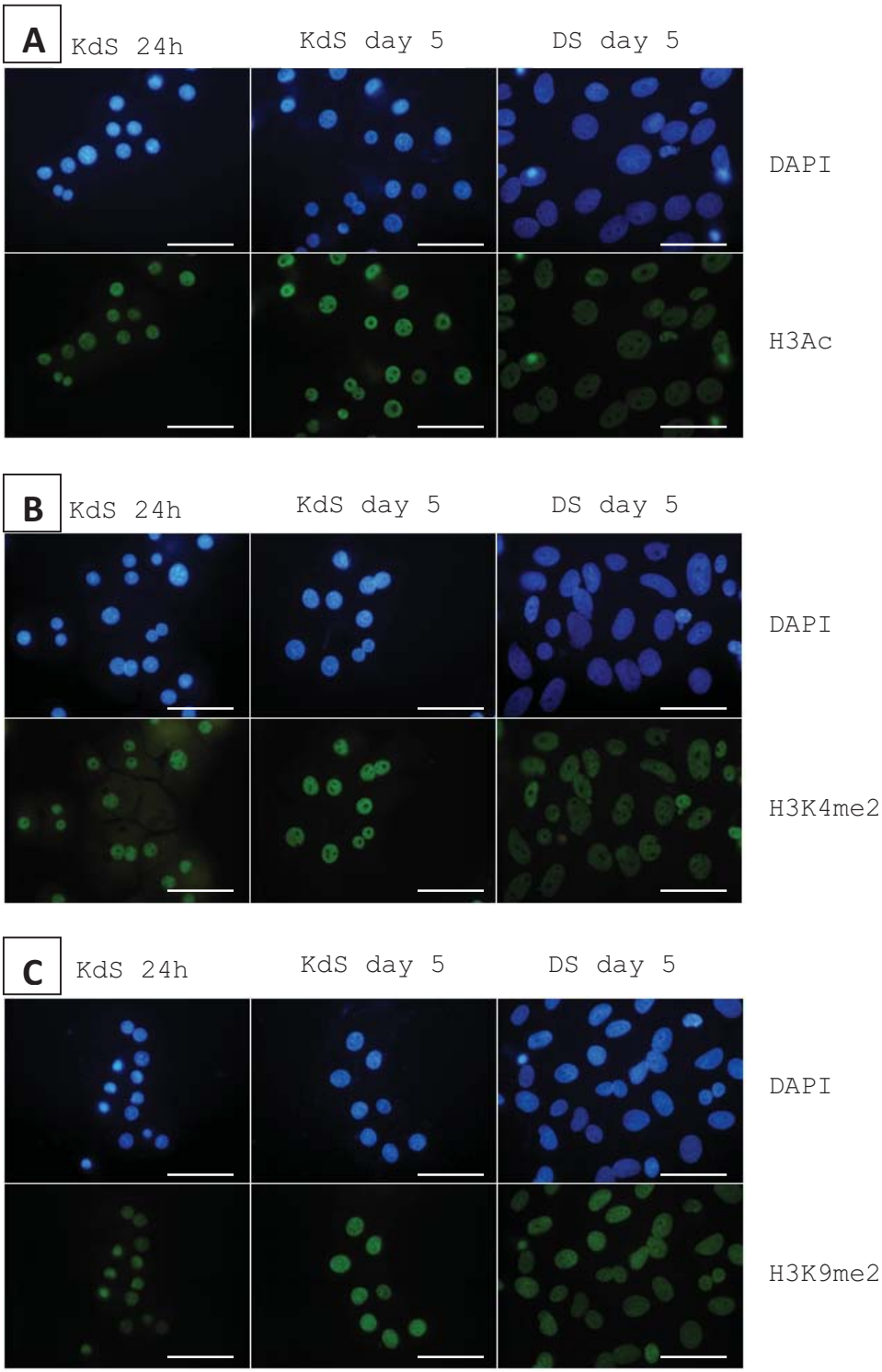

Figure 5.6: Comparative analysis of histone modifications in differentiated and dedifferentiated hepatocytes. Hepatocytes cultured in KdS medium for 24 hours or 5 days, or in DS medium for 5 days were immunostained for H3Ac (A), H3K4me2 (B) or H3K9me2 (C) (green) and counterstained with DAPI (blue). The fluorescence is more diffuse in the large nuclei of dedifferentiated hepatocytes than in the smaller nuclei of differentiated cells. Scale bar represents 50µm.

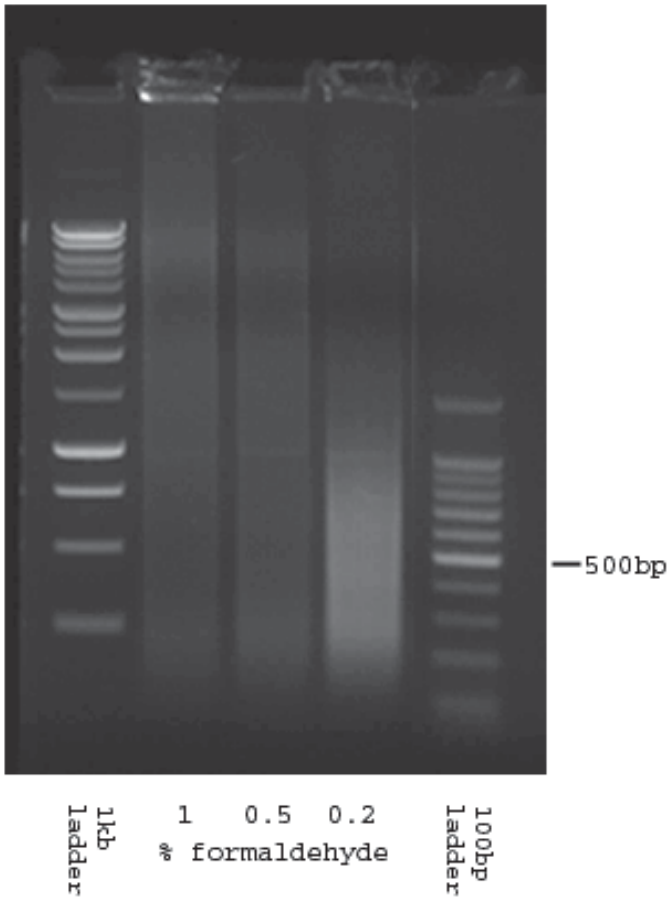

Figure 5.7: Optimisation of DNA fragment size for chromatin immunoprecipitation. Hepatocytes were cross-linked with 1, 0.5 or 0.2% formaldehyde for 10 minutes at room temperature and then lysed. The lysate was subjected to 10 x 5 second pulses of sonication at 60% amplitude with a duty cycle of 8% (each 5 second pulse was followed by 55 seconds rest). After cross-link reversal, the product was run on a 1% agarose gel and visualised with ethidium bromide. Cross-linking with 1% or 0.5% formaldehyde results in DNA fragments that range in size from 200bp to >10,000bp. Where 0.2% formaldehyde is used, DNA fragment sizes fall between 200bp and 1500bp, the majority of fragments being approximately 500bp.

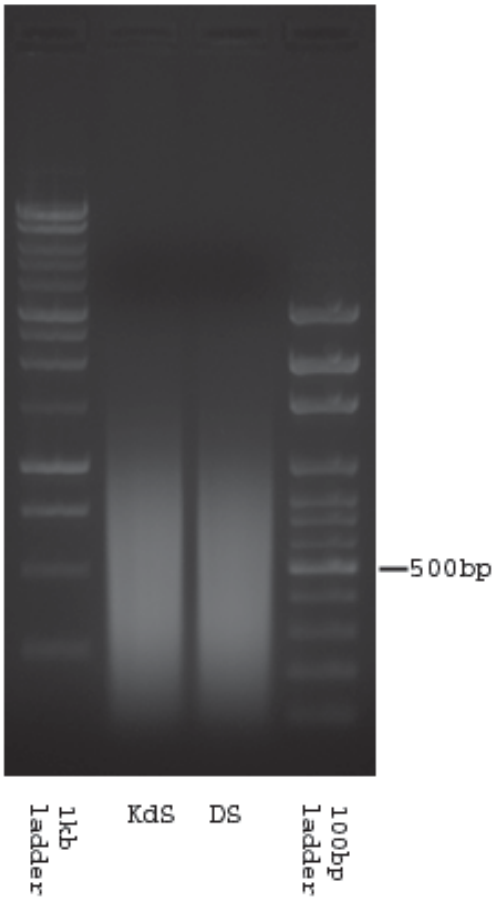

Figure 5.8: DNA fragments derived from differentiated and dedifferentiated hepatocytes are the same size. Differentiated and dedifferentiated hepatocytes were cross-linked with 0.2% formaldehyde for 10 minutes at room temperature and then lysed. The lysate was subjected to 10 x 5 second pulses of sonication at 60% amplitude with a duty cycle of 8%. After cross-link reversal, the product was run on a 1% agarose gel and visualised with ethidium bromide. The average size of DNA fragments obtained from KdS and DS cells is the same.

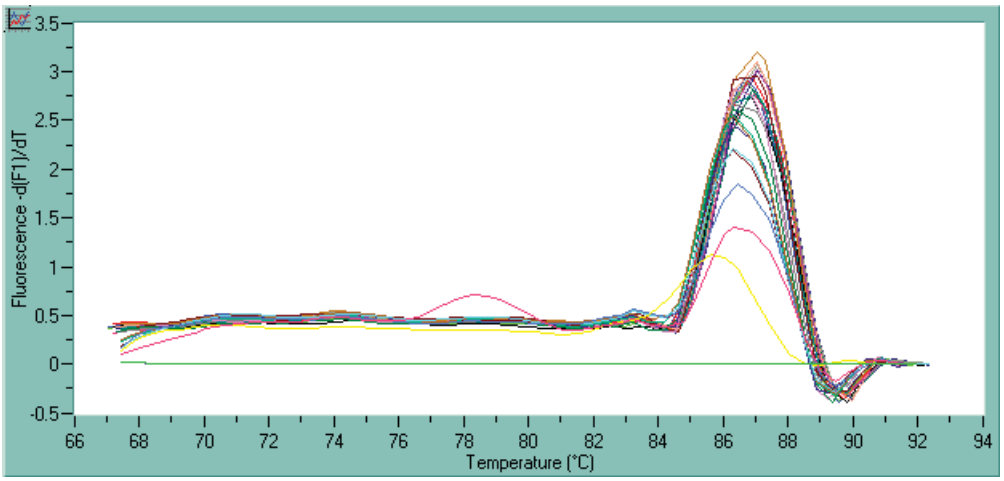

Figure 5.9: Melting curve analysis of Sox9 real-time PCR. A plot of melting behaviour reveals a single, sharply defined narrow peak representing the target PCR product. There is no evidence of primer dimer formation, which results in a second broader peak at a lower temperature than the product peak. Melting curve analysis was conducted under the following conditions: 95°C, 0s, 20°C/s; 65°C, 15s, 20°C/s; 95°C, 0s, 0.1°C/s. F1=fluorescence, T=temperature.

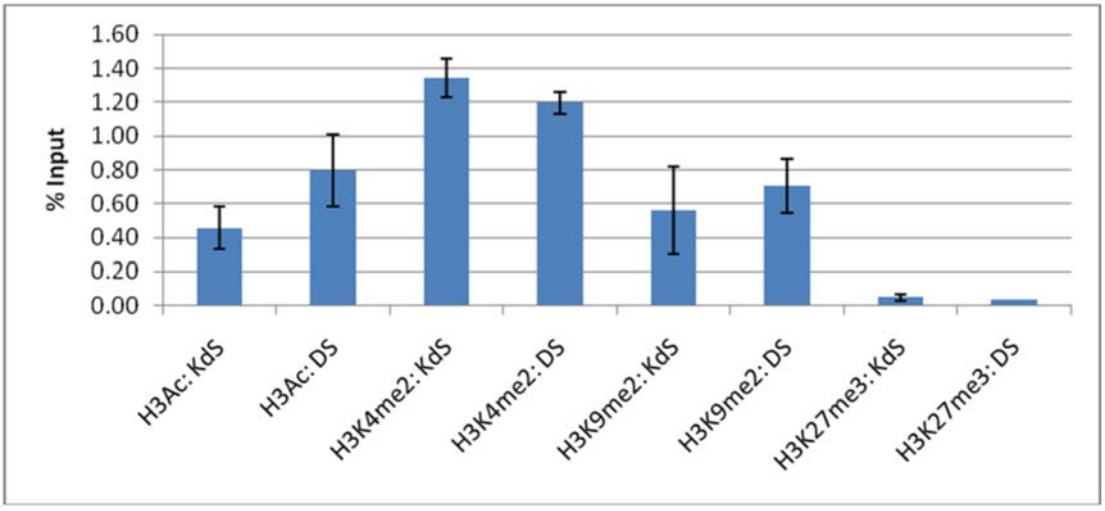

Figure 5.10: Induction of Sox9 in dedifferentiated hepatocytes is not associated with histone modification at the promoter. Hepatocytes cultured for 5 days in KdS or DS medium were cross-linked with 0.2% formaldehyde for 10 minutes at room temperature and then lysed. The lysate was subjected to 10 x 5 second pulses of sonication at 60% amplitude with an 8% duty cycle. 25ug of sonicated chromatin was incubated with 5ug of antibody overnight at 4^{o}C, and the immunoprecipitated material was collected with proteinA-agarose beads. Following elution, the formaldehyde cross-links were reversed, and protein was cleaved with proteinaseK. DNA was phenol-chloroform extracted and then ethanol precipitated. The *sox9* promoter was amplified by SYBR green real-time PCR under the following conditions: Initial denaturation: 95^{o}C, 10s, 20^{o}C/s. PCR: 95^{o}C, 5s, 20^{o}C/s; 60^{o}C, 20s, 20^{o}C/s; 40 cycles. Error bars represent ± 1 standard error.

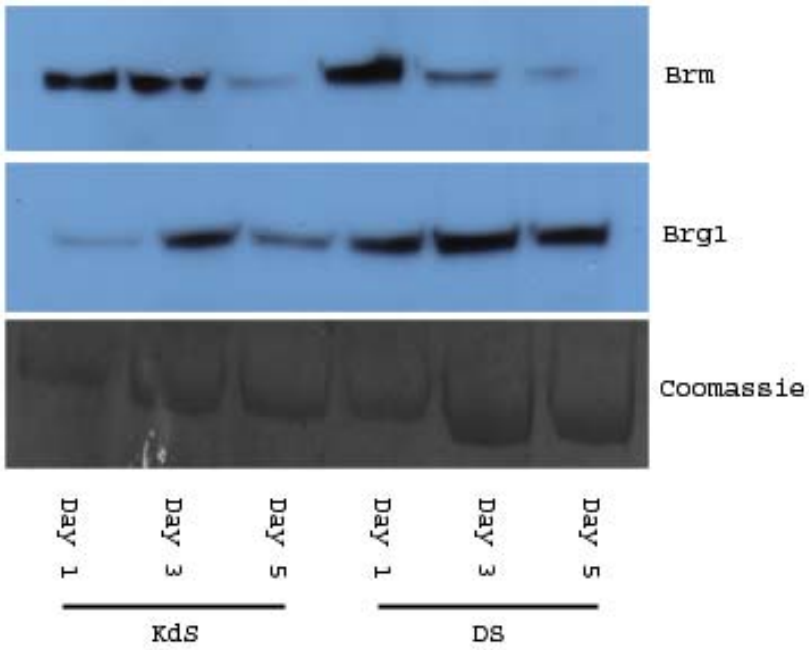

Figure 5.11: Brm is downregulated in dedifferentiated hepatocytes. Nuclear extracts were prepared from hepatocytes cultured for 1, 3 or 5 days in either KdS or DS medium. 10µg of each sample was separated by electrophoresis on a 5% Tris-HCl gel and blotted onto a PVDF membrane. Blots were probed with primary antibodies against Brm or Brg1 and then with HRP-conjugated secondary antibodies. The signal was detected by ECL chemiluminescence. Coomassie staining was used as a loading control. Brm is repressed in day 5 differentiated hepatocytes and in dedifferentiated hepatocytes on days 3 and 5. Brg1 is upregulated in dedifferentiated hepatocytes in comparison to differentiated hepatocytes.

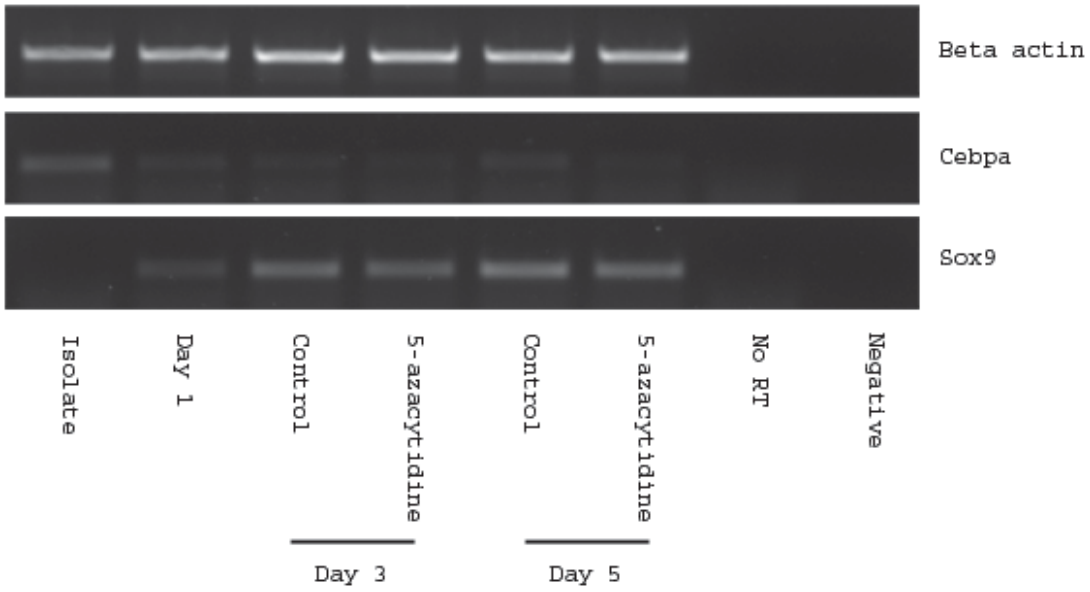

Figure 5.12: 5-azacytidine may not provoke DNA demethylation in dedifferentiated hepatocytes. Dedifferentiated hepatocytes were treated on day 1 with 10µM 5-azacytidine. The compound was reapplied every day and total RNA was extracted on day 3 or day 5. 5µg of RNA was DNase-treated, of which 2µg was reverse transcribed. 100ng of cDNA was amplified by PCR using specific primers. 5-azacytidine does not affect expression of *cebpα* or *sox9*, perhaps because it does not cause DNA demethylation in dedifferentiated hepatocytes under the conditions described. Cycle numbers: *Beta actin* 22, *cebpα* 27, *sox9*, 27.

5.3 DISCUSSION

5.3.1 Chromatin decompaction in dedifferentiated hepatocytes may occur at the level of higher-order structure

The nuclei of dedifferentiated hepatocytes are significantly larger than those of differentiated hepatocytes (*Figure 5.4*), suggesting that dedifferentiation involves global decompaction of chromatin. As activation of *sox9* is not accompanied by histone modification at the promoter (*Figure 5.10*), this global reorganisation may depend on histone modification-independent mechanisms. Francis *et al*. (2004) showed by electron microscopy that the core components of Polycomb repressive complex 1 (PCC) can induce compaction of nucleosomal arrays in a classical "beads-on-a-string" conformation into higher order structures. Interestingly, PCC can also compact arrays assembled with histones that lack N-terminal tails, thus demonstrating that PCC-meditated chromatin compaction does not require histone modifications (Francis *et al.* 2004). Decompaction of chromatin in dedifferentiated hepatocytes may therefore reflect deregulation of Polycomb repressive complex 1, or loss of an alternative transcriptional repressor that operates at the level of higher order chromatin structure, for example HP1.

5.3.2 Induction of *sox9* may depend on histone modification at an enhancer

Induction of *sox9* in the absence of promoter-localised histone modification activity is also consistent with recent work by Heintzman *et al*. (2009), who showed that the chromatin state at human promoters is largely invariant across diverse cell types. Enhancers, in contrast, were found to be marked with highly cell-type specific histone modifications. Enrichment of H3K4me1 in particular correlates with functional enhancer activity and cell-type specific gene expression (Heintzman *et al*. 2009). *Sox9* is regulated by numerous enhancers, reflecting its complex spatiotemporal expression pattern (*Figure 5.13*) (Bagheri-Fam *et al*. 2006) (Sekido and Lovell-Badge 2008). It is therefore possible that *sox9* expression in the hepatic

ducts depends on cell-type specific activation of an as yet unidentified enhancer. In this case *sox9* induction in dedifferentiated hepatocytes is likely to correlate with enhancer-localised enrichment of H3K4me1, rather than with histone modification at the promoter.

5.3.3 Sox9 may be a pioneer factor

Sox9 induces duct gene expression in both differentiated hepatocytes (*Figure 4.2*) and primary fibroblasts (*Figure 4.11*), suggesting that it can activate its targets even in a repressive chromatin environment. Sox9 is one of about twenty Sox proteins in the mammalian genome, all of which contain an approximately eighty amino acid high mobility group (HMG) domain. The crystal structure of the Sox17 HMG domain bound to DNA reveals that it is comprised of three α-helices that adopt a characteristic L-shape (*Figure 5.14*). By targeting the minor groove of the DNA, the HMG domain introduces an 80^{o} bend, widening the minor grove and compressing the major groove (Palasingam *et al.* 2009). During hepatocyte reprogramming, such dramatic remodelling of DNA architecture may facilitate recruitment of other transcription factors to the regulatory elements of duct genes, thus endowing Sox9 with pioneer activity similar to that described for FoxA transcription factors. Duct gene activation in dedifferentiated hepatocytes may be further enhanced by Sox9-mediated recruitment of the histone acetyltransferase p300, which potentiates Sox9-dependent transcription of chromatinised templates (Furumatsu *et al.* 2005).

5.3.4 Downregulation of Brm may contribute to hepatocyte dedifferentiation

Downregulation of Brm in dedifferentiated hepatocytes and day 5 differentiated hepatocytes (*Figure 5.11*) suggests that loss of Brm activity may contribute to the early stages of dedifferentiation. In support of this idea, Brm also correlates with differentiation state during development, being more highly expressed in differentiated adult hepatocytes than in embryonic liver (Inayoshi *et al.* 2006). Furthermore, Brm physically interacts with C/EBPα in adult hepatocytes and potentiates C/EBPα-mediated transactivation of the albumin promoter *in vitro*

(Inayoshi *et al*. 2006). Downregulation of both Brm and C/EBPα during dedifferentiation may therefore combine to inhibit transcriptional activation of C/EBPα targets such as *cps1* and *gck*. The importance of chromatin remodelling in hepatocyte differentiation is also highlighted by deletion of BAF47, a core SWI/SNF subunit, in developing liver (*Alb-Afp-Cre; Baf47*$^{fl/-}$). Mutant livers fail to activate 70% of genes that are normally upregulated during liver development, including those involved in glycogen synthesis, gluconeogenesis and cell-cell adhesion (Gresh *et al.* 2005). In addition, hepatocyte proliferation is increased, according with the observation that Brm is required for C/EBPα-mediated proliferation arrest in SWI/SNF-defective cells (Muller *et al.* 2004). Downregulation of Brm during dedifferentiation may therefore contribute to cell cycle re-entry as well as reduced transcription of liver genes.

5.3.5 Summary

Activation of ductal genes in dedifferentiated hepatocytes is likely to depend on extracellular signalling as well as endogenous transcription factors. However induction of *sox9* is not enhanced by TGFβ or Notch ligands under the experimental conditions adopted here. Chromatin-mediated control of gene transcription may contribute to reprogramming as dedifferentiation correlates with downregulation of the chromatin remodeller Brm and with an increase in nuclear area. However activation of *sox9* does not require promoter-localised histone modification.

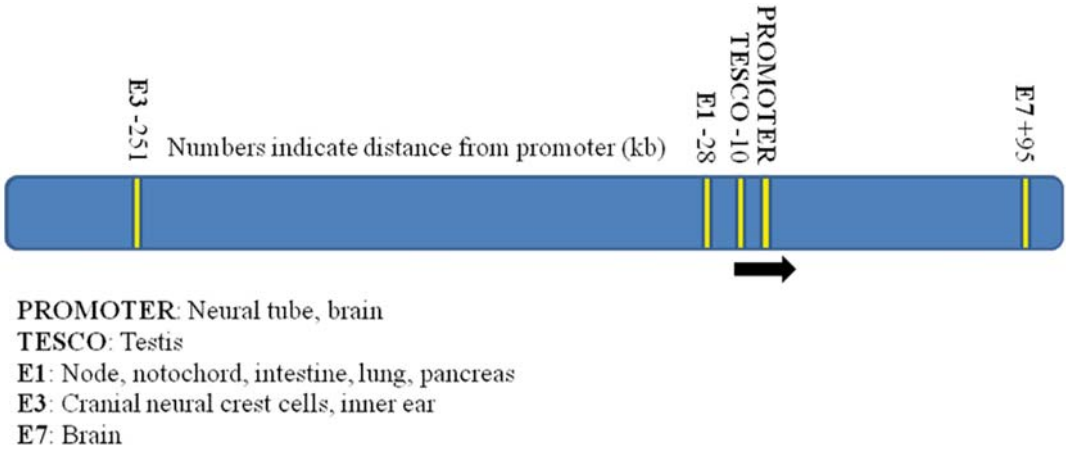

Figure 5.13: Sox9 enhancers. Sox9 is regulated by numerous upstream and downstream enhancers that facilitate expression in multiple different cell types (Bagheri-Fam *et al.* 2006) (Sekido and Lovell-Badge 2008).

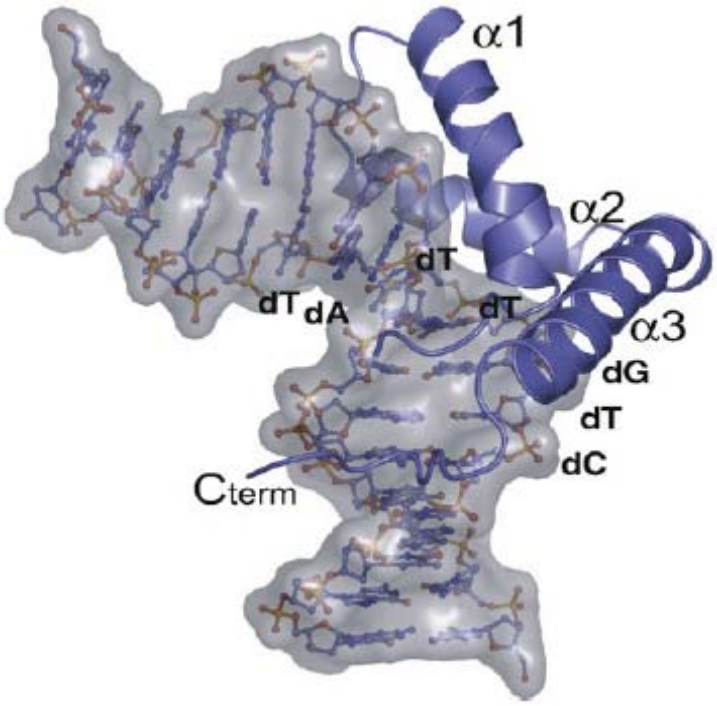

Figure 5.14: Model of the Sox17 HMG domain bound to DNA. DNA and the Sox17 HMG domain are shown in ball-and-stick/van der Waals surface representation and as a cartoon respectively. Nucleotides of the core TATTGTC motif are labelled (Palasingam *et al.* 2009).

6. DISCUSSION

Dedifferentiation of primary hepatocytes has been considered simply as a hindrance to their use as an *in vitro* model of liver function. However the results presented here demonstrate that hepatocyte dedifferentiation also provides a useful model of cellular reprogramming. In addition to progressively downregulating hepatocyte-specific genes, dedifferentiated hepatocytes induce ductal genes, including the ductal transcription factor Sox9. This work has identified a mutually antagonistic relationship between Sox9 and the hepatic transcription factor C/EBPα, which has implications both for the mechanism of hepatocyte lineage commitment and the therapeutic interconversion of differentiated cell types.

6.1 The mechanism of lineage commitment

The spontaneous expression of ductal genes in dedifferentiated hepatocytes supports the idea that lineage commitment is an active process requiring continuous repression of opposing gene expression profiles. In hepatocytes, lineage commitment appears to be maintained by persistent C/EBPα-mediated repression of *sox9*. As Sox9 is in turn capable of repressing *Cebpα*, mutually exclusive expression of these factors may underlie the tightly coordinated antagonism of hepatocyte and ductal programs *in vivo*.

6.2 Reprogramming of differentiated cells for cell replacement therapy

In comparison to embryonic stem cell and iPS cell-based protocols, interconversion of differentiated cell types is potentially an efficient and rapid method of generating substantial populations of cells for transplant. Reprogramming of hepatocytes to duct-like cells exhibits two features that may inform the use of differentiated cells in cell replacement therapy. Firstly, the activation of ductal, but not pancreatic gene expression in dedifferentiated hepatocytes suggests that reprogramming is likely to

be most successful when the starting and target cell types have a close developmental relationship. Secondly, the role of dedifferentiation in facilitating this conversion highlights the importance of repressing the existing gene expression profile in order to activate the target program. Where the starting and target cell types are developmentally related, transcription factors that both activate genes characteristic of the starting population, and repress genes associated with the target population may be common. Examples include C/EBPα in reprogramming hepatocytes to duct-like cells and Pax5 in reprogramming B cells to macrophages (Xie *et al.* 2004). Specific knockdown of these factors, either by siRNA or by overexpression of a negative regulator, may be used to reverse lineage commitment, relieve repression of the target program, and therefore increase the efficiency of reprogramming.

6.3 Future work

Although dedifferentiated hepatocytes induce ductal genes, expression of numerous hepatic factors, including HNF4α and UGT, is maintained. To understand the barriers that prevent resolution of this hybrid phenotype, future work should include modification of the extracellular signalling environment, or of the extracellular matrix, which has previously been shown to contribute to ductal differentiation (Nishikawa *et al.* 2005). Complete hepatocyte-BEC reprogramming may also require ectopic expression of transcription factors other than Sox9. FoxM1b, which is required for biliary differentiation of periportal hepatoblasts and IHBD formation (Krupczak-Hollis *et al.* 2004), is one possible candidate. Another is Sal-like 4 (Sall4), which is expressed in hepatoblasts but not adult hepatocytes and functions both to promote ductal differentiation and repress hepatic differentiation (Oikawa *et al.* 2009). In addition to gene expression data, functional analysis is required to monitor the extent of hepatocyte-BEC conversion. For example, the potential of reprogrammed BECs to adjust bile pH by secreting bicarbonate ions could be measured by microfluorimetry, which allows intracellular pH to be calculated from the emission intensity of a fluorescent indicator such as 2',7'-bis-(2-carboxyethyl)-5-(and-6)-carboxyfluorescein (BCECF).

Hepatocyte dedifferentiation is a complex process, potentially involving downregulation of liver-specific transcription factors other than C/EBPα. Therefore the degree to which loss of C/EBPα alone recapitulates the permissive effect of dedifferentiation on ductal gene induction should be confirmed by specific, conditional ablation of *Cebpα* in adult hepatocytes. Conditional inactivation of *Cepb*α would also make it possible to assess the relative contribution of C/EBPα repression to the downregulation of hepatic genes during dedifferentation. In addition to regulating dedifferentiation and induction of ductal genes, repression of C/EBPα may play an important role in maintaining BEC lineage commitment. This hypothesis could be tested by ectopically expressing C/EBPα in intrahepatic bile duct cells and analysing the effect on expression of ductal and hepatic genes.

More detailed analysis is required to address the nature of the interaction between C/EBPα and Sox9. As the *sox9* promoter contains C/EBPα binding sites, C/EBPα is likely to directly repress *sox9* transcription. The necessary binding of C/EBPα to the *sox9* promoter and the existence of repressive activity could be confirmed by chromatin immunoprecipitation and luciferase assay respectively. The *cebp*α promoter does not contain Sox9 binding sites, leaving open the possibility that Sox9 represses *cebp*α transcription indirectly.

Mutual antagonism of transcription factors commonly underlies binary cell fate decisions during development, suggesting that C/EBPα and Sox9 may regulate the differentiation of hepatoblasts into hepatocytes and BECs. This idea is consistent with data obtained by liver-specific deletion of *cebpα* and *sox9*, described in *section 4.3.5*. The mechanism of hepatoblast differentiation could be further elucidated using BMEL cells, which were isolated from e14 embryos and are likely to originate from hepatoblasts (Strick-Marchand and Weiss 2002). If the ratio of C/EBPα and Sox9 is a key determinant of hepatoblast fate, then adenovirus-mediated overexpression of Sox9 or C/EBPα siRNA should induce ductal differentiation. Equally overexpression of C/EBPα or Sox9 siRNA should result in hepatocyte differentiation.

6.4 Conclusion

Differentiation of specialised cell types from a totipotent zygote is a largely unidirectional process characterised by increasing commitment to a single fate (Gurdon and Melton 2008). However the results presented here show that lineage commitment is reversible and requires continuous repression of alternative gene expression profiles even in adult cells. Mutually antagonistic lineage-activating transcription factors may underlie maintenance of lineage commitment in a wide range of developmental contexts. Repression of these factors, for example by dedifferentiation, may promote successful reprogramming of differentiated cells for cell replacement therapy.

REFERENCES

Ahlgren, U., et al. (1996). "The morphogenesis of the pancreatic mesenchyme is uncoupled from that of the pancreatic epithelium in IPF1/PDX1-deficient mice." Development **122**(5): 1409-1416.

Antoniou, A., et al. (2009). "Intrahepatic Bile Ducts Develop According to a New Mode of Tubulogenesis Regulated by the Transcription Factor SOX9." Gastroenterology **136**(7): 2325-2333.

Aoi, T., et al. (2008). "Generation of pluripotent stem cells from adult mouse liver and stomach cells." Science **321**(5889): 699-702.

Arendt, D. (2008). "The evolution of cell types in animals: emerging principles from molecular studies." Nat Rev Genet **9**(11): 868-882.

Bagheri-Fam, S., et al. (2006). "Long-range upstream and downstream enhancers control distinct subsets of the complex spatiotemporal Sox9 expression pattern." Dev Biol **291**(2): 382-397.

Bhutani, N., et al. (2010). "Reprogramming towards pluripotency requires AID-dependent DNA demethylation." Nature **463**(7284): 1042-1047.

Bossard, P. and K. S. Zaret (1998). "GATA transcription factors as potentiators of gut endoderm differentiation." Development **125**(24): 4909-4917.

Bostick, M., et al. (2007). "UHRF1 plays a role in maintaining DNA methylation in mammalian cells." Science **317**(5845): 1760-1764.

Burke, Z. D. and D. Tosh (2006). "The Wnt/beta-catenin pathway: master regulator of liver zonation?" Bioessays **28**(11): 1072-1077.

Cairns, B. R. (2009). "The logic of chromatin architecture and remodelling at promoters." Nature **461**(7261): 193-198.

Chakrabarti, S. K., et al. (2002). "Quantitative assessment of gene targeting in vitro and in vivo by the pancreatic transcription factor, Pdx1. Importance of chromatin structure in directing promoter binding." J Biol Chem **277**(15): 13286-13293.

Chen, S. S., et al. (2000). "C/EBPbeta, when expressed from the C/ebpalpha gene locus, can functionally replace C/EBPalpha in liver but not in adipose tissue." Mol Cell Biol **20**(19): 7292-7299.

Christoffels, V. M., et al. (1998). "Glucocorticoid receptor, C/EBP, HNF3, and protein kinase A coordinately activate the glucocorticoid response unit of the carbamoylphosphate synthetase I gene." Mol Cell Biol **18**(11): 6305-6315.

Cirillo, L. A., et al. (2002). "Opening of compacted chromatin by early developmental transcription factors HNF3 (FoxA) and GATA-4." Mol Cell **9**(2): 279-289.

Clotman, F., et al. (2002). "The onecut transcription factor HNF6 is required for normal development of the biliary tract." Development **129**(8): 1819-1828.

Clotman, F., et al. (2005). "Control of liver cell fate decision by a gradient of TGF beta signaling modulated by Onecut transcription factors." Genes Dev **19**(16): 1849-1854.

Coffinier, C., et al. (2002). "Bile system morphogenesis defects and liver dysfunction upon targeted deletion of HNF1beta." Development **129**(8): 1829-1838.

Dabeva, M. D., et al. (1998). "Liver regeneration and alpha-fetoprotein messenger RNA expression in the retrorsine model for hepatocyte transplantation." Cancer Res **58**(24): 5825-5834.

D'Amour, K. A., et al. (2006). "Production of pancreatic hormone-expressing endocrine cells from human embryonic stem cells." Nat Biotechnol **24**(11): 1392-1401.

Deutsch, G., et al. (2001). "A bipotential precursor population for pancreas and liver within the embryonic endoderm." Development **128**(6): 871-881.

Eberhard, D., et al. (2008). "Origin of pancreatic endocrine cells from biliary duct epithelium." Cell Mol Life Sci **65**(21): 3467-3480.

Eggan, K., et al. (2004). "Mice cloned from olfactory sensory neurons." Nature **428**(6978): 44-49.

Egli, D., et al. (2008). "Mediators of reprogramming: transcription factors and transitions through mitosis." Nat Rev Mol Cell Biol **9**(7): 505-516.

Elaut, G., et al. (2006). "Molecular mechanisms underlying the dedifferentiation process of isolated hepatocytes and their cultures." Curr Drug Metab **7**(6): 629-660.

Fausto, N. and J. S. Campbell (2003). "The role of hepatocytes and oval cells in liver regeneration and repopulation." Mech Dev **120**(1): 117-130.

Flodby, P., et al. (1996). "Increased hepatic cell proliferation and lung abnormalities in mice deficient in CCAAT/enhancer binding protein alpha." J Biol Chem **271**(40): 24753-24760.

Fougere-Deschatrette, C., et al. (2006). "Plasticity of hepatic cell differentiation: bipotential adult mouse liver clonal cell lines competent to differentiate in vitro and in vivo." Stem Cells **24**(9): 2098-2109.

Francis, N. J., et al. (2004). "Chromatin compaction by a polycomb group protein complex." Science **306**(5701): 1574-1577.

Furumatsu, T., et al. (2005). "Sox9 and p300 cooperatively regulate chromatin-mediated transcription." J Biol Chem **280**(42): 35203-35208.

Godoy, P., et al. (2010). "Dexamethasone-dependent versus -independent markers of epithelial to mesenchymal transition in primary hepatocytes." Biol Chem **391**(1): 73-83.

Gordon, G. J., et al. (2000). "Liver regeneration in rats with retrorsine-induced hepatocellular injury proceeds through a novel cellular response." Am J Pathol **156**(2): 607-619.

Gradwohl, G., et al. (2000). "neurogenin3 is required for the development of the four endocrine cell lineages of the pancreas." Proc Natl Acad Sci U S A **97**(4): 1607-1611.

Graf, T. and T. Enver (2009). "Forcing cells to change lineages." Nature **462**(7273): 587-594.

Gresh, L., et al. (2005). "The SWI/SNF chromatin-remodeling complex subunit SNF5 is essential for hepatocyte differentiation." EMBO J **24**(18): 3313-3324.

Gualdi, R., et al. (1996). "Hepatic specification of the gut endoderm in vitro: cell signaling and transcriptional control." Genes Dev **10**(13): 1670-1682.

Gurdon, J. B. (1962). "The developmental capacity of nuclei taken from intestinal epithelium cells of feeding tadpoles." J Embryol Exp Morphol **10**: 622-640.

Gurdon, J. B. and D. A. Melton (2008). "Nuclear reprogramming in cells." Science **322**(5909): 1811-1815.

Hanley, K. P., et al. (2008). "Ectopic SOX9 mediates extracellular matrix deposition characteristic of organ fibrosis." J Biol Chem **283**(20): 14063-14071.
Hanna, J., et al. (2008). "Direct reprogramming of terminally differentiated mature B lymphocytes to pluripotency." Cell **133**(2): 250-264.
Heintzman, N. D., et al. (2009). "Histone modifications at human enhancers reflect global cell-type-specific gene expression." Nature **459**(7243): 108-112.
Henkens, T., et al. (2007). "Trichostatin A, a critical factor in maintaining the functional differentiation of primary cultured rat hepatocytes." Toxicol Appl Pharmacol **218**(1): 64-71.
Hirota, T., et al. (2005). "Histone H3 serine 10 phosphorylation by Aurora B causes HP1 dissociation from heterochromatin." Nature **438**(7071): 1176-1180.
Ho, L. and G. R. Crabtree (2010). "Chromatin remodelling during development." Nature **463**(7280): 474-484.
Hochedlinger, K. and R. Jaenisch (2002). "Monoclonal mice generated by nuclear transfer from mature B and T donor cells." Nature **415**(6875): 1035-1038.
Hochedlinger, K. and K. Plath (2009). "Epigenetic reprogramming and induced pluripotency." Development **136**(4): 509-523.
Huang, S. (2009). "Reprogramming cell fates: reconciling rarity with robustness." Bioessays **31**(5): 546-560.
Huangfu, D., et al. (2008). "Induction of pluripotent stem cells by defined factors is greatly improved by small-molecule compounds." Nat Biotechnol **26**(7): 795-797.
Inayoshi, Y., et al. (2006). "Mammalian chromatin remodeling complex SWI/SNF is essential for enhanced expression of the albumin gene during liver development." J Biochem **139**(2): 177-188.
Inoue, K., et al. (2005). "Generation of cloned mice by direct nuclear transfer from natural killer T cells." Curr Biol **15**(12): 1114-1118.
Inoue, Y., et al. (2004). "Disruption of hepatic C/EBPalpha results in impaired glucose tolerance and age-dependent hepatosteatosis." J Biol Chem **279**(43): 44740-44748.
Jaenisch, R. and R. Young (2008). "Stem cells, the molecular circuitry of pluripotency and nuclear reprogramming." Cell **132**(4): 567-582.
Jonsson, J., et al. (1994). "Insulin-promoter-factor 1 is required for pancreas development in mice." Nature **371**(6498): 606-609.
Jung, J., et al. (1999). "Initiation of mammalian liver development from endoderm by fibroblast growth factors." Science **284**(5422): 1998-2003.
Kajimura, S., et al. (2009). "Initiation of myoblast to brown fat switch by a PRDM16-C/EBP-beta transcriptional complex." Nature **460**(7259): 1154-1158.
Kaneda, M., et al. (2004). "Essential role for de novo DNA methyltransferase Dnmt3a in paternal and maternal imprinting." Nature **429**(6994): 900-903.
Krupczak-Hollis, K., et al. (2004). "The mouse Forkhead Box m1 transcription factor is essential for hepatoblast mitosis and development of intrahepatic bile ducts and vessels during liver morphogenesis." Dev Biol **276**(1): 74-88.
Kyrmizi, I., et al. (2006). "Plasticity and expanding complexity of the hepatic transcription factor network during liver development." Genes Dev **20**(16): 2293-2305.

Lagha, M., et al. (2009). "Pax3:Foxc2 reciprocal repression in the somite modulates muscular versus vascular cell fate choice in multipotent progenitors." Dev Cell **17**(6): 892-899.
Law, J. A. and S. E. Jacobsen (2010). "Establishing, maintaining and modifying DNA methylation patterns in plants and animals." Nat Rev Genet **11**(3): 204-220.
Lee, C. S., et al. (2005). "The initiation of liver development is dependent on Foxa transcription factors." Nature **435**(7044): 944-947.
Lemaigre, F. P. (2009). "Mechanisms of liver development: concepts for understanding liver disorders and design of novel therapies." Gastroenterology **137**(1): 62-79.
Li, J., et al. (2000). "Mammalian hepatocyte differentiation requires the transcription factor HNF-4alpha." Genes Dev **14**(4): 464-474.
Li, W. C., et al. (2007). "Keratinocyte serum-free medium maintains long-term liver gene expression and function in cultured rat hepatocytes by preventing the loss of liver-enriched transcription factors." Int J Biochem Cell Biol **39**(3): 541-554.
Lodish, H. F. (2004). Molecular cell biology. New York, W. H. Freeman.
Lopez, R. G., et al. (2009). "C/EBPalpha and beta couple interfollicular keratinocyte proliferation arrest to commitment and terminal differentiation." Nat Cell Biol **11**(10): 1181-1190.
Martinez-Balbas, M. A., et al. (1995). "Displacement of sequence-specific transcription factors from mitotic chromatin." Cell **83**(1): 29-38.
McCright, B., et al. (2002). "A mouse model of Alagille syndrome: Notch2 as a genetic modifier of Jag1 haploinsufficiency." Development **129**(4): 1075-1082.
Meivar-Levy, I., et al. (2007). "Pancreatic and duodenal homeobox gene 1 induces hepatic dedifferentiation by suppressing the expression of CCAAT/enhancer-binding protein beta." Hepatology **46**(3): 898-905.
Michalopoulos, G. K., et al. (2005). "Transdifferentiation of rat hepatocytes into biliary cells after bile duct ligation and toxic biliary injury." Hepatology **41**(3): 535-544.
Mikkelsen, T. S., et al. (2008). "Dissecting direct reprogramming through integrative genomic analysis." Nature **454**(7200): 49-55.
Mikkola, I., et al. (2002). "Reversion of B cell commitment upon loss of Pax5 expression." Science **297**(5578): 110-113.
Morgan, R. (2004). "Conservation of sequence and function in the Pax6 regulatory elements." Trends Genet **20**(7): 283-287.
Muller, C., et al. (2004). "The CCAAT enhancer-binding protein alpha (C/EBPalpha) requires a SWI/SNF complex for proliferation arrest." J Biol Chem **279**(8): 7353-7358.
Nerlov, C., et al. (2000). "GATA-1 interacts with the myeloid PU.1 transcription factor and represses PU.1-dependent transcription." Blood **95**(8): 2543-2551.
Nishikawa, Y., et al. (2005). "Transdifferentiation of mature rat hepatocytes into bile duct-like cells in vitro." Am J Pathol **166**(4): 1077-1088.
Niwa, H., et al. (2000). "Quantitative expression of Oct-3/4 defines differentiation, dedifferentiation or self-renewal of ES cells." Nat Genet **24**(4): 372-376.
Offield, M. F., et al. (1996). "PDX-1 is required for pancreatic outgrowth and differentiation of the rostral duodenum." Development **122**(3): 983-995.

Oikawa, T., et al. (2009). "Sall4 regulates cell fate decision in fetal hepatic stem/progenitor cells." Gastroenterology **136**(3): 1000-1011.
Okita, K., et al. (2007). "Generation of germline-competent induced pluripotent stem cells." Nature **448**(7151): 313-317.
Orphanides, G. and D. Reinberg (2002). "A unified theory of gene expression." Cell **108**(4): 439-451.
Palasingam, P., et al. (2009). "The structure of Sox17 bound to DNA reveals a conserved bending topology but selective protein interaction platforms." J Mol Biol **388**(3): 619-630.
Parviz, F., et al. (2003). "Hepatocyte nuclear factor 4alpha controls the development of a hepatic epithelium and liver morphogenesis." Nat Genet **34**(3): 292-296.
Rai, K., et al. (2008). "DNA demethylation in zebrafish involves the coupling of a deaminase, a glycosylase, and gadd45." Cell **135**(7): 1201-1212.
Ramji, D. P. and P. Foka (2002). "CCAAT/enhancer-binding proteins: structure, function and regulation." Biochem J **365**(Pt 3): 561-575.
Rekhtman, N., et al. (1999). "Direct interaction of hematopoietic transcription factors PU.1 and GATA-1: functional antagonism in erythroid cells." Genes Dev **13**(11): 1398-1411.
Rooman, I., et al. (2000). "Modulation of rat pancreatic acinoductal transdifferentiation and expression of PDX-1 in vitro." Diabetologia **43**(7): 907-914.
Rossi, J. M., et al. (2001). "Distinct mesodermal signals, including BMPs from the septum transversum mesenchyme, are required in combination for hepatogenesis from the endoderm." Genes Dev **15**(15): 1998-2009.
Rozen, S. and H. Skaletsky (2000). "Primer3 on the WWW for general users and for biologist programmers." Methods Mol Biol **132**: 365-386.Ruthenburg, A. J., et al. (2007). "Multivalent engagement of chromatin modifications by linked binding modules." Nat Rev Mol Cell Biol **8**(12): 983-994.
Seale, P., et al. (2008). "PRDM16 controls a brown fat/skeletal muscle switch." Nature **454**(7207): 961-967.
Sekido, R. and R. Lovell-Badge (2008). "Sex determination involves synergistic action of SRY and SF1 on a specific Sox9 enhancer." Nature **453**(7197): 930-934.
Sharif, J., et al. (2007). "The SRA protein Np95 mediates epigenetic inheritance by recruiting Dnmt1 to methylated DNA." Nature **450**(7171): 908-912.
Shi, Y., et al. (2008). "A combined chemical and genetic approach for the generation of induced pluripotent stem cells." Cell Stem Cell **2**(6): 525-528.
Shih, D. Q., et al. (2001). "Hepatocyte nuclear factor-1alpha is an essential regulator of bile acid and plasma cholesterol metabolism." Nat Genet **27**(4): 375-382.
Shogren-Knaak, M., et al. (2006). "Histone H4-K16 acetylation controls chromatin structure and protein interactions." Science **311**(5762): 844-847.
Si-Tayeb, K., et al. (2010). "Organogenesis and development of the liver." Dev Cell **18**(2): 175-189.
Soriano, H. E., et al. (1998). "Lack of C/EBP alpha gene expression results in increased DNA synthesis and an increased frequency of immortalization of freshly isolated mice [correction of rat] hepatocytes." Hepatology **27**(2): 392-401.
Spence, J. R., et al. (2009). "Sox17 regulates organ lineage segregation of ventral foregut progenitor cells." Dev Cell **17**(1): 62-74.

Stadtfeld, M., et al. (2008). "Reprogramming of pancreatic beta cells into induced pluripotent stem cells." Curr Biol **18**(12): 890-894.
Stadtfeld, M., et al. (2008). "Induced pluripotent stem cells generated without viral integration." Science **322**(5903): 945-949.
Stopka, T., et al. (2005). "PU.1 inhibits the erythroid program by binding to GATA-1 on DNA and creating a repressive chromatin structure." EMBO J **24**(21): 3712-3723.
Strick-Marchand, H. and M. C. Weiss (2002). "Inducible differentiation and morphogenesis of bipotential liver cell lines from wild-type mouse embryos." Hepatology **36**(4 Pt 1): 794-804.
Suzuki, A., et al. (2008). "Tbx3 controls the fate of hepatic progenitor cells in liver development by suppressing p19ARF expression." Development **135**(9): 1589-1595.
Takahashi, K. and S. Yamanaka (2006). "Induction of pluripotent stem cells from mouse embryonic and adult fibroblast cultures by defined factors." Cell **126**(4): 663-676.
Takeuchi, J. K. and B. G. Bruneau (2009). "Directed transdifferentiation of mouse mesoderm to heart tissue by defined factors." Nature **459**(7247): 708-711.
Tanimizu, N. and A. Miyajima (2004). "Notch signaling controls hepatoblast differentiation by altering the expression of liver-enriched transcription factors." J Cell Sci **117**(Pt 15): 3165-3174.
Tateishi, K., et al. (2008). "Generation of insulin-secreting islet-like clusters from human skin fibroblasts." J Biol Chem **283**(46): 31601-31607.
Tolhuis, B., et al. (2002). "Looping and interaction between hypersensitive sites in the active beta-globin locus." Mol Cell **10**(6): 1453-1465.
Tosh, D., et al. (1988). "Glucagon regulation of gluconeogenesis and ketogenesis in periportal and perivenous rat hepatocytes. Heterogeneity of hormone action and of the mitochondrial redox state." Biochem J **256**(1): 197-204.
Uhlenhaut, N. H., et al. (2009). "Somatic sex reprogramming of adult ovaries to testes by FOXL2 ablation." Cell **139**(6): 1130-1142.
Waddington, C. H. (1957). The strategy of the genes : a discussion of some aspects of theoretical biology. London, Allen & Unwin.
Wernig, M., et al. (2007). "In vitro reprogramming of fibroblasts into a pluripotent ES-cell-like state." Nature **448**(7151): 318-324.
Wilmut, I., et al. (1997). "Viable offspring derived from fetal and adult mammalian cells." Nature **385**(6619): 810-813.
Xie, H., et al. (2004). "Stepwise reprogramming of B cells into macrophages." Cell **117**(5): 663-676.
Yamasaki, H., et al. (2006). "Suppression of C/EBPalpha expression in periportal hepatoblasts may stimulate biliary cell differentiation through increased Hnf6 and Hnf1b expression." Development **133**(21): 4233-4243.
Yovchev, M. I., et al. (2007). "Novel hepatic progenitor cell surface markers in the adult rat liver." Hepatology **45**(1): 139-149.
Zaret, K. S. (2002). "Regulatory phases of early liver development: paradigms of organogenesis." Nat Rev Genet **3**(7): 499-512.
Zaret, K. S. (2008). "Genetic programming of liver and pancreas progenitors: lessons for stem-cell differentiation." Nat Rev Genet **9**(5): 329-340.
Zaret, K. S. and M. Grompe (2008). "Generation and regeneration of cells of the liver and pancreas." Science **322**(5907): 1490-1494.

Zhang, C., et al. (2005). "MafA is a key regulator of glucose-stimulated insulin secretion." Mol Cell Biol **25**(12): 4969-4976.
Zhang, P., et al. (1999). "Negative cross-talk between hematopoietic regulators: GATA proteins repress PU.1." Proc Natl Acad Sci U S A **96**(15): 8705-8710.
Zhou, Q., et al. (2008). "In vivo reprogramming of adult pancreatic exocrine cells to beta-cells." Nature **455**(7213): 627-632.
Zong, Y., et al. (2009). "Notch signaling controls liver development by regulating biliary differentiation." Development **136**(10): 1727-1739.

APPENDIX

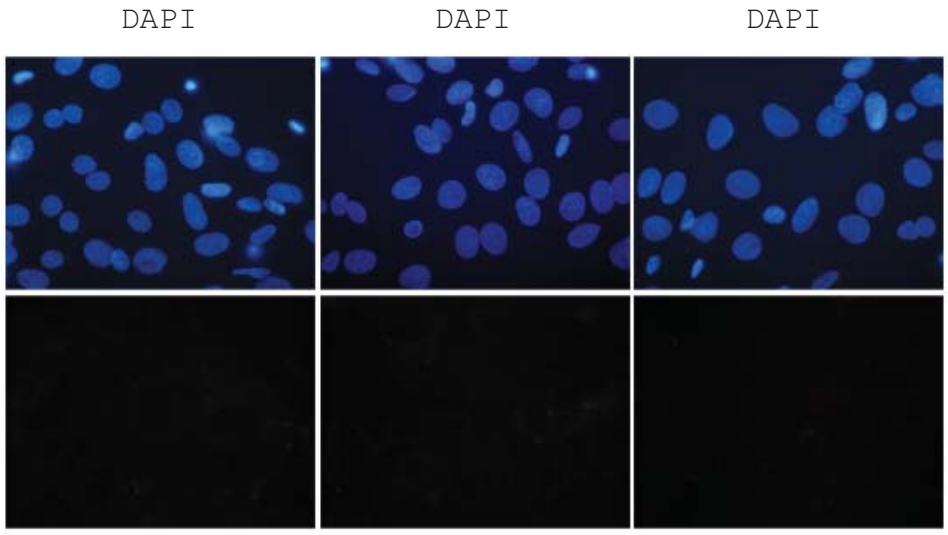

Figure 7.1: No primary antibody controls for immunocytochemistry. Immunocytochemistry was conducted as described in section 2B.4, except that blocking buffer was used instead of a primary antibody. There was no non-specific binding of the secondary antibodies.

Figure 7.2: No primary antibody control for immunohistochemistry. Immunohistochemistry was conducted as described in section 2B.5, except that blocking buffer was used instead of a primary antibody. There was no non-specific binding of the secondary antibody.

A

KdS Day 1 1	KdS Day 1 2	KdS Day 1 3	KdS Day 5 1	KdS Day 5 2	KdS Day 5 3	DS Day 5 1	DS Day 5 2	DS Day 5 3
117.063	131.899	129.736	168.015	173.054	184.818	331.055	233.607	248.767
139.576	72.253	83.11	130.017	165.809	164.554	287.63	287.889	174.33
122.016	98.183	91.782	146.302	156.985	192.885	248.183	580.558	157.612
177.431	242.625	80.104	184.321	202.379	113.170	128.806	203.417	232.418
111.613	98.183	94.875	169.269	186.786	157.007	372.448	123.140	229.412
117.842	98.205	76.406	98.940	157.958	161.073	309.689	291.306	212.608
126.903	165.506	109.624	183.002			567.042	283.023	279.152
193.880	77.682	43.512	152.011			338.603	346.129	242.496
124.589	109.213	113.279	175.562			355.515	130.363	269.788
98.724	73.097	97.340	118.080			352.855	210.402	258.261
	140.787	58.326	89.792			290.960	357.180	150.476
	109.883		178.157			273.724	154.239	196.907
	127.660		61.289				285.099	301.665
			85.446				149.589	259.126
							316.371	227.898
							362.003	162.111
							299.351	320.891
								157.915

B

	1	2	3	Mean	St Dev	SE
KdS Day 1	132.964	118.860	88.918	113.581	22.493	12.986
KdS Day 5	138.586	173.829	162.251	158.222	17.964	10.371
DS Day 5	321.376	271.392	226.769	273.179	47.329	27.325

C

	p-value
T-Test KdS Day 1, KdS Day 5	0.055
T-Test KdS Day 5, DS Day 5	0.017
T -Test KdS Day 1, DS Day 5	0.006

Table 7.1: The nuclear area of KdS and DS hepatocytes. (A) For each cell type, the nuclear area (μm^2) of every cell in 3 independent fields of view (1, 2 and 3) was measured under 40X magnification and 10X eyepiece. **(B)** The mean nuclear area, standard deviation (St Dev) and standard error (SE) were calculated for each cell type. **(C)** The mean nuclear areas of each cell type were compared using 2-tailed T-tests.

		1	2	3	Mean % input	SE	T-Test
2% K	Ct1	26.59	27.46	26.94			
	Ct2	26.44	26.79	27.06			
	Mean Ct	26.52	27.13	27.00			
	Adjusted	20.87	21.48	21.36			
2% D	Ct1	25.57	26.59	25.85			
	Ct2	25.74	26.46	25.77			
	Mean Ct	25.66	26.53	25.81			
	Adjusted	20.01	20.88	20.17			
KA	Ct1	29.47	28.54	29.30			
	Ct2	29.23	28.77	29.01			
	Mean Ct	29.35	28.66	29.16			
	dCt	-8.48	-7.17	-7.98			
	100*2^dCt	0.28	0.69	0.40	0.46	0.12	
DA	Ct1	28.06	27.68	27.15			
	Ct2	28.11	27.20	27.08			
	Mean Ct	28.09	27.44	27.12			
	dCt	-8.07	-6.56	-6.71			
	100*2^dCt	0.37	1.06	0.96	0.80	0.21	0.13
K4	Ct1	27.61	27.64	27.62			
	Ct2	27.12	27.50	27.31			
	Mean Ct	27.37	27.57	27.47			
	dCt	-6.49	-6.09	-6.11			
	100*2^dCt	1.11	1.47	1.45	1.34	0.12	
D4	Ct1	26.38	27.63	26.47			
	Ct2	26.64	26.99	26.35			
	Mean Ct	26.51	27.31	26.41			
	dCt	-6.50	-6.43	-6.24			
	100*2^dCt	1.11	1.16	1.32	1.20	0.06	0.24
K9	Ct1	28.83	30.64	28.08			
	Ct2	28.87	30.06	27.74			
	Mean Ct	28.85	30.35	27.91			
	dCt	-7.98	-8.87	-6.55			
	100*2^dCt	0.40	0.21	1.06	0.56	0.26	
D9	Ct1	28.23	27.92	26.96			
	Ct2	27.72	27.90	26.82			
	Mean Ct	27.98	27.91	26.89			
	dCt	-7.96	-7.03	-6.72			
	100*2^dCt	0.40	0.77	0.95	0.70	0.16	0.55
K27	Ct1	32.22	33.90	31.29			
	Ct2	33.11	32.67	31.70			

	Mean Ct	32.67	33.29	31.50			
	dCt	-11.79	-11.80	-10.14			
	100*2^dCt	0.03	0.03	0.09	0.05	0.02	
D27	Ct1	31.45	32.89	31.92			
	Ct2	31.71	32.11	31.57			
	Mean Ct	31.58	32.50	31.75			
	dCt	-11.57	-11.62	-11.58			
	100*2^dCt	0.03	0.03	0.03	0.03	0.00	0.51
2%K NaB	Ct1	26.81					
	Ct2	26.83					
	Mean Ct	26.82					
	Adjusted	21.18					
2%D NaB	Ct1	26.12					
	Ct2	25.98					
	Mean Ct	26.05					
	Adjusted	20.41					

Table 7.2: Sox9 real-time PCR data. Mean threshold cycle (mean Ct) numbers were calculated for each of three independent experiments (1, 2 and 3) from two replicate Ct values (Ct1 and Ct2). Ct values for 2% input samples were adjusted by subtracting $\log_2 50$ (adjusted). The mean Ct value for output (immunoprecipitated) samples was subtracted from the mean Ct value for the appropriate input sample (dCt). Fold differences were calculated as 2^dCt and multiplied by 100 to give % input. Mean % input values and standard error (SE) were obtained by combining % input values from the three experiments. For each histone modification, mean % input values for KdS and DS cells were compared with 2-tailed T-tests. K=KdS, D=DS, A=H3Ac, 4=H3K4me2, 9=H3K9me3, 27=H3K27me3, NaB=sodium butyrate.